# The multiperiod electric vehicle routing problem: model and solution approaches

Laura Echeverri

# UNIVERSITÉ DE TOURS

ÉCOLE DOCTORALE MIPTIS

Laboratoire d'Informatique Fondamentale
et Appliquée de Tours (EA 6300)

## THÈSE présentée par :

**Laura Catalina ECHEVERRI GUZMÁN**

Soutenue le : 15 décembre 2020

pour obtenir le grade de : Docteur de l'université de Tours

Discipline/ Spécialité : INFORMATIQUE

# The Multi-period Electric Vehicle Routing problem: model and solution approaches

THÈSE DIRIGÉE PAR :

| | |
|---|---|
| MENDOZA Jorge E. | Professeur agrégé, HEC Montréal, Canada |
| NÉRON Emmanuel | Professeur des universités, Université de Tours |

RAPPORTEURS :

| | |
|---|---|
| JUSSIEN Christelle | Professeur des universités, Université d'Angers |
| LEHUÉDÉ Fabien | Professeur des universités, IMT Atlantique |

JURY :

| | |
|---|---|
| BILLAUT Jean-Charles | Professeur des universités, Université de Tours |
| FROGER Aurélien | Maître de Conférences, Université de Bordeaux |
| JUSSIEN Christelle | Professeur des universités, Université d'Angers |
| LEHUÉDÉ Fabien | Professeur des universités, IMT Atlantique |
| MENDOZA Jorge E. | Professeur agrégé, HEC Montréal, Canada |
| NÉRON Emmanuel | Professeur des universités, Université de Tours |

# Acknowledgment

Earning this degree would have been impossible without the help of many others. First, I want to thank my advisors, Jorge Mendoza and Emmanuel Néron. Thank you for your wisdom and dedication along these years.

I give special thanks to Aurélien Froger. Thank you for your availability and for all the research advices you have given me.

I thank very sincerely Christelle Jussien and Fabien Lehuédé for having accepted to be the reporters of my thesis. I also thank Jean-Charles Billaut for having accepted to be part of the jury.

I want to thank the colleagues I have met during these years at LIFAT. Thank you for your help, for your advice, for the deep conversations, and the baby foot breaks. Life in Tours would not be the same without you.

I also thank *my girls*, Brenda, Gaby, and Diana, for all the fun we had and your support during my stay in Montreal, and afterwards.

I want to thank my parents for supporting me during these years with their prayers. Also, I thank my sister and my brother-in-law. Thank you for your life and research advices, and for being there to help me no matter the time difference.

Finally, I want to thank God for opening a door that no one could close. The adventure continues by your side.

# Résumé

Cette thèse étudie l'optimisation du routage et de la programmation de la charge des véhicules électriques (VEs) sur un horizon de planification de plusieurs périodes dans le but de limiter la dégradation des batteries associée à ces opérations. Nous introduisons le problème qui en résulte sous le nom de « Multi-period Electric Vehicle Routing Problem » (MP-E-VRP). Nous définissons formellement le MP-E-VRP et développons des méthodes pour le résoudre.

Pour tenir compte de l'impact des pratiques de charge et des tournées sur le vieillissement des batteries des VE, nous associons les coûts de dégradation aux opérations de charge et aux routes. Nous transformons la relation non linéaire entre les paramètres de fonctionnement et l'état de santé de la batterie en coûts linéaires par morceaux qui peuvent être inclus dans le MP-E-VRP.

Nous fournissons ensuite une formulation de programmation linéaire mixte en nombres entiers (PLNE) pour le MP-E-VRP, ci-après dénommée $[F^1]$. Notre formulation modélise le temps de manière continue et utilise des variables de suivi basées sur les arcs. En outre, elle utilise des modèles de flux pour tenir compte des contraintes de capacité du réseau électrique et de l'infrastructure de charge, et des modèles de combinaison convexe pour représenter le coût de dégradation des batteries et les fonctions de charge. Étant donné que le MP-E-VRP est un nouveau problème dans la littérature sur les E-VRP, nous présentons la procédure que nous avons suivie pour générer des instances basées sur des informations fournies par des entreprises utilisant des VE. Les résultats des calculs indiquent que, généralement, le modèle ne peut pas être utilisé directement pour résoudre des cas réalistes. Par conséquent, $[F^1]$ nous permet d'avoir une idée de la difficulté du problème et de la pertinence de concevoir des stratégies plus complexes.

Nous proposons ensuite une stratégie de décomposition dans laquelle nous générons d'abord un pool de routes de bonne qualité, puis nous sélectionnons les routes du pool, nous leur attribuons des VEs et nous ordonnons les opérations de chargement. Nous proposons trois méthodes qui suivent cette stratégie de décomposition. Elles utilisent toutes une heuristique existante pour échantillonner l'espace des routes possibles. Pour résoudre le second sous-problème (la sélection de routes et l'affectation des VE), nous proposons une heuristique constructive, une formulation PLNE et une approche basée sur « *local branching* ». L'heuristique constructive, bien que simple, permet de trouver une solution réalisable en peu de temps. Pour chaque période, l'heuristique attribue la route ayant la plus grande consommation d'énergie au VE ayant la plus grande énergie disponible et poursuit l'attribution jusqu'à ce que toutes les routes de la période soient

attribuées. En outre, l'heuristique vérifie la satisfaction des contraintes de l'infrastructure de recharge. La solution obtenue peut alors être fournie pour accélérer le processus de recherche dans les autres stratégies de décomposition.

La méthode de décomposition basée sur une formulation PLNE s'appuie sur $[F^1]$, ci-après dénommée $[F^{2m}]$. Peu de modifications sont nécessaires dans $[F^1]$ pour formuler le nouveau problème concernant l'affectation des VE aux routes et l'ordonnancement des opérations de chargement. Enfin, la matheuristique « *local branching* » basée sur $[F^{2m}]$ consiste à ajouter des contraintes linéaires à cette formulation, pour explorer l'espace de solution en effectuant des recherches locales sur des voisinages définis en vue de trouver des solutions de bonne qualité. La définition du voisinage et la stratégie de diversification sont modifiées pour tenir compte des caractéristiques du MP-E-VRP. Les résultats expérimentaux nous permettent d'identifier cette méthode comme la meilleure pour trouver des solutions pour des instances de grande taille.

# Abstract

This thesis discusses the optimization of electric vehicle (EV) routing and charging scheduling over a planning horizon of multiple periods with the aim of mitigating the battery degradation associated with these operations. We introduce the resulting problem as the Multi-period Electric Vehicle Routing Problem (MP-E-VRP). We formally define the MP-E-VRP and develop methods for solving it.

To account for the impact of charging and routing practices on EVs battery aging, we associate degradation costs with charging operations and routes. We transform the nonlinear relationship between operating parameters and battery health into piecewise linear costs that can be easily included in the MP-E-VRP.

We then provide a Mixed integer linear programming (MILP) formulation for the MP-E-VRP, hereinafter referred to as $[F^1]$. Our formulation models time on a continuous basis and uses arc-based tracking variables. Moreover, it uses flow models to account for the power grid and charging infrastructure capacity constraints, and convex combination models to represent the battery degradation cost and charging functions. Since the MP-E-VRP is a new problem in the E-VRP literature, we present the procedure we followed to generate instances based on some insights provided by companies using EVs. Computational results indicate that, generally, the model cannot be directly used to solve realistic instances. Therefore, $[F^1]$ allows us to have an idea about the difficulty of the problem and the relevance of designing more complex strategies.

We then propose a decomposition strategy in which we first generate a pool of high-quality routes and then we select the routes from the pool, assign EVs to them, and schedule the charging operations. We propose three methods following this decomposition strategy. All of them use an existing heuristic to sample the space of feasible routes. To solve the second subproblem (routes selection, assignment of EVs, and scheduling of charging operations), we propose a constructive heuristic, a MILP formulation, and a local branching-based approach. The constructive heuristic, yet simple, allows finding a feasible solution in a short time. For each period, the heuristic assigns the route with the highest energy consumption to the EV with the most available energy and continues the assignment until all routes of the period are assigned. In addition, the heuristic checks for the satisfaction of the charging infrastructure constraints. The solution obtained can then be provided to speed up the search process in the other decomposition strategies.

The decomposition method based on a MILP formulation is built upon $[F^1]$, referred to as $[F^{2m}]$. Few modifications are needed in $[F^1]$ to formulate the new problem concerning the assignment of EVs to routes and the scheduling of the charging operations. Finally,

the local branching matheuristic is based on $[F^{2m}]$ and lies in adding linear inequalities to this formulation, to explore the solution space by performing local searches on defined neighborhoods looking for good quality solutions. The neighborhood definition and the diversification strategy are modified to consider MP-E-VRP features. Computational experiments allow us to identify this method as the best for finding solutions in large-size instances.

# Contents

# List of Tables

# List of Figures

# Abbreviations used along the manuscript

| | |
|---|---|
| AFV | Alternative-fuel powered vehicle |
| Ah | Ampere-hour |
| C-rate | The measure of the speed at which a battery is charged relative to its maximum capacity |
| CS | Charging station |
| DOD | (Battery's) Depth of discharge |
| EV | Electric vehicle |
| E-VRPs | Electric Vehicle Routing Problems |
| GHG | Greenhouse gas |
| ICEV | Internal combustion engine vehicle |
| kW | Kilowatt |
| kWh | Kilowatt-hour |
| Li-ion | Lithium-ion |
| MILP | Mixed integer linear programming |
| MP-E-VRP | Multi-period Electric Vehicle Routing Problem |
| MP-E-VRACSP | Multi-period Electric Vehicle Route Assignment and Charging Scheduling Problem |
| OR | Operations Research |
| SOC | (Battery's) State of charge |
| VRP | Vehicle Routing Problem |

# Chapter 1

# Introduction

## 1.1 Version française

Les accords internationaux sur le changement climatique sont principalement axés sur la réduction des gaz à effet de serre (GES) et des émissions de pollution atmosphérique, ayant un impact sur l'augmentation des températures mondiales (Bektaş et al., 2019). Le secteur des transports est particulièrement concerné car il représente un pourcentage important des émissions mondiales (de Campos et al., 2019). Par exemple, il représente près de 25% des émissions en Europe et 29% aux États-Unis (Eurostat, 2019; USEPA, 2019). Le transport dépend principalement des combustibles fossiles comme source d'énergie. Lors de leur combustion, les combustibles fossiles émettent du dioxyde de carbone ($CO_2$), qui représente environ 80% des émissions totales de GES (Ahmad, 2004). Parmi les différents modes de transport, le transport routier est le plus grand producteur d'émissions de GES dans les pays membres de l'Organisation de Coopération et de Développement Économiques (OCDE) (McKinnon and Piecyk, 2009). Le fret routier représentant un peu moins de la moitié du transport routier total, les entreprises de transport de marchandises sont encouragées à réduire leurs émissions de GES (Li et al., 2013).

L'un des principaux moyens pour réduire les émissions dans les transports est l'utilisation de modes de transport plus « verts ». Dans le domaine du transport routier, des alternatives aux véhicules à moteur à combustion interne (VMCI), couramment utilisés, sont recherchées. Les véhicules électriques (VEs) sont présentés comme une solution prometteuse pour améliorer l'efficacité énergétique et réduire les émissions de GES et la dépendance aux combustibles fossiles (Felipe et al., 2014; Zheng and Peeta, 2017). En général, le terme VE couvre les véhicules hybrides, les véhicules hybrides rechargeables et les véhicules électriques à batterie, mais, pour ce qui concerne cette thèse, le terme ne couvrira que les véhicules électriques à batterie. Ceux-ci utilisent un moteur électrique et sont alimentés par une batterie électrique rechargeable. Les VEs n'ont aucune émission de gaz d'échappement, ce qui contribue à réduire la pollution localisée. Les émissions totales de GES dépendent du processus de fabrication des VEs et de la source d'énergie utilisée pour charger leurs batteries (Casals et al., 2016; Quak et al., 2016). Les entreprises de transport de marchandises sont prêtes à intégrer les VEs dans leurs opérations logistiques, car ils permettent de réaliser des économies de carburant, de réduire les émissions de GES et d'adopter une «

image verte » (Franceschetti et al., 2017). En fait, plusieurs grandes entreprises utilisent déjà des VEs dans leur parc automobile. Il s'agit notamment de DHL, UPS, Japan Post, Frito Lay, Fed Ex, AT&T, General Electric, Coca-Cola et Staples (Lebeau et al., 2015; Benedikt Sobotka, 2019; Suizo, 2013). L'adoption généralisée des VEs est toutefois entravée par certaines contraintes technologiques que les VMCI n'ont pas. Par exemple, l'autonomie des VEs est généralement plus réduite que celui des VMCI.

Les infrastructures de recharge des VEs sont encore rares par rapport au réseau de stations de ravitaillement des VMCI, et la durée de la recharge est beaucoup plus longue que celle du ravitaillement des VMCI, allant de 30 minutes à plusieurs heures (Høyer, 2008; Pelletier et al., 2016). En outre, le prix d'achat des VEs reste supérieur à celui des VMCI, la batterie représentant une part importante du surcoût. Le prix d'achat des VEs s'est révélé être l'un des principaux obstacles à l'adoption des VEs (Bühne et al., 2015; Bullard, 2019). Alors que la recherche sur la technologie des batteries progresse à un rythme lent vers des VEs moins chers, il est nécessaire de progresser dans le développement d'outils de gestion du parc automobile qui puissent gérer les restrictions des VEs (Felipe et al., 2014).

La communauté de la Recherche Opérationnelle (RO) a montré un intérêt croissant pour la conception de techniques d'optimisation pour résoudre des problèmes du routage des véhicules électriques (E-VRPs). Ces problèmes sont axés sur la mise en place d'itinéraires *efficaces* pour la livraison de biens et de services aux clients en tenant compte des contraintes technologiques des VEs. Pour surmonter leur autonomie limitée, les VEs peuvent être rechargés en cours de route. Cela introduit des décisions supplémentaires par rapport aux problèmes classiques de routage des véhicules (VRP) : où et combien les recharger. Schneider et al. (2014) ont introduit le problème du routage des véhicules électriques avec des fenêtres de temps et des stations de recharge. Dans ce problème, les clients doivent être visités dans des fenêtres temporelles prédéfinies et les VEs peuvent faire un détour par les stations de recharge (CSs) où ils récupèrent une batterie complètement chargée. Pour économiser de l'énergie et du temps, des politiques de recharge partielle ont été introduites par Felipe et al. (2014). Montoya et al. (2017) ont proposé de remplacer l'hypothèse classique du processus de charge linéaire en introduisant une approximation linéaire par morceaux de la fonction de charge. L'approximation linéaire par morceaux reflète la non-linéarité de la relation entre le temps passé à charger et la quantité d'énergie chargée. En outre, la disponibilité actuelle (limitée) de l'infrastructure de recharge en dehors du dépôt a motivé la conception de stratégies visant à résoudre le problème de la localisation des CSs et du routage des VEs. Yang and Sun (2015) ont étudié ce problème dans un contexte de stations d'échange de batteries. Plus tard, Schiffer and Walther (2017) ont introduit le problème du routage de la localisation électrique avec des fenêtres temporelles et une recharge partielle dans les CSs. D'autres améliorations ont été apportées au problème du routage de la localisation électrique en tenant compte des installations intra-route, des ressources multiples, de l'incertitude des habitudes des clients et des CSs partagées (Koç et al., 2018; Schiffer et al., 2018; Schiffer and Walther, 2018a,b). Une grande partie de la littérature sur les E-VRPs se concentre sur le routage mais néglige généralement les limites de l'infrastructure de recharge. Par exemple, pratiquement toutes les études partent du principe que les CSs sont de propriété privée et peuvent simultanément charger un nombre illimité de VEs. Ainsi, les VEs ont un accès prioritaire à l'infrastructure et peuvent commencer à charger lorsqu'ils arrivent au CS. Toutefois, ces hypothèses peuvent

conduire à des programmes de recharge irréalisables, car les CSs disposent d'un nombre limité de chargeurs (Froger et al., 2019a). En outre, la plupart des entreprises n'ont pas les ressources nécessaires pour acquérir une infrastructure de recharge en dehors du dépôt, et doivent donc faire face à l'incertitude quant à la disponibilité des CSs publiques. À notre connaissance, il existe peu de références traitant de l'incertitude quant à la disponibilité des CSs publiques (voir Sweda et al. (2017), Kullman et al. (2020), et Keskin et al. (2019) pour plus de détails).

Les innovations récentes dans la technologie des batteries permettent de surmonter l'autonomie limitée des VEs. Les batteries au lithium-ion (li-ion), le type de batterie le plus courant pour les VEs, peuvent désormais atteindre une autonomie de 230 à 480 km (Nykvist et al., 2019). D'ici 2025, les améliorations apportées aux matériaux des anodes et des cathodes devraient porter le rayon d'action à plus de 500 km (Nathan, 2019; Sedran, 2018). En outre, de nouvelles technologies de batteries encore plus performantes devraient être disponibles dans les années à venir. La technologie des batteries à semi-conducteurs est l'alternative la plus connue. À la différence des batteries li-ion, qui utilisent des électrolytes liquides pour conduire le courant électrique, les batteries à semi-conducteurs utilisent un matériau conducteur sec. Les batteries à l'état solide pourraient atteindre une autonomie de 800 km (Middlehurst, 2019; Sedran, 2018). Néanmoins, de nombreux chercheurs conviennent que cette technologie ne sera pas commercialisée avant 2030 (Collins, 2019; Middlehurst, 2019). D'autres technologies, telles que le lithium-soufre et le lithium-air, sont également en cours de développement, avec la promesse de densités énergétiques extrêmement élevées qui se traduisent par des VEs à grande autonomie (Collins, 2019).

L'augmentation de l'autonomie des VEs modifie la manière dont les opérations logistiques avec les VEs sont effectuées. Jusqu'à très récemment, l'autonomie limitée des VEs obligeait les entreprises exploitant des VEs pour des opérations urbaines et semi-urbaines à prévoir une recharge des batteries en milieu de parcours (Quak et al., 2016). Avec l'avènement des nouvelles technologies de batteries, la distance parcourue par un itinéraire dans la distribution urbaine est généralement plus courte que l'autonomie des VEs nouvellement disponibles. En Europe, plus de 80% des trajets de fret urbains sont inférieurs à 80 km, ce qui est bien inférieur à la portée que peuvent atteindre les VEs de nos jours (Lebeau et al., 2016). Sans qu'il soit nécessaire de faire une recharge à mi-parcours, les opérations de recharge peuvent être limitées à la nuit (ou entre deux quarts de travail) au dépôt. En fait, la recharge au dépôt est le mode de recharge le plus courant pour les entreprises. Cela est dû au manque d'infrastructures publiques de recharge et aux longs délais de recharge qui rendent incertaine la disponibilité des CSs (Kullman et al., 2020; Quak et al., 2016; Sweda et al., 2017). En outre, la possibilité de recharger entre deux quarts de travail est avantageuse car elle permet d'utiliser le temps des conducteurs de manière plus efficace (Lebeau et al., 2016; Taefi et al., 2016).

Lorsque la recharge des batteries est limitée au dépôt, les exploitants de parcs de VEs doivent tenir compte des contraintes liées au réseau et à l'infrastructure de recharge. Il peut être impossible de charger tous les VEs simultanément, car cela peut nécessiter une connexion au réseau de plus grande capacité que celle déjà disponible au dépôt (Quak et al., 2017). En outre, l'alternative consistant à améliorer la capacité du réseau nécessite un investissement initial important qui peut être excessivement coûteux pour de

Table 1.1: Spécifications de l'infrastructure de recharge des VEs aux États-Unis. Source: Nicholas (2019)

| Niveau de recharge | Voltage | Puissance typique | EV km d'autonomie par heure de recharge |
|---|---|---|---|
| Niveau 2 | 208 V–240 V CA | 3.3–6.6 kW CA | 16–32 km |
| Rapide CC | 400 V–1000 V CC | 50 kW ou plus | 241–1609 km |

Note: CA = courant alternatif; CC = courant continu; kW = kilowatt; V = volt; km = kilomètre

nombreuses entreprises. Par exemple, UPS a récemment procédé à une mise à niveau de l'infrastructure du réseau dans son dépôt de Londres, pour un coût de plus de £600,000 (plus de €702000), mais peu d'entreprises peuvent se permettre des investissements de cette ampleur (FREVUE, 2016). En outre, les plans tarifaires de l'électricité peuvent comporter des restrictions de puissance maximale qui doivent être respectées lors de la recharge des VEs (voir, par exemple, Southern California Edison (2019)). En ce qui concerne l'infrastructure de recharge, une entreprise peut disposer d'un nombre limité de chargeurs au dépôt. Les chargeurs de VEs utilisés dans les dépôts peuvent être classés en deux grandes catégories : Niveau 2 et courant continu (CC) rapide. Le tableau 1.1 présente les principales caractéristiques de ces deux types de chargeurs. Le coût d'acquisition d'un chargeur dépend de la puissance de l'appareil, de ses capacités de communication et de la nécessité d'un socle. Le coût d'un chargeur varie entre environ €1000 (pour les chargeurs de niveau 2) et €125000 (pour les chargeurs rapides CC). Les coûts d'installation par chargeur peuvent être d'environ €2070 lorsque l'on installe six chargeurs de niveau 2 ou plus et varient de €16000 à €60000 pour les chargeurs rapides CC, en fonction du niveau de puissance et du nombre de chargeurs à installer (Nicholas, 2019). Contraintes par ces fourchettes de prix élevées, les entreprises possèdent généralement plusieurs chargeurs de niveau 2 mais seulement quelques chargeurs rapides CC.

Les opérations de recharge doivent alors être programmées en tenant compte de la capacité de l'infrastructure de recharge. Bien que la programmation de la recharge des VEs ait reçu beaucoup moins d'attention que le routage dans la littérature en RO, certaines études ont récemment tenté de tenir compte des contraintes d'infrastructure. Froger et al. (2019a) ont mis l'accent sur le routage et la programmation de la recharge des CSs. Ils ont développé un modèle de programmation linéaire mixte en nombres entiers (PLNE) en temps continu pour traiter les CSs avec capacités et des fonctions de charge non linéaires. L'objectif est de minimiser la durée totale du plan de route. Ce dernier comprend la conduite, le service aux clients et la recharge des VEs. Betz et al. (2016), Sassi et al. (2015) et Sassi et Oulamara (2017) ont envisagé la programmation de la recharge des VEs dans un contexte avec un parc de VEs et de VMCI. Sassi et al. (2015) ont traité de la programmation et du routage de la recharge dans le but de minimiser le nombre de véhicules employés et le total des coûts de déplacement et de recharge. Les opérations de chargement peuvent être effectuées à la fois dans les CSs et au dépôt. Les CSs ont des coûts de chargement dépendant du temps et différents types de chargeurs. Ils sont soumis à des fenêtres de temps de fonctionnement et à la puissance de charge maximale qu'ils peuvent fournir. L'infrastructure de chargement disponible au dépôt consiste en un nombre limité de chargeurs de différentes technologies. Sassi et Oulamara (2017) traite de l'affectation des VEs et des VMCI à des itinéraires soumis à la disponibilité des chargeurs et à la

capacité du réseau électrique au dépôt. L'objectif est de maximiser l'utilisation des VEs et de minimiser les coûts de charge. Ils ont fourni une formulation PLNE pour ce problème. Dans Sassi et Oulamara (2017) et Sassi et al. (2015), l'horizon temporel (un jour) est discrétisé en périodes de temps et le processus de charge est linéaire par rapport à la puissance de charge. Betz et al. (2016) ont abordé la programmation des véhicules et de la recharge en utilisant une formulation PLNE en temps discret pour un modèle de disposition de flotte d'une société exploitant des VEs et des VMCI. Les opérations de charge doivent être programmées au dépôt, où un nombre limité de chargeurs avec un processus de charge linéaire est disponible. L'objectif est de minimiser les coûts globaux (coûts d'exploitation et coûts énergétiques en fonction du temps) ou les émissions globales de $CO_2$ en fonction du temps. Rinaldi et al. (2018) ont formulé un modèle PLNE en temps discret pour le problème de la répartition des bus électriques et hybrides soumis à des contraintes de programmation et de charge au dépôt, telles que la disponibilité des chargeurs. L'objectif est de minimiser les coûts opérationnels, à savoir les coûts énergétiques, les coûts de chargement au dépôt et une pénalité pour avoir commencé les trajets après l'heure de départ souhaitée. Pelletier et al. (2018) ont étudié le problème de la programmation de la charge au dépôt dans un horizon de planification de plusieurs jours, afin de minimiser les coûts de charge intégrant la dégradation des batteries. La définition du problème tient compte des différents modes de charge, des fonctions de charge non linéaires, d'un nombre limité de chargeurs disponibles et des contraintes du réseau électrique.

La dégradation des batteries est un processus physico-chimique qui peut être accéléré par certaines conditions de stockage et de fonctionnement (Pelletier et al., 2017). Ceci est d'autant plus critique que la batterie est le composant le plus coûteux d'un VE. En effet, les batteries représentent entre 30 et 40% du coût d'acquisition d'un VE (Casals et al., 2017). En outre, les procédures actuelles de production et d'élimination des batteries ont des effets néfastes sur la santé humaine et la biodiversité (voir Sonoc et al. (2015); Wanger (2011); Zeng et al. (2014) pour plus de détails sur les questions environnementales concernant les batteries li-ion). Le vieillissement et le remplacement des batteries au cours de la durée de vie d'un VE ont un impact négatif sur les performances et la durabilité des VEs (Uddin et al., 2014). Cela affecte à son tour la flexibilité à long terme et la durabilité des opérations de distribution des VEs. Néanmoins, à notre connaissance, il n'existe qu'une poignée de références concernant la modélisation de la dégradation des batteries dans le contexte du routage et de la programmation de la charge des VEs (voir, par exemple, Barco et al. (2017); Arslan et al. (2015); Pelletier et al. (2018))

Afin d'atténuer la dégradation à long terme des batteries, les entreprises doivent planifier simultanément les opérations d'acheminement et de chargement sur un horizon de planification de (au moins) quelques jours/quarts de travail. En effet, le découplage des décisions de routage et de planification sur une seule journée entraîne généralement une dégradation accélérée des batteries. Pour autant que nous sachions, la littérature ne fait pas état d'études traitant simultanément de ces décisions sur un horizon de planification à plusieurs périodes. Il convient de noter que le problème qui en résulte est considérablement plus difficile à résoudre que le traditionnel VRP multipériode (MP-VRP). En effet, le MP-VRP consiste à concevoir un ensemble de routes pour chaque période sur un horizon de planification de plusieurs périodes (généralement, mais pas nécessairement, des jours) pour répondre à la demande requise des clients, où la demande par client dans chaque

période est connue (Angelelli et al., 2007; Chandra and Fisher, 1994; Wen et al., 2010). Le problème d'acheminement peut être résolu indépendamment pour chaque jour, puisqu'il n'y a pas de contraintes de couplage entre les jours. Ce n'est plus le cas lorsqu'il s'agit de VEs. En effet, l'énergie d'un VE au début d'une période dépend des décisions de charge et d'acheminement de la période précédente. Pour ajouter à la complexité du problème qui en résulte, les contraintes liées à l'infrastructure de recharge doivent être prises en compte dans la programmation de ces opérations.

À la lumière de ces questions, l'objectif de cette thèse est d'élargir la recherche sur les VEs en étudiant un nouveau problème qui intègre la planification du routage et de la recharge des dépôts sur un horizon de planification de plusieurs jours : le problème de tournées de véhicules électriques multiperiodique (MP-E-VRP). L'objectif du MP-E-VRP est d'atténuer la dégradation des batteries par un couplage approprié des itinéraires et des calendriers de charge sur plusieurs périodes de travail.

Le reste de ce manuscrit est organisé comme suit. Le Chapitre 2 passe en revue la littérature correspondante concernant le VRP et les E-VRPs. Le Chapitre 3 fournit un contexte sur la dégradation des batteries au li-ion. En outre, il présente la procedure que nous avons suivie pour approximer la fonction de dégradation de la batterie en tant que coûts de dégradation de la batterie. Ces coûts peuvent être facilement inclus dans les E-VRPs. Le Chapitre 4 définit formellement le MP-E-VRP et en fournit une formulation PLNE. Le Chapitre 5 présente la stratégie de décomposition que nous proposons pour aborder le MP-E-VRP. Le chapitre présente aussi trois méthodes qui suivent cette stratégie de décomposition et une évaluation expérimentale des méthodes proposées. Enfin, nous résumons l'ensemble de la recherche, présentons la conclusion finale et exposons quelques perspectives de recherche. Chaque chapitre est accompagné d'une introduction en français qui définit les grandes lignes du chapitre tout en présentant les contributions de ce travail.

Cette thèse est financée en France par l'Agence Nationale de la Recherche à travers le projet e-VRO (ANR-15-CE22-0005-01) et a été rendue possible en partie grâce au soutien de Calcul Québec (www.calculquebec.ca) et de Compute Canada (www.computecanada.ca). De plus, j'ai été stagiaire de recherche de mars à septembre 2019 au Centre interuniversitaire de recherche sur les réseaux d'entreprises, la logistique et le transport (CIRRELT) à Montréal (Canada). Ce stage a été financé en France par le GDR R.O. dans le cadre de son programme Mobilité Doctorant/Jeune Chercheur du GDR R.O.

Les résultats de cette recherche ont été présentés lors de six conférences avec les références suivantes :

- Echeverri, L.C., Froger, A., Mendoza, J.E., and Néron, E.
  The multi-period electric vehicle routing problem.
  *19ème Congrès ROADEF*, Lorient (France), 2018.

- Echeverri, L.C., Froger, A., Mendoza, J.E., and Néron, E.
  Scheduling charging operations for electric vehicles while minimizing battery degradation.
  *INFORMS Annual Meeting*, Phoenix (United States), 2018.

- Echeverri, L.C., Froger, A., Mendoza, J.E.

Multi-period electric vehicle routing and charging scheduling problems.
*Optimization Days*, Montreal (Canada), 2019.

- Echeverri, L.C., Froger, A., Mendoza, J.E.
Multi-period routing and battery charge scheduling for electric vehicles.
*Seventh meeting of the EURO working group on vehicle routing and logistics optimization (VeRoLog)*, Seville (Spain), 2019.

- Echeverri, L.C., Froger, A., Mendoza, J.E., and Néron, E.
A matheuristic for the Multi-period Electric Vehicle Routing Problem.
*13th Metaheuristics International Conference*, Cartagena de Indias (Colombia), 2019.

- Echeverri, L.C., Froger, A., Mendoza, J.E., and Néron, E.
Solving the Multi-period Electric Vehicle Routing Problem with matheuristics.
*21ème Congrès ROADEF*, Montpellier (France), 2020.

## 1.2 English version

International agreements on climate change are mainly focused in the reduction of greenhouse gases (GHGs) and air pollution emissions, as they have been linked to increases in global temperatures (Bektaş et al., 2019). The transportation sector is particularly concerned as it accounts for an important percentage of emissions worldwide (de Campos et al., 2019). For instance, it accounts for almost 25% of emissions in Europe and 29% in the United States (Eurostat, 2019; USEPA, 2019). Transportation mainly depends on fossil fuels as the energy source. During combustion, fossil fuels emit carbon dioxide ($CO_2$), which represents roughly 80% of the total GHGs emissions (Ahmad, 2004). Among the different transportation modes, road transportation is the largest producer of GHG emissions in the member countries of the Organization for Economic Cooperation and Development (OECD) (McKinnon and Piecyk, 2009). With road freight being slightly less than half of the road transportation total, freight transportation companies are encouraged to reduce GHG emissions (Li et al., 2013).

One main leverage to reduce emissions in transportation is the use of 'greener' transportation modes. In road transportation, alternatives to the commonly used internal-combustion engine vehicles (ICEVs) are being sought. Electric vehicles (EVs) are presented as a promising solution to improve energy efficiency and reduce GHG emissions and fossil fuel dependency (Felipe et al., 2014; Zheng and Peeta, 2017). In general, the term EVs covers hybrid, plug-in hybrid and battery electric vehicles, but, for the purpose of this thesis, the term will only cover battery electric vehicles. These use an electric motor and are powered by a rechargeable electric battery. EVs have zero tailpipe emissions, which helps to reduce localized pollution. Total GHG emissions depend on the manufacturing process of EVs and the energy source used to charge their batteries (Casals et al., 2016; Quak et al., 2016). Freight transportation companies are willing to integrate EVs in their logistic operations, as they allow for fuel savings, GHG emissions reduction and 'green branding' (Franceschetti et al., 2017). In fact, several major companies are already using EVs in their fleets. These include DHL, UPS, Japan Post, Frito Lay, Fed Ex, AT&T, General Electric, Coca-Cola, and Staples (Lebeau et al., 2015; Benedikt Sobotka, 2019;

Suizo, 2013). Widespread adoption of EVs is, however, impeded by some technological constraints that ICEVs do not have. For example, EVs' driving range is generally shorter compared to that of ICEVs'.

Charging infrastructure for EVs is still scarce compared to the network of refueling stations for ICEVs, and charging duration is much longer than refueling duration for ICEVs, the former taking from 30 minutes to several hours (Høyer, 2008; Pelletier et al., 2016). Moreover, EVs purchasing price is still higher than ICEVs' price, with the battery representing an important part of the extra cost. EVs purchasing price has shown to be one of the biggest barriers to the adoption of EVs (Bühne et al., 2015; Bullard, 2019). While research in battery technology is moving at a low pace forward longer range - cheaper EVs, it is necessary to progress in the development of fleet management tools that can handle the EVs' restrictions (Felipe et al., 2014).

The Operations Research (OR) community has shown a growing interest in the design of optimization techniques to solve electric vehicle routing problems (E-VRPs). These problems are focused on building *efficient* routes to deliver goods and services to customers taking into account the EVs technological constraints. To overcome their limited driving range, EVs can be recharged en route. This introduces additional decisions compared to classical vehicle routing problems (VRPs): where and how much to charge. Schneider et al. (2014) introduced the electric vehicle routing problem with time windows and recharging stations. In this problem, the customers must be visited within predefined time windows and EVs can detour to charging stations (CSss) where they recover a fully charged battery. To save energy and time, partial recharging policies were introduced by Felipe et al. (2014). Montoya et al. (2017) proposed to replace the classical linear charging process assumption by introducing a piecewise linear approximation of the charging function. The piecewise linear approximation reflects the nonlinearity of the relation between the time spent charging and the amount of energy charged. Furthermore, the current (limited) availability of charging infrastructure outside the depot has motivated the design of strategies to solve the problem of CS location and EV routing. Yang and Sun (2015) studied this problem in a context with battery swapping stations. Later on, Schiffer and Walther (2017) introduced the electric location routing problem with time windows and partial recharging in CSs. Further enhancement to the electric location routing problem have been made by considering intra-route facilities, multiple resources, uncertainty in customers' patterns, and shared CSs (Koç et al., 2018; Schiffer et al., 2018; Schiffer and Walther, 2018a,b). Much of the literature on E-VRPs focuses on the routing but usually neglects the charging infrastructure limitations. For instance, virtually all studies assume that CSs are privately owned and can simultaneously charge an unlimited number of EVs. Thus, the EVs have priority access to the infrastructure and may start charging when they arrive at the CS. However, making these assumptions can lead to infeasible charging schedules as CSs have a limited number of chargers (Froger et al., 2019a). Additionally, most companies do not have the resources to acquire charging infrastructure outside the depot, so they have to deal with the uncertainty with respect to public CS availability. As far as we know, there are few references addressing uncertainty in public CS availability (see Sweda et al. (2017), Kullman et al. (2020), and Keskin et al. (2019) for more details).

Recent innovations in battery technology are allowing to overcome EVs' restrictive driving range. Lithium-ion (li-ion) batteries, the most common type of batteries for EVs,

are now able to reach 230 to 480 km of range (Nykvist et al., 2019). By 2025, improvements in anode and cathode materials are expected to increase the driving range to more than 500 km (Nathan, 2019; Sedran, 2018). Moreover, new battery technologies with even better performance are expected to become available in the years to come. Solid-state battery technology is the best-known alternative. Differing from li-ion batteries that use liquid electrolytes to conduct the electric current, solid-state batteries use dry conductive material. Solid-state batteries could achieve a driving range of up to 800 km (Middlehurst, 2019; Sedran, 2018). Nevertheless, many researchers agree that this technology will not be commercially available before 2030 (Collins, 2019; Middlehurst, 2019). Other technologies, such as lithium-sulfur and lithium-air, are also under development, with the promise of extremely high energy densities which translate into EVs with large driving ranges (Collins, 2019).

The increase on EVs' driving range is changing the way logistic operations with EVs are carried out. Up to very recently, the limited range of EVs forced companies exploiting EVs for urban and semi-urban operations to plan for mid-route battery charging (Quak et al., 2016). With the advent of new battery technologies, the distance covered by a route in urban distribution is typically shorter than the autonomy of the newly available EVs. In Europe, more than 80% of urban freight trips are shorter than 80 km, which is far less than the range achievable by EVs nowadays (Lebeau et al., 2016). Without the need for mid-route charging, the charging operations can be restricted to take place overnight (or between shifts) at the depot. As a matter of fact, depot charging is the most common charging manner for companies. This is due to the lack of public charging infrastructures and the long charging times that make uncertain the availability of the CSs (Kullman et al., 2020; Quak et al., 2016; Sweda et al., 2017). Further, the possibility to charge between working shifts is advantageous as it helps to use the drivers' time more efficiently (Lebeau et al., 2016; Taefi et al., 2016).

When battery charging is limited to the depot, EV fleet operators must take into account grid and charging infrastructure constraints. Charging all EVs simultaneously may be impossible as it can require a higher capacity grid connection than the capacity already available at the depot (Quak et al., 2017). Furthermore, the alternative of upgrading the grid capacity requires a significant initial investment that can be excessively expensive for many companies. For instance, UPS recently carried out a grid infrastructure upgrade process in its depot in London with a cost of over £600,000 (more than €702000), but few companies can afford investments of that amount (FREVUE, 2016). Moreover, electricity rate plans may comprise maximum power restrictions that must be respected when charging EVs (see, e.g., Southern California Edison (2019)). Regarding the charging infrastructure, a company may have a limited number of chargers available at the depot. EV chargers used in depot charging can be classified in two main categories: Level 2 and direct current (DC) fast. Table 1.2 presents the main characteristics of these two types of chargers. Acquisition cost of a charger depends on the power of the unit, its communication capabilities, and the need for a pedestal. The cost of a charger ranges from about €1000 (for Level 2 chargers) to €125000 (for DC fast chargers). Installation costs per charger can be about €2070 when installing six or more Level 2 chargers and range from €16000 to €60000 for DC fast chargers, depending on the power level and the number of chargers to install (Nicholas, 2019). Constrained by these high price ranges, companies

Table 1.2: EV charging infrastructure specifications in the United States. Source: Nicholas (2019)

| Charging level | Voltage | Typical power | EV km of range per charging hour |
|---|---|---|---|
| Level 2 | 208 V–240 V AC | 3.3–6.6 kW AC | 16–32 km |
| DC fast | 400 V–1000 V DC | 50 kW or more | 241–1609 km |

Note: AC = alternating current; DC = direct current; kW = kilowatt; V = volt; km = kilometer

typically own several Level 2 chargers but just a few DC fast chargers.

Charging operations must then be scheduled taking into account the capacity of the charging infrastructure. Although EV charging scheduling has received far less attention than routing in the OR literature, some studies have recently attempted to account for the infrastructure constraints. Froger et al. (2019a) focused on routing and CS charging scheduling. They developed a continuous-time mixed-integer linear programming (MILP) model to deal with capacitated CSs with nonlinear charging functions. The objective is to minimize the total time of the route plan. The latter includes driving, servicing customers, and charging the EVs. Betz et al. (2016), Sassi et al. (2015) and Sassi and Oulamara (2017) considered EVs charging scheduling in a context with a fleet of EVs and internal combustion engine vehicles (ICEVs). Sassi et al. (2015) dealt with charging scheduling and routing with the aim of minimizing the number of employed vehicles and the total travel and charging costs. Charging operations can be performed both at CSs and at the depot. CSs have time dependent charging costs and different types of chargers. They are subject to operating time windows and the maximum charging power they can deliver. The charging infrastructure available at the depot consists of a limited number of chargers with different technologies. Sassi and Oulamara (2017) addressed the assignment of EVs and ICEVs to routes subject to charger availability and power grid capacity at the depot. The objective is to maximize the use of EVs and minimize the charging costs. They provided a MILP formulation for this problem. In Sassi and Oulamara (2017) and Sassi et al. (2015) the time horizon (a day) is discretized into time periods and the charging process is linear with respect to the charging power. Betz et al. (2016) tackled vehicle and charging scheduling using a discrete-time MILP formulation for a fleet disposition model of a company running EVs and ICEVs. Charging operations must be scheduled at the depot, where a limited number of chargers with a linear charging process is available. The objective is to minimize the overall costs (running costs and time-dependent energy costs) or the overall time-dependent $CO_2$-emissions. Rinaldi et al. (2018) formulated a discrete-time MILP model for the problem of dispatching electric and hybrid buses subject to scheduling and depot charging constraints, such as chargers availability. The objective is to minimize the operational costs consisting of the energy costs, the depot charging costs and a penalty for starting the trips after their preferred departure time. Pelletier et al. (2018) studied the problem of depot charging scheduling in a planning horizon of several days, in order to minimize charging costs incorporating battery degradation. The definition of the problem accounts for different charging modes, nonlinear charging functions, a limited number of available chargers, and power grid constraints.

Battery degradation is a physiochemical process that may be accelerated by some

storage and operating conditions (Pelletier et al., 2017). This is especially critical since the battery is the most expensive component of an EV. Indeed, battery packs represents between 30 and 40% of the acquisition cost of an EV (Casals et al., 2017). Moreover, current battery production and disposal procedures have adverse effects on human health and biodiversity (see Sonoc et al. (2015); Wanger (2011); Zeng et al. (2014) for details on environmental issues regarding li-ion batteries). Battery aging and replacement over an EV lifetime adversely impact EV performance and durability (Uddin et al., 2014). This in turn affects the long-term flexibility and the sustainability of the distribution operations with EVs. Nonetheless, to the best of our knowledge, there exist only a handful of references considering battery degradation modeling in the context of EV routing and charging scheduling (see, for example, Barco et al. (2017); Arslan et al. (2015); Pelletier et al. (2018)).

In order to mitigate the long-term degradation of batteries, companies must simultaneously plan routing and charging operations over a planning horizon of (at least) a few days/shifts. Indeed, decoupling routing and scheduling decision and planning for a single day usually leads to accelerated battery degradation. As far as we know, the literature does not report on studies simultaneously addressing these decisions over a multi-period planning horizon. One should note that the resulting problem is considerably harder to solve than the traditional multi-period VRP (MP-VRP). As a matter of fact, the MP-VRP consists in designing a set of routes for each period on a planning horizon of several periods (typically, but not necessarily, days) to meet the required demand of customers, where the demand per customer in each period is known (Angelelli et al., 2007; Chandra and Fisher, 1994; Wen et al., 2010). The routing problem can be independently solved for each day, since there are no coupling constraints between days. This is no longer true when dealing with EVs. Indeed, the energy of an EV at the beginning of a period depends on the charging and routing decisions of the previous period. Adding to the complexity of the resulting problem, the charging infrastructure constraints must be accounted in the scheduling of these operations.

In light of these issues, the purpose of this thesis is to expand the research on E-VRPs by studying a new problem that integrates routing and depot charging scheduling over a planning horizon of several days: the Multi-period Electric Vehicle Routing Problem (MP-E-VRP). The aim of the MP-E-VRP is to mitigate battery degradation by a proper coupling of routes and charging schedules over multiple working periods.

## Contributions

The contributions of this work are multifold and are reported subsequently while we define the outline of this thesis.

### Chapter 2 - Literature review

We start this chapter by positioning OR in transportation planning, to highlight its importance and usefulness. We latter focus on the vehicle routing problem (VRP), one of the most studied topics in OR, providing an overview of its most important variants. We

finish this overview by identifying a new stream of research on VRPs concerned by the environmental impact of transportation activities, called green vehicle routing problems. These include the E-VRPs, that extend classical routing problems to consider the limited driving range and long charging durations of EVs. At this point, we concentrate on the E-VRPs. We emphasize on modeling rather than solution methods, to highlight the most important contributions on incorporating real-life characteristics. We point out how improvements in battery technology entail a new line of E-VRPs based on depot charging rather than en route recharging. Furthermore, we call attention to the importance of considering battery degradation concerns in transportation planning. In this way, we identify the lack in the literature of E-VRPs coupling routing and charging scheduling over multiple days, to address battery aging properly. We also present a classification of references on EV routing and charging scheduling by charging infrastructure characteristics, battery charging function, solution method used, among other features.

### Chapter 3 - Approximating the battery degradation function

This chapter provides a background on battery degradation modelling for lithium-ion (li-ion) batteries, one of the most generally used technologies for EVs. The chapter highlights the importance of considering battery degradation in both economic and environmental perspectives. Moreover, it draws attention to the effects of accelerated battery degradation on the sustainability of distribution operations with EVs. Next, it summarizes the most representative battery degradation models found in the literature. Battery degradation modeling is very complex, owing to the electrochemical processes involved in it and the interrelation of the factors that accelerate it. For this reason, models must be approximated to be incorporated in E-VRPs. We provide the procedure we followed to approximate the battery degradation function as battery degradation costs that can be easily included to E-VRPs. These costs are composed by (charging) fixed costs and cumulative wear costs associated with charging operations and routes. Fixed costs are intended to penalize the number of charges and using fast-charging and can be easily computed with only the battery pack price and the charging rate as input. The cumulative wear cost function was obtained by use of the model of Han et al. (2014). This model computes the wear cost per unit of energy charged or discharged depending on the percentage of available battery capacity. To facilitate its inclusion in a model, we proposed a function that maps the energy charged or discharged over a defined time interval to the wear cost incurred. For modeling purposes, we approximated this function with a piecewise linear function which shows to be adequate to represent the cumulative wear cost. The fit's adjusted $R^2$ is equal to 0.99. Moreover, we tested for a significant difference-in-slope by performing the Davies' test, which rejected the null hypothesis of no breakpoint at 1% level. The battery degradation costs are used in the rest of this thesis.

### Chapter 4 - The Multi-period Electric Vehicle Routing problem

In this chapter we introduce and formally define the MP-E-VRP. The MP-E-VRP consists on designing routes to be performed by a fleet of EVs to serve a set of customers over a planning horizon of several periods. EVs are charged at the depot at any time,

subject to the charging infrastructure capacity constraints. Due to the impact of charging and routing practices on EVs battery aging, degradation costs are associated with charging operations and routes. Chapter 3 describes how these costs are obtained. The objective of the MP-E-VRP is to determine, for each period, a set of routes visiting all the customers and to schedule the charging operations of the EVs while minimizing the degradation costs. The MP-E-VRP integrates EV routing and depot charging scheduling, and has coupling constraints between days. These features make the MP-E-VRP a complex problem to solve. We provide a MILP formulation in continuous time using arc-based tracking variables. Our formulation uses flow models to account for the power grid and charging infrastructure capacity constraints, and convex combination models to represent the cumulative wear cost and charging functions. We present the procedure we followed to generate instances for the MP-E-VRP. Computational results indicate that, generally, the model cannot be directly used to solve realistic instances. Indeed, a MILP commercial solver is unable to solve to optimality the small-size instances provided (3 periods and 10 customers per period) after 3 hours, and the gap with respect to best known upper bounds is still very large. This MILP formulation allows us to have an idea about the difficulty of the problem and the relevance of designing more complex strategies. Chapter 5 accounts for the different strategies implemented to solve the MP-E-VRP.

Results of this research were presented at two conferences with the following references:

- Echeverri, L.C., Froger, A., Mendoza, J.E., and Néron, E.
  The multi-period electric vehicle routing problem.
  *19ème Congrès ROADEF*, Lorient (France), 2018.
- Echeverri, L.C., Froger, A., Mendoza, J.E., and Néron, E.
  Scheduling charging operations for electric vehicles while minimizing battery degradation.
  *INFORMS Annual Meeting*, Phoenix (United States), 2018.

### Chapter 5 - Decomposition methods for solving the MP-E-VRP

In this chapter, we present a decomposition strategy to tackle the MP-E-VRP. The first subproblem to be solved consists on designing a high-quality and diverse pool of feasible routes. The second subproblem refers to selecting the routes to be performed, assigning EVs to them, and scheduling the charging operations that make this assignment feasible. We propose three methods following this decomposition strategy. All of them use an existing heuristic to sample the space of feasible routes. To solve the second subproblem, we propose a constructive heuristic, a MILP formulation, and a local branching-based approach. The constructive heuristic, yet simple, allows to find a feasible solution in short time. For each period, the heuristic assigns the route with the highest energy consumption to the EV with the most available energy and continues the assignment until all routes of the period are assigned. In addition, the heuristic checks for the satisfaction of the charging infrastructure constraints. The solution obtained can then be provided to speed up the search process in the other decomposition strategies. The MILP formulation is built upon the MILP formulation presented for the MP-E-VRP. Few modifications are needed to formulate the new problem concerning the assignment of EVs to routes and the

scheduling of the charging operations. Finally, the local branching based approach is based in the MILP formulation presented in this chapter and lies in adding linear inequalities to this formulation, to explore the solution space by performing local searches on defined neighborhoods looking for good quality solutions. The neighborhood definition and the diversification strategy are modified to consider MP-E-VRP features. Computational experiments allow us to identify this method as the best for finding solutions in large-size instances.

Results of this research were presented at four conferences with the following references:

- Echeverri, L.C., Froger, A., Mendoza, J.E.
  Multi-period electric vehicle routing and charging scheduling problems.
  *Optimization Days*, Montreal (Canada), 2019.

- Echeverri, L.C., Froger, A., Mendoza, J.E.
  Multi-period routing and battery charge scheduling for electric vehicles.
  *Seventh meeting of the EURO working group on vehicle routing and logistics optimization (VeRoLog)*, Seville (Spain), 2019.

- Echeverri, L.C., Froger, A., Mendoza, J.E., and Néron, E.
  A matheuristic for the Multi-period Electric Vehicle Routing Problem.
  *13th Metaheuristics International Conference*, Cartagena de Indias (Colombia), 2019.

- Echeverri, L.C., Froger, A., Mendoza, J.E., and Néron, E.
  Solving the Multi-period Electric Vehicle Routing Problem with matheuristics.
  *21ème Congrès ROADEF*, Montpellier (France), 2020.

Finally we summarize the overall research, present the final conclusion and outline some research perspectives.

This thesis is funded in France by Agence Nationale de la Recherche through project e-VRO (ANR-15-CE22-0005-01) and was enabled in part by support provided by Calcul Québec (www.calculquebec.ca) and Compute Canada (www.computecanada.ca). Additionally, I was a research intern from March to September 2019 at the Interuniversity research center on enterprise networks, logistics, and transportation (CIRRELT) in Montreal (Canada). This intership was funded in France by the GDR R.O. through their program Mobilité Doctorant/Jeune Chercheur du GDR R.O.

# Chapter 2

# Literature review

Nous commençons ce chapitre en positionnant la Recherche Opérationnelle dans la planification des transports, afin de souligner son importance et son utilité. Nous nous concentrons ensuite sur le problème du routage des véhicules (VRP), l'un des sujets les plus étudiés en matière de RO, en donnant un aperçu de ses variantes les plus importantes. Nous terminons ce tour d'horizon en identifiant un nouveau courant de recherche sur les PRV concernés par l'impact environnemental des activités de transport, appelé problèmes de routage des véhicules verts. Il s'agit des E-VRP, qui étendent les problèmes classiques de routage pour tenir compte de l'autonomie limitée et des longues durées de chargement des VE. À ce stade, nous nous concentrons sur les E-VRP. Nous mettons l'accent sur la modélisation plutôt que sur les méthodes de résolution, afin de mettre en évidence les contributions les plus importantes sur l'incorporation des caractéristiques de ces problémes dans les modéles. Nous soulignons comment les améliorations de la technologie des batteries impliquent une nouvelle gamme de PREV basés sur la recharge au dépôt plutôt que sur la recharge en route. En outre, nous attirons l'attention sur l'importance de prendre en compte les problèmes de dégradation des batteries dans la planification des transports. Ainsi, nous identifions le manque dans la littérature d'E-VRPs couplant le routage et la programmation de la charge sur plusieurs jours, pour traiter correctement le vieillissement des batteries. Nous présentons également une classification des références sur le routage et la programmation de la recharge des VE en fonction des caractéristiques de l'infrastructure de recharge, de la fonction de recharge de la batterie, de la méthode de solution utilisée, entre autres.

## 2.1 Operations Research and transportation

Operations Research (OR) is a vast discipline concerned with the development of scientific models and techniques to support decision-making problems arising in the direction and management of systems in industry, business, government, and defense (Operational Research Society, 1962). This discipline has considerably contributed to the efficiency of transportation systems. It has proved to be suitable for solving complex transportation problems that can be found at the different levels of decision making: strategic, tactical and operational. Strategic level decisions include the design of the physical network, the location of main facilities and resource acquisition. Tactical decisions include the design of the service network (the long distance movement of goods) and the solution of vehicle routing problems (the distribution of goods at a local or regional level). Finally, operational planning refers to the short term decisions that ensure demand satisfaction and resource efficiency, taking into account the dynamic nature of operations (Crainic and Laporte, 1997).

The OR community has been studying transportation problems for a long time. Indeed, a first contribution dates back to 1930 (see Schrijver (2002)). This research has not only produced advances of knowledge but also models and algorithms present in software used by private and public companies (Speranza, 2018). A particular area of interest is the solution of vehicle routing problems. Companies face immense pressure to be competitive, having to deliver goods to their customers ever faster and more efficiently. Fortunately, the vehicle routing problem (VRP), as an optimization problem, is one of the most studied topics in OR, resulting in a large set tools and applications (see, for example, the survey on software by Partyka and Hall (2014) and the books Toth and Vigo (2014) and Corberán and Laporte (2013)).

The new policies intended to reduce GHGs emissions in the transport sector have persuaded companies to consider the use of alternative-fuel powered vehicles (AFVs), such as EVs and biodiesel vehicles. Companies are adapting their logistics operations to integrate EVs in their fleets, as they are a promising solution to improve energy efficiency and reduce GHGs and fossil fuel dependency (Felipe et al., 2014; Zheng and Peeta, 2017). As a response, recent years have witnessed a growing interest in the OR community for the design of optimization techniques to solve EV routing problems (E-VRPs), which consider the EVs technological constraints, such as their reduced driving range and their long battery charging duration.

After this brief presentation of the positioning of OR, and VRPs, in transportation, we provide in Section 2.2 an overview of the VRP and its most important variants. Following, in Section 2.3, we focus on E-VRPs.

## 2.2 The Vehicle Routing Problem

The VRP consists of designing a set of minimum cost routes for vehicles serving a set of customer locations such that each route starts and ends at a common depot and some side constraints are satisfied (Laporte, 2007). In its classical version, only the vehicles capacity constraints must be met and the fleet is assumed to be homogeneous, i.e., all vehicles have

the same capacity. This problem is also referred to as the Capacitated VRP (CVRP). The VRP was introduced by Dantzig and Ramser in 1959 to describe a real-world problem related with the delivery of gasoline to service stations. Since then, a large number of different variants have been proposed, with the purpose of incorporating more real-life characteristics. A natural variant is to consider a limited fleet of vehicles with different capacities, variable and fixed costs, speeds or customers they can visit, a problem known as the Heterogeneous Fleet VRP (HFVRP) or the Mixed Fleet VRP. A variant related to the HFRVRP is the Fleet Size and Mix VRP (FSM), that address the strategic decision of the optimal fleet size and assortment of vehicles from an unlimited heterogeneous fleet (see Baldacci et al. (2008) and Soonpracha et al. (2014)).

Other variant, the VRP with Time Windows (VRPTW; see Desaulniers et al. (2014)), involves scheduling visits to customers who are only available during specific time intervals, called time windows. Vehicles are subject to travel, service and waiting times. Time windows can be hard or soft. In presence of hard time windows, if a vehicle arrives too early to service a customer, it must wait until the time window opens, with no cost for early arrival, in general. In presence of soft time windows, the violation of a time window is penalized with a cost that is non-decreasing with respect to time. To account for traffic congestion, travel time may depend on the time of the day. Solving VRPs with time-dependent travel times is proved to increase the accuracy of route plans as compared to solving VRPs modeled with time-independent travel times (see for example, Figliozzi (2012) and Kok et al. (2012)).

In the VRP with Pickup and Delivery (VRPPD), a heterogeneous vehicle fleet must satisfy a set of requests, with the requests defined by a pickup point, a delivery point and a demand to be transported between these two points (Desaulniers et al., 2001). This problem is known as the Dial-a-Ride problem (DARP) in passenger transportation, with applications in point-to-point transportation for patients, handicapped persons, and elderly (see Cordeau and Laporte (2007)). The Vehicle Routing Problem with Backhauls (VRPB) is also a pickup/delivery problem with the assumption that on each route all deliveries are required to be made before any pickups. This is based on the fact that vehicles are normally rear-loaded and the rearrangement of the loads on the vehicles at the delivery points may be costly or infeasible (Goetschalckx and Jacobs-Blecha, 1989).

The Multi-Depot VRP (MDVRP) considers that customers are served by vehicles located in different depots geographically spread (Montoya-Torres et al., 2015). Vehicles may be obligated to return to the starting depot or not, and depots may have a maximum vehicle capacity. Solutions to the MDVRP frequently group customers into clusters to be served by vehicles located in the nearest depot. For a review of literature on the MDVRP, see Vidal et al. (2012).

The Multi-period VRP (MP-VRP) consists of designing a set of routes for each period on a given planning horizon of several periods (typically, but not necessarily, days) to meet the required demand of customers, where the demand per customer in each period is known (Angelelli et al., 2007; Chandra and Fisher, 1994; Wen et al., 2010). It should not be confused with the Periodic VRP (PVRP), that faces the design of routes in a multi-period planning horizon to satisfy the visit frequency of customers, with the visits occurring in one of a set of different period combinations (Christofides and Beasley, 1984).

In Dynamic VRPs (DVRPs) some data is not known beforehand, but revealed dynamically over the course of the operation. This data can include travel time, vehicle availability, customers' locations and demands (see, e.g., Haghani and Jung (2005), Li et al. (2009)). A review of the literature on DVRP can be found in Psaraftis et al. (2016). If some data are not known in advance but are described by a random variable following a probability distribution, the problem is known as stochastic VRP (SVRP). Stochastic data can include travel times, and customer demands and availability. A survey on SVRP can be found in Gendreau et al. (1996).

VRPs are in general focused on the minimization of internal costs related to the routes, these costs incurred by the organization carrying out the routing plan. The growing awareness of human activities' influence on climate change has driven organizations to account for the environmental impact of transportation activities. This has motivated the emergence of VRP variants called Green VRPs (GVRPs). The aim of GVRPs is to reduce the environmental externalities of transportation, such as air pollution and GHGs emissions. Lin et al. (2014) provide a survey on these problems by identifying the most representative problems: pollution routing problems, VRPs in Reverse Logistics, and VRPs concerning energy consumption. Pollution routing problems concern the reduction of GHG emissions and in particular $CO_2$ emissions. VRPs in Reverse Logistics focus on the distribution channels of the reverse flows of a supply chain, such as waste and end-of-life goods collection. Finally, VRPs concerning energy consumption are focused on reducing fossil fuel consumption by optimizing transportation's energy usage. A first line of research in these problems deals with the inclusion of fuel consumption and emissions models in the routing problem. Eglese and Bekta¸s (2014) provide an overview of such problems. A second line of research involves the refueling or recharging of AFVs. These problems take into consideration the AFVs' distance limitation associated with their fuel tank capacity. Accordingly, they are related to the distance-constrained VRP (DCVRP), where vehicles have a limit on the total length of the route they can perform. Moreover, they must deal with AFVS's scarce refueling infrastructure. Additionally, for EVs, the recharging duration can take hours. Thus, appropriate strategies are required to incorporate recharging time into EV routing.

## 2.3 Electric Vehicle Routing Problems

Conrad and Figliozzi (2011) introduced the recharging vehicle routing problem as an extension of the DCVRP. In this problem, vehicles with a limited range (potentially EVs) may charge at certain customer locations to continue the route, if needed. In addition, vehicles can fully charge the battery or up to 80% of its capacity. Erdoğan and Miller-Hooks (2012) considered the use of dedicated alternative fuel stations by introducing a GVRP where AFVs are allowed to completely refuel at these stations in constant time. Schneider et al. (2014) presented the E-VRP with time windows (E-VRPTW) and recharging stations. In the E-VRPTW, EVs can detour to charging stations (CSs) to fully charge their batteries following a linear charging function. Motivated by potential cost savings in recharging time and energy, Felipe et al. (2014) addressed the possibility of executing partial recharges at CSs with multiple charging technologies. Partial recharging was also

considered by Bruglieri et al. (2015) and Keskin and Çatay (2016, 2018), among others, in the context of the E-VRPTW. Keskin and Çatay (2018) additionally considered different charging technologies. Finally, Montoya et al. (2017) introduced a piecewise linear approximation of the charging function to reflect the nonlinear charging behavior of the charging process. Froger et al. (2019b) proposed two new formulations for the problem introduced by Montoya et al. (2017).

Several other E-VRP extensions have been considered in the last years. In most studies, EVs are charged at the depot or at CS, but there are other available alternatives. To reduce the waiting time for charging, some studies have considered using battery swap stations (BSSs), where the discharged battery is replaced by a fully charged one in short time (Jie et al., 2019; Liao et al., 2016; Masmoudi et al., 2018; Paz et al., 2018; Wang et al., 2018), or wireless charging systems (WCSs), where EVs are charged while driving without the need to stop to recharge (Li et al., 2018). The idea of BSS is slowly being reconsidered after the bankruptcy of battery-switching services company Better Place in 2013 (David Pearson, 2013). WCSs, for their part, are still in the early stages of development (Li et al., 2018). As most companies do not operate pure (homogeneous) EVs fleets, several studies have considered the use of a heterogeneous fleet. Some of them have analyzed the case with ICEVs (Goeke and Schneider, 2015; Hiermann et al., 2019; Kopfer and Vornhusen, 2019; Lebeau et al., 2015; Sassi et al., 2015; Sassi and Oulamara, 2017; Villegas et al., 2018) whereas others have considered a heterogeneous EV fleet (Desaulniers et al., 2016). Furthermore, some studies have addressed the scarcity of CSs by dealing with both CS location and EV routing (Schiffer and Walther, 2017; Yang and Sun, 2015), some of them also including other features such as multiple depots, intra-route facilities, multiple resources, uncertainty in customers patterns and shared CS (Koç et al., 2018; Li-ying and Yuan-bin, 2015; Paz et al., 2018; Schiffer et al., 2018; Schiffer and Walther, 2018a,b).

Most of the literature on E-VRPs tackles the routing of EVs but disregards the charging infrastructure limitations. For example, many of the studies assume that CSs are privately owned and can simultaneously charge an unlimited number of EVs. As a consequence, EVs have priority access to the CSs and may start charging when arriving at a CS. Nevertheless, such assumptions can lead to infeasible charging schedules because CSs have a limited number of chargers (Froger et al., 2019a). Moreover, most companies do not have their own charging infrastructure because their installation requires significant investments they cannot afford (Koç et al., 2018). As a consequence, they must deal with the uncertain availability of public CSs. As far as we know, there is a small body of literature that is concerned with this issue. Sweda et al. (2017) assigned a probability to the unavailability of stations. If an EV arrives to an unavailable CS, it must wait a random time interval before recharging. Bruglieri et al. (2019b) dealt with the capacity of AFSs by allowing for reservations at them, with the introduction of time windows at the stations. Kullman et al. (2020) introduced the E-VRP with public-private recharging strategy where EVs may be recharged at a privately-owned depot and en-route at public CSs. They modeled the charging queuing dynamics at the CSs as a $M/M/\psi_c/\infty$ queuing system. Keskin et al. (2019) considered time-dependent waiting times at the CSs using a M/G/1 queuing system. Froger et al. (2019a) proposed the E-VRP with capacitated CSs. This problem considers the scheduling of the charging operations at CSs with multiple charging technologies.

Historically, studies on E-VRPs had dealt with EVs limited driving range by including mid-route battery charging in their modeling, as it was the case in real applications. Recent improvements in battery technology are now allowing for performing daily urban and semi-urban operations without the need for mid-route charging, as the driving range becomes sufficient for this type of operation. In such cases, charging operations can be limited to be performed overnight (or between shifts) at the depot. With the phasing-out of en-route charging, new E-VRPs are focusing on depot charging and, along with this, grid and charging infrastructure limitations at the depot. Sassi et al. (2015) presented a Mixed Fleet VRP with heterogeneous EVs and homogeneous ICEVs in which EVs can charge at the depot and at CSs. When charging at the depot, the constraints related to the power grid must be satisfied. CSs are subject to operating time windows and have with different technologies and time dependent charging costs. Betz et al. (2016) proposed a fleet disposition model for a company running EVs and ICEVs in which vehicles must be assigned to routes. Charging operations are performed at the depot subject to the limited number of chargers available. Sassi and Oulamara (2017) introduced the EV scheduling and optimal charging problem, in which EVs and ICEVs must be assigned to pre-constructed routes. EVs are subject to charger availability and power grid capacity at the depot. Rinaldi et al. (2018) presented a problem of dispatching electric and hybrid buses subject to scheduling and depot charging constraints, such as chargers availability. Pelletier et al. (2018) introduced the electric freight vehicle (EFV) charging scheduling problem in which a fleet of EFVs must be charged at the depot to perform a set of routes in a planning horizon of several days while minimizing charging costs including battery degradation. The definition of the problem accounts for different charging modes, nonlinear charging functions, a limited number of available chargers, and power grid constraints.

Battery degradation is a physiochemical process that may be accelerated by some storage and operating conditions (Pelletier et al., 2017). Accelerated battery aging affects the sustainability of distribution operations with EVs, as it is explained in Section 3.1. Thus, battery degradation concerns must be considered in transportation planning with EVs. To our knowledge, there are few approaches to model the battery degradation in EV routing and scheduling problems. Sassi and Oulamara (2017) restrict the interval of the battery's state of charge (SOC) to improve the battery lifetime. The SOC of a battery is the percentage of available battery capacity (usually represented in values from 0 to 1). Sweda et al. (2017) go a little further, accounting for the battery degradation due to battery's overcharging and number of charging cycles in recharging policies for EVs. A charging cycle is the process of charging and discharging a rechargeable battery. Arslan et al. (2015) model the number of cycles as a non-linear function of the depth of discharge (DOD). The DOD is the inverse of the SOC, the percentage of the battery that has been discharged relative to the total battery capacity. Arslan et al. (2015) assign a battery degradation cost per cycle based on the DOD and use it in a minimum cost path problem for Plug-in Hybrid Electric Vehicles. Pelletier et al. (2018) use the model of Han et al. (2014) in its discrete version to compute the wear costs per unit of energy going in or out of the battery according to the battery's SOC. Barco et al. (2017) apply a simplified version of the battery degradation model of Hoke et al. (2011) to an E-VRP in public transportation. They propose a two-stage model where they first solve to optimality an E-VRP that minimizes energy consumption, and then they use a heuristic approach to

assign the routes to the EVs and solve a charging optimization problem with battery degradation. The degradation is considered to be due to temperature, SOC and DOD. Their approach could lead to infeasible solutions if the optimum routes cannot be assigned to the available vehicles so that the vehicles can be charged enough to meet the energy demands of the following routes. In order to avoid it, an optimization model is needed with a better articulation of vehicle routing and charging, and battery degradation.

To lessen battery degradation in the long-term, companies using EVs must jointly plan routes and charging schedules over multiple days/shifts. In fact, decoupling routing and scheduling decision and planning for a single day usually leads to accelerated battery degradation. To the best of our knowledge, there are no studies in the literature that address these decisions simultaneously over multiple periods. Kouider et al. (2018) proposed the periodic electric vehicle routing problem (PEVRP), dealing with routing and charging (both at the depot and at CSs) over multiple periods subject to frequency constraints. However, they fail to clarify how the charging decisions taken in each period are coupled and they do not take into account the charging infrastructure limitations. Coupling routing and charging scheduling in a multiple period framework increases the difficulty of solving a MP-VRP with EVs. In the traditional MP-VRP, the routing decisions can be taken independently each day, since there are no coupling constraints between days. This is no longer true when dealing with EVs. As a matter of fact, the energy of an EV at the beginning of a period depends on the charging and routing decisions of the previous period. Adding to the complexity of the resulting problem, the charging infrastructure constraints must be accounted in the scheduling of these operations.

As discussed above, the progression on battery technology is now allowing for performing daily urban and semi-urban operations with EVs without the need for mid-route charging. Consequently, some recent studies on E-VRPs are focusing on depot charging together with the power grid and charging infrastructure limitations. Furthermore, concerns about the impact of operating conditions on battery degradation and, thereby, on the sustainability of operations with EVs, claim for a proper management in EV routing applications. This implies coupling EV routing and charging over a planning horizon of multiple days/shifts to mitigate battery aging. Such configuration entails several challenges. First, considering the power grid and charging infrastructure limitations at the depot requires the scheduling of the charging operations to make it feasible. Second, battery degradation modeling must be both easy to incorporate and sufficiently realistic to be able to reflect the degradation caused by the operation conditions. Third, coupling routing and scheduling decisions adds complexity to the problem. The research to date has not studied such a problem. This thesis responds to this void by introducing the multi-period EV routing problem (MP-E-VRP). Chapter 3 considers in more depth on battery degradation modeling and details how we obtained the battery degradation approximation to embed it in the MP-E-VRP. Subsequent chapters focus on the MP-EV-VRP definition and solution methods.

Table 2.2 classifies the EV routing and charging scheduling studies according to:

- The problem it solves: if it is focused on the EV routing (R) problem or in the charging scheduling (Sch.) problem

- The charging infrastructure:
  - Ownership (Own.): if it is private (Pr.) and hence always available, or public (Pub.), and hence the user must compete with others for access
  - Capacity (Cap.): if it considers an unlimited (Unlim.) number of chargers, so that all vehicles can be simultaneously charged, or a limited (Lim.) number of chargers, and so the access must be synchronized
  - Charging mode (Charg. mode): if it considers a single (S) mode, multiple (M) modes, BSSs or WCSs.
- The battery charging function (Battery charging fcn.):
  - Charging policy (Charg. policy): choosing between whether the battery is always charged up to its full capacity (F) or whether the amount of charge is a decision variable and so the battery can be partially charged (P)
  - Charging function approximation (Charg. fnc.): whether it is linear (L) or non linear (NL)
- The energy consumption function (Energy cons. fnc.): whether it is linear (L), generally proportional to the distance, or non-linear (NL), and based on vehicle and arc characteristics such as speed, acceleration, mass, rolling friction and air drag
- The fleet composition: whether it is a homogeneous fleet (Ho) or heterogeneous (He) fleet
- The objective function (Obj. fcn.), with the explanation of the numbers given in Table 2.1
- The solution method it proposes, with A-, G-, EVO-VNS, ALNS, TS, ILS, SA, MSH, HC, AC, DP, CG, WSM, PBA, and PSO representing adaptive-, general-, evolutionary-variable neighborhood search, adaptive large neighborhood search, tabu search, iterated local search, simulated annealing, multi-space sampling heuristic, heuristic concentration, ant colony, dynamic programming, column generation, weighted sum method, path based approach, and particle swarm optimization, respectively. MILP is used for the papers that only formulate the mathematical model and report results obtained by a solver
- Other features such as the existence of time windows (TW), station location decisions (Loc.), multiple periods (Per.) and battery degradation modeling (Deg.)

E-VRPs are NP-hard in the strong sense as they are a natural extension of the VRP, which is also NP-hard (Afroditi et al., 2014; Lenstra and Kan, 1981).

Table 2.1: Meanings of objective functions in Table 2.2

| | |
|---|---|
| 1 Vehicle cost | 9 Station installation cost |
| 2 Total travel cost | 10 Stopping cost at a station |
| 3 Total time cost | 11 Recharging cost |
| 4 Operational costs | 12 Waiting cost |
| 5 Battery cost | 13 Battery degradation cost |
| 6 Charging cost | 14 Penalty for violated time windows |
| 7 Fuel cost | 15 Profit of visits |
| 8 Battery swapping cost | |

Table 2.2: EV routing and charging scheduling literature overview

| Papers | Problem | Charging Infrastructure | | | Battery charging fcn. | | Energy cons. | Fleet composition | | Obj. fcn. | Solution method | Others |
|---|---|---|---|---|---|---|---|---|---|---|---|---|
| | | Own. | Cap. | Charg. mode | Charg. policy | Charg. fnc. | fnc. | Ho | He | | | |
| Conrad and Figliozzi (2011) | R | Pr. | Unlim. | S | F, P | – | L | EVs | | 1, 2, 3, 11 | Iterative construction, improvement heuristics | – |
| Erdoğan and Miller-Hooks (2012) | R | Pr. | Unlim. | S | F | – | L | AFVs | | 2 | Several heuristics | – |
| Schneider et al. (2014) | R | Pr. | Unlim. | S | F | L | L | EVs | | 1, 2 | Hybrid VNS and TS | TW |
| Felipe et al. (2014) | R | Pr. | Unlim. | M | P | L | L | EVs | | 2, 11 | Several heuristics and SA | TW |
| Sassi et al. (2015) | R,Sch | Pr. | Lim. | M | P | L | L | | EVs, ICEVs | 1, 2, 11 | Several heuristics | TW |
| Li-ying and Yuan-bin (2015) | R | Pr. | Unlim. | M | F | ◇ ◇ ◇ | L | EVs | | 3, 9, 11 | Hybrid AVNS and TS | TW, Loc. |
| Goeke and Schneider (2015) | R | Pr. | Unlim. | S | P | L | ◇ | | EVs, ICEVs | 2, 3, 7, 5, 11 | ALNS | TW |
| Bruglieri et al. (2015) | R | Pr. | Unlim. | S | P | L | L | EVs | | 1, 2, 11, 12 | VNS branching | TW |
| Yang and Sun (2015) | R | Pr. | Unlim. | BSS | – | – | L | EVs | | 2, 9 | Several heuristics | – |
| Arslan et al. (2015) | R | Pr. | Unlim. | S | P | L | L | PHEVs | | 7, 5, 10 | DP | – |
| Lebeau et al. (2015) | R | Pr. | Unlim. | S | P | L | NL | | EVs, ICEVs, PHEVs | 1, 2, 4 | Savings heuristic | TW |
| Keskin and Çatay (2016) | R | Pr. | Unlim. | S | P | L | L | EVs | | 1, 2 | ALNS | TW |
| Desaulniers et al. (2016) | R | Pr. | Unlim. | S | F | L | L | EVs | | 2 | Branch-price-and-cut | TW |
| Hiermann et al. (2016) | R | Pr. | Unlim. | S | F | L | L | | EVs | 1, 2 | Branch-price, and ALNS | TW |
| Wen et al. (2016) | R | Pr. | Unlim. | S | P | L | L | EVs | | 1, 2 | ALNS | TW |
| Roberti and Wen (2016) | R | Pr. | Unlim. | S | F | L | L | EVs | | 2 | GVNS, DP | TW |
| Lin et al. (2016) | R | Pr. | Unlim. | S | F | L | L | EVs | | 1, 2, 11 | MILP | – |
| Liao et al. (2016) | R | Pr. | Unlim. | BSS | – | – | NS | EVs | | 3 | DP | – |
| Grandinetti et al. (2016) | R | Pr. | Unlim. | S | P | L | L | EVs | | 1, 2, 14 | WSM | TW |
| Koç and Karaoglan (2016) | R | Pr. | Unlim. | S | F | – | L | AFVs | | 2 | Brach-and-cut | – |
| Montoya et al. (2016) | R | Pr. | Unlim. | S | F | – | L | AFVs | | 2 | MSH | – |
| Betz et al. (2016) | Sch | Pr. | Lim. | S | P | L | - | | EVs, ICEVs | 2, 7 | MILP | – |
| Hof et al. (2017) | R | Pr. | Unlim. | BSS | – | – | L | EVs | | 2, 9 | AVNS | – |
| Sweda et al. (2017) | R | Pub. | Lim. | M | P | ◇ ◇ | L | EVs | | 2, 7, 11, 12 | Several optimal and heuristic procedures | Deg. |
| Bruglieri et al. (2017) | R | Pr. | Unlim. | S | P | L | L | EVs | | 1, 3 | VNS branching based matheuristic | TW |
| Barco et al. (2017) | R,Sch | Pr. | Unlim. | S | P | L | NL | | EVs, ICEVs | 11, 13 | Differential evolution algorithm | Deg. |
| Montoya et al. (2017) | R | Pr. | Unlim. | M | P | NL | L | EVs | | 3 | Hybrid ILS and HC | – |
| Schiffer and Walther (2017) | R | Pr. | Unlim. | S | F | L | L | EVs | | 1, 2, 9 | MILP | TW |

NS: The paper does not mention the characteristics of the function
◇ depends on vehicle mass, speed and gradient of the terrain
◇ ◇ linear but has different cost components for different charge levels
◇ ◇ ◇ linear but has different cost and rates for different chargers

Table 2.1: EV routing and charging scheduling literature overview

| Papers | Problem | Charging Infrastructure | | | Battery charging fcn. | | Energy cons. | Fleet composition | | Obj. fcn. | Solution method | Others |
|---|---|---|---|---|---|---|---|---|---|---|---|---|
| | | Own. | Cap. | Charg. mode | Charg. policy | Charg. fnc. | fnc. | Ho | He | | | |
| Leggieri and Haouari (2017) | R | Pr. | Unlim. | S | P | L | L | AFVs | | 2 | MILP | – |
| Andelmin and Bartolini (2017) | R | Pr. | Unlim. | S | F | – | L | AFVs | | 2 | An exact algorithm | – |
| Sassi and Oulamara (2017) | Sch | Pr. | Lim. | S | P | L | - | | EVs, ICEVs | 2, 11 | Several heuristic procedures | Deg. |
| Paz et al. (2018) | R | Pr. | Unlim. | BSS | F | ◇ ◇ ◇ ◇ | L | EVs | | 1, 2, 9 | MILP | TW |
| Li et al. (2018) | R | Pr. | Unlim. | S, WCS | P | L | L | EVs | | 3, 11 | MILP | – |
| Wang et al. (2018) | R | Pr. | Unlim. | BSS | F | – | L | EVs | | 15 | Heuristic procedures | TW |
| Zhang et al. (2018a) | R | Pr. | Unlim. | S | F | – | NL | EVs | | 11 | AC and ALNS | – |
| Schiffer and Walther (2018b) | R | Pr. | Unlim. | S | P | L | L | EVs | | 1, 3, 9 | ALNS, DP | TW |
| Zhang et al. (2018b) | R | Pr. | Unlim. | S | P | L | L | EVs | | 1, 2, 3, 11, 12 | TS | TW |
| Keskin and Çatay (2018) | R | Pr. | Unlim. | M | P | L | L | EVs | | 1, 11 | ALNS based matheuristic | TW |
| Villegas et al. (2018) | R | Pr. | Unlim. | M | P | NL | L | EVs,ICEVs | | 1, 2, 10, 11 | GRASP based matheuristic | TW |
| Masmoudi et al. (2018) | R | Pr. | Unlim. | BSS | – | – | ◇ | | EVs | 2 | EVO-VNS | TW |
| Madankumar and Rajendran (2018) | R | Pr. | Unlim. | S | F, P | – | L | AFVs | | 2 | MILP | TW |
| Koç et al. (2018) | R | Pr. | Unlim. | M | P | NL | L | EVs | | 3, 9 | ALNS based matheuristic | TW, Loc. |
| Rinaldi et al. (2018) | Sch | Pr. | Lim. | S | F | - | - | | EVs,PHEVs | 6, 11, 14 | MILP | TW |
| Kouider et al. (2018) | R | Pr. | Unlim. | S | P | - | L | EVs | | 2, 10 | Several heuristics | Per. |
| Pelletier et al. (2018) | Sch | Pr. | Lim. | M | P | NL | - | EVs | | 11, 13 | MILP | Per., Deg. |
| Bruglieri et al. (2019b) | R | Pub. | Lim. | S | F | – | L | AFVs | | 2 | An exact method | – |
| Jie et al. (2019) | R | Pr. | Unlim. | BSS | P | – | L | | EVs | 2, 4, 8 | Hybrid CG and ALNS | – |
| Macrina et al. (2019) | R | Pr. | Unlim. | S | P | L | L | EVs,ICEVs | | 2, 11 | ILS | TW |
| Hiermann et al. (2019) | R | Pr. | Unlim. | S | P | L | L | | EVs,ICEVs,PHEVs | 1, 7, 11 | GA, LNS with IP solver | TW |
| Bruglieri et al. (2019a) | R | Pr. | Unlim. | S | F | – | L | AFVs | | 2 | PBA | – |
| Keskin et al. (2019) | R | Pub. | Lim. | S | P | NL | L | EVs | | 2, 4, 11, 14 | ALNS based matheuristic | TW |
| Froger et al. (2019a) | R,S | Pub. | Lim. | M | P | NL | L | EVs | | 3 | Two-stage matheuristic | – |
| Froger et al. (2019b) | R | Pr. | Unlim. | M | P | NL | L | EVs | | 3 | MILP | – |
| Kopfer and Vornhusen (2019) | R | Pr. | Unlim. | S | P | L | NL | | EVs, ICEVs | 6 | MILP | TW |
| Breunig et al. (2019) | R | Pr. | Unlim. | S | F | L | L | EVs | | 1, 2 | LNS, Exact algorithm | – |
| Kullman et al. (2020) | R | Pub. | Lim. | S | P | NL | L | EVs | | 3 | Several exact and heuristic methods | – |

◇ ◇ ◇ ◇ linear, constant for battery swapping and parallel with service time

# Chapter 3

# Approximating the battery degradation function

Ce chapitre fournit des éléments de modelisation de la dégradation des batteries au lithium-ion (li-ion), l'une des technologies les plus généralement utilisées pour les VE. Le chapitre souligne l'importance de prendre en compte cette dégradation tant du point de vue économique qu'environnemental. En outre, nous attirons l'attention sur les effets de la dégradation accélérée des batteries sur la durabilité des opérations de distribution des VE. Ensuite, nous présentons les modèles de dégradation des batteries les plus représentatifs trouvés dans la littérature. La modélisation de la dégradation des batteries est très complexe, en raison des processus électrochimiques qu'elle implique et de l'interrelation des facteurs qui l'accélèrent. Pour cette raison, les modèles doivent être approximés pour être incorporés dans les modèles. Nous fournissons la procédure que nous avons suivie pour approximer la fonction de dégradation de la batterie en tant que coûts de dégradation de la batterie qui peuvent être facilement inclus dans les E-VRPs. Ces coûts sont composés des coûts fixes (de charge) et des coûts d'usure cumulées associés aux opérations de charge et aux itinéraires. Les coûts fixes sont destinés à pénaliser le nombre de charges et à utiliser la charge rapide et peuvent être facilement calculés avec seulement le prix du bloc de batteries et le taux de charge. La fonction de coût d'usure cumulée a été obtenue en utilisant le modèle de Han et al. (2014). Ce modèle calcule le coût d'usure par unité d'énergie chargée ou déchargée en fonction du pourcentage de la capacité disponible de la batterie. Pour faciliter son inclusion dans un modèle, nous proposons une fonction qui met en correspondance l'énergie chargée ou déchargée sur un intervalle de temps défini avec le coût d'usure entraîné. À des fins de modélisation, nous avons approché cette fonction par une fonction linéaire par morceaux qui s'avère adéquate pour représenter le coût d'usure cumulé. Les coûts de dégradation des batteries sont utilisés dans la suite de cette thèse.

## 3.1 Introduction

Lithium-ion (li-ion) battery is one of the most widely used technologies in EV. It offers high energy density, power and cell voltage, low memory effect and self-discharge, and good cycle life (Notter et al., 2010; Dunn et al., 2011; Majeau-Bettez et al., 2011). In fact, the 2019 Nobel Prize in Chemistry was awarded to John Goodenough, M. Stanley Whittingham and Akira Yoshino for the development of this type of batteries. Li-ion batteries are also widely used to power portable electronics and their introduction laid the foundation of a wireless, fossil fuel-free society (NobelPrize.org, 2019). Research on other battery technologies, such as lithium–sulfur (Li–S), zinc-air (Zn-air) and lithium-air (Li-air), has not yet succeeded in beating li-ion battery's high capacity and voltage (Fotouhi et al., 2016; Greim et al., 2020; Yong et al., 2015).

Li-ion batteries, however, have a limited useful life due to their degradation mechanisms. This physiochemical process, inherent to battery functioning, may be accelerated by some storage and operating conditions (Pelletier et al., 2017). This is especially critical since the battery is the most expensive component of an EV. Indeed, battery packs price represents between 30 and 40% of the final EV price (Casals et al., 2017). This cost is, however, falling faster than expected. By 2025, it is expected that the cost will have been reduced to 20% of total EV cost (Bullard, 2019).

Since battery prices continue falling, the careful management of a battery to reduce degradation, avoiding premature disposal and replacement, may not be critical from the economic perspective in some years. Nevertheless, from the environmental point of view, such disposal and replacement is not desirable. Even though spent li-ion batteries are not generally considered as dangerous waste, they contain flammable and toxic substances that lead to a risky disposal (Lv et al., 2018). Lithium recycling strategies, as an alternative to disposal, are in their early stages and are seldom produced in industrial scale (Liu et al., 2019; Lv et al., 2018; Sonoc et al., 2015; Wanger, 2011). Regarding the production of new batteries, the extraction of materials has negative consequences on the reserves of metal resources and the environment. Moreover, lithium exploitation is detrimental to local human health and biodiversity, and larger mining operations will increase this problem (Wanger, 2011; Zeng et al., 2014). Parallel consequences can be seen in the extraction of other metals for these batteries such as ferrite, manganese and copper (McManus, 2012; Zeng et al., 2014).

Li-ion battery demand is expected to increase more than ten-fold by 2029 (MINING.COM, 2020). Although there are still plenty of lithium reserves, a balance of lithium supply and demand throughout this century depends on several conditions such as the development of better recycling systems and the reduction of material demand per battery capacity (Greim et al., 2020). The latter implies, besides the improvement of li-ion batteries technology and the development of new battery chemistries, the search for strategies that prevent premature excessive battery wear.

Regarding EVs operation, battery degradation leads to capacity fade and power fade. The capacity fade reduces the vehicle's range and the power fade decreases its efficiency (Uddin et al., 2014; Pelletier et al., 2016). A battery is commonly said to reach its end of life for vehicle applications when it has reduced its available capacity or maximum power

by 20% of its original value. Generally, the capacity loss is the reference condition as the initial power of the battery is superior to the vehicle's needs (Lam, 2011). Battery aging and replacement over an EV lifetime adversely impact EV performance and durability (Uddin et al., 2014). This in turn affects the long-term flexibility and the sustainability of the distribution operations with EVs (Pelletier et al., 2017).

The above-mentioned situations make evident the need to consider battery degradation concerns in transportation planning with EVs. However, battery degradation modeling is very complex due to the electrochemical processes involved in it and the interrelation of the factors that accelerate its aging (Vetter et al., 2005). Battery degradation models use non-linear functions, interactions between variables and multiple parameters that make their inclusion in optimization strategies a challenging task (Abdulla et al., 2018). In order to formulate E-VRPs to be solved using optimization solvers, battery degradation models must be approximated. In this chapter we present the procedure we followed to approximate the battery degradation function. Sections 3.2 and 3.3 provide a short overview of the li-ion battery degradation process and modelling approaches. Based on models presented in Section 3.3, we obtained battery degradation costs that can be easily incorporated to E-VRPs. The procedure is presented in Section 3.4. Battery degradation costs are composed by (charging) fixed costs and cumulative wear costs associated with charging operations and routes. We approximate the latter using piecewise linear functions.

## 3.2 Lithium-ion battery degradation

Battery degradation takes place during storage, charging and discharging. The process of charging and discharging a battery is called a cycle. The degradation during storage, named calendar aging, is measured through the calendar life of the battery. Specifically, it refers to the number of years during which the battery can remain stored, losing capacity, before it gets to its end of life. The degradation that takes place while cycling, named cycle aging, is measured through the cycle life of the battery, that is, the number of cycles a battery can undergo before it reaches its end of life (Pelletier et al., 2017).

Battery aging is due to several physical and chemical processes that interact with each other (for an overview of these processes the reader is referred to Pelletier et al. 2017). This interaction makes the modelling very difficult (Vetter et al., 2005). Nevertheless, battery deterioration is worsened by some operating and storage conditions that can be more easily included in E-VRPs . Literature agrees that the most important stress factors are: high and low temperatures, high SOC while the battery is stored, large DOD, high charging and discharging rates, overcharging and over-discharging (see, for example, Wohlfahrt-Mehrens et al. 2004; Wang et al. 2011; Baghdadi et al. 2016; Bordin et al. 2017; Pelletier et al. 2017; Xu 2013; Omar et al. 2014; Sarasketa-Zabala et al. 2014, 2015). These stress factors can be included in a battery degradation model without delving into the electrochemistry of the battery.

Table 3.1: Key elements of presented battery degradation models. Source: Pelletier et al. (2017)

| Source | Stress factors | Type of aging | Model output |
|---|---|---|---|
| Wang et al. (2011) | Temperature, C-rate, charge throughput | Cycle aging | Remaining capacity |
| Peterson et al. (2010) | Energy throughput | Cycle aging | Remaining capacity |
| Sarasketa-Zabala et al. (2015) | DOD, charge throughput | Cycle aging | Remaining capacity |
| Sarasketa-Zabala et al. (2014) | Temperature, SOC | Calendar aging | Remaining capacity |
| Xu (2013)* | DOD, SOC, C-rate, temperature, time | Cycle and calendar aging | Remaining capacity |
| Hoke et al. (2011)** | Temperature, SOC, DOD, energy throughput | Cycle and calendar aging | Daily battery degradation cost |
| Omar et al. (2014) | Temperature, C-rate, DOD | Cycle aging | Number of achievable cycles before end of life |
| Han et al. (2014)*** | DOD | Cycle aging | Wear cost per unit of energy transferred to/from battery |

C-rate: the measure of the speed at which the battery is charged relative to its maximum capacity. For example, a 1C-rate means that an empty battery can be charged in 1 hour.
Parameters calibrated for lithium iron phosphate batteries.
Exceptions:
* for lithium manganese oxide.
** for lithium nickel cobalt aluminium oxide.
*** for any battery type.

## 3.3 Battery degradation models

There are three modelling approaches for battery degradation: electrochemical, empirical and semi-empirical. Electrochemical models rely on theory to capture physical processes that cause degradation. They are the most precise but are too complex to be included in an optimization framework (Abdulla et al., 2018; Pelletier et al., 2017). Empirical models use experimental measurements to relate battery aging with factors that cause it, but are subjected to specific experimental conditions and large amounts of data (Xu, 2013; Muenzel et al., 2015). Semi-empirical models combine both theoretical models and experimental data to fit parameters to the models. They are simpler than electrochemical models and more adaptable for use in different conditions than empirical models (Pelletier et al., 2017). Since electrochemical models are very complex, we focus our attention on empirical and semi-empirical models. Pelletier et al. (2017) gathered the most relevant models for transportation planning. Table 3.1 presents the key elements of these models, such as the stress factors they consider, the type of aging and the output. Models are mostly focused on capacity fade because power fade of li-ion batteries is not problematic for EVs.

## 3.4 Obtaining the battery degradation costs

We focus battery degradation modeling on cycle aging since it is more directly related to charging and routing decisions. We preferred an empirical approach that can be easily integrated to E-VRPs. The operating parameters that affect cycle aging include temperature, charging rate, and SOC (Han et al., 2014). Considerations about temperature control go beyond the usual components for VRPs and so we disregard them. We use models that transform the nonlinear relationship between battery degradation and the remaining parameters into costs, so that degradation is easier to interpret. The greater the degradation, the greater the cost.

### 3.4.1 Fixed costs

The charging rate is the measure of the speed at which the battery is charged relative to its maximum. The unit of measure is called C-rate. For example, a 1 C-rate means that an empty battery can be charged in one hour. High C-rates represent higher power, faster charging and discharging, and more stress on the battery.

The charging rate has a strong impact on cycle aging (Omar et al., 2014). To model this, we introduce the fixed cost $u_{ch}$ (in USD \$) that translates into a monetary cost the battery degradation attributable to charging with a given charging rate $ch$ (in C-rate). $u_{ch}$ reflects the decrease of the battery capacity due to the charging rate applied. The faster the rate, the larger the cost. To set $u_{ch}$ we rely on the model presented by Omar et al. (2014). These authors conducted cycle life tests to examine the influence of the charging rate in cycle aging. The tests were performed on lithium iron phosphate based battery cells, a li-ion battery largely used for EVs (Satyavani et al., 2016). Based on the results of their tests, Omar et al. (2014) obtained the following relationship:

$$CL(ch) = 5963\exp(-0.6531ch) + 321.4\exp(0.03168ch) \tag{3.1}$$

where $CL(ch)$ is the number of times the cell can be charged at a constant C-rate of $ch$ and fully discharged at a 1 C-rate before the end of its life. Using a procedure similar to the one presented by Arslan et al. (2015), we compute $u_{ch}$, as follows:

$$u_{ch} = \frac{1}{CL(ch)}BP \tag{3.2}$$

where $BP$ corresponds to the cost of the battery pack in USD ($).

### 3.4.2 Cumulative wear costs

We computed the cumulative wear costs using the semi-empirical model for EV charging applications introduced by Han et al. (2014). The model computes the wear cost per unit of energy charged or discharged depending on the SOC of the battery. Specifically, let $\xi$ be the SOC of the EV, the wear cost $W(\xi)$ per unit of energy charged or discharged is presented in Equation (3.3)

$$W(\xi) = \frac{BP}{2 \times BS \times \mu^2} \times \frac{\mathfrak{b}(1-\xi)^{\mathfrak{b}-1}}{\mathfrak{a}} \tag{3.3}$$

where $BP$ is the cost of the battery pack in USD ($), $BS$ is the capacity of the battery pack in kWh, $\mu$ is the cycle efficiency, and $\mathfrak{a}$ and $\mathfrak{b}$ are battery-dependent parameters. The cycle efficiency is the ratio of the discharge percentages of two successive cycles. Parameters $\mathfrak{a}$ and $\mathfrak{b}$ can be obtained by curve fitting of battery cycle aging test data. For example, Choi and Kim (2016) find these values for three different types of batteries.

To compute the wear cost related with the energy charged or discharged over a defined time interval, we calculated the indefinite integral of $W(\xi)$ in Eq. (3.4). We call this integral the cumulative wear cost function, $\mathcal{W}(\xi)$. This function maps the SOC $\xi$ to the sum of the wear cost associated to charging the battery to every SOC from 0% to $\xi$ or discharging it from every SOC $\xi$ to 0%.

$$\mathcal{W}(\xi) = \frac{BP}{2 \cdot BS \cdot \mu^2 \cdot \mathfrak{a}}(1 - (1-\xi)^{\mathfrak{b}}) \tag{3.4}$$

For modeling purposes, we approximate the cumulative wear cost function by fitting a regression model with segmented relationships (Muggeo, 2003). We fit a piecewise linear approximation of (3.4) for a 16 kWh li-ion battery with cycle efficiency of 0.95, parameters $\mathfrak{a} = 694$ and $\mathfrak{b} = 0.795$ and a price of $6560. We obtained a model with three breakpoints with an adjusted $R^2 = 0.99$. We also tested for a significant difference-in-slope by performing the Davies' test. The test rejected the null hypothesis of not having breakpoints at 1% level. This result supports our claim of the adequacy of a piecewise linear function to approximate the cumulative wear cost function. Fig. 3.1 presents the piecewise linear approximation.

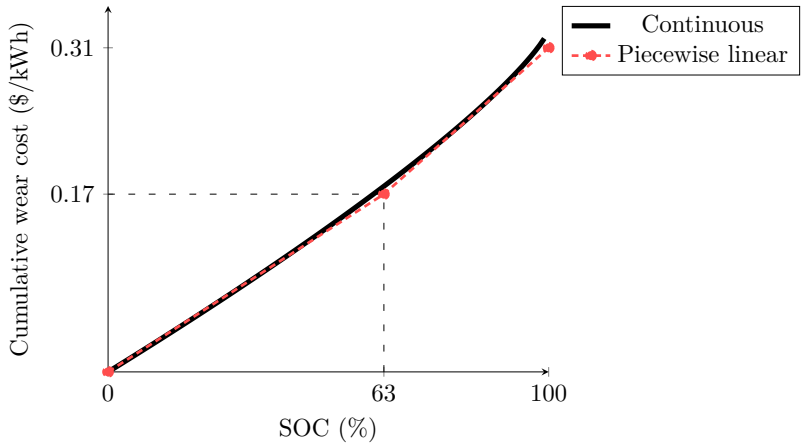


**Fig. 3.1.** Cumulative wear cost vs. piecewise linear approximation for a 16 kWh, $6560 li-ion battery with $\mathfrak{a} = 694$, $\mathfrak{b} = 0.795$ and $\mu = 0.95$. Parameters $\mathfrak{a}$ and $\mathfrak{b}$ taken from Han et al. (2014).

### 3.4.3 Example

We provide a numerical example illustrating how the battery degradation costs are computed. Consider an EV with a 16kWh li-ion battery with a price of $6560. The EV can be charged using two charging rates: 0.25 C-rate or 0.5 C-rate. The calculation for the fixed costs using (3.2) yields $1.22 for 0.25 C-rate and $1.42 for 0.5 C-rate. Additionally, the piecewise linear cumulative wear cost function is as presented in Fig. 3.1. For computing the cumulative wear cost in monetary units, it suffices to multiply the cost obtained by the EV battery capacity (16kWh). Table 3.2 provides the battery degradation costs incurred in four EV charging scenarios. The scenarios result from a combination of two options for the charging rate, 0.25 C-rate or 0.5 C-rate, and two options for the initial energy of the EV, 0% or 75% of the battery capacity. In all scenarios, the battery is charged 25% of its capacity.

Table 3.2: Computation of the battery degradation costs for an EV with a 16kWh battery being charged in four EV charging scenarios

| | Scenario | | | |
|---|---|---|---|---|
| | 1 | 2 | 3 | 4 |
| Charging rate (C-rate) | 0.25 | 0.25 | 0.5 | 0.5 |
| SOC charging interval | 0%-25% | 75%-100% | 0%-25% | 75%-100% |
| (1) Fixed cost ($) | 1.22 | 1.22 | 1.42 | 1.42 |
| Cumulative wear cost ($/kWh) | 0.07 | 0.09 | 0.07 | 0.09 |
| (2) Cumulative wear cost ($) | 1.07 | 1.51 | 1.07 | 1.51 |
| Total ($): (1)+(2) | 2.29 | 2.73 | 2.49 | 2.93 |

# Chapter 4

# The Multi-period Electric Vehicle routing problem

Dans ce chapitre, nous présentons et définissons formellement le MP-E-VRP. Le MP-E-VRP consiste à concevoir des itinéraires à effectuer par une flotte de VE pour desservir un ensemble de clients sur un horizon de planification de plusieurs périodes. Les VE sont chargés au dépôt à tout moment, sous réserve des contraintes de capacité de l'infrastructure de chargement. En raison de l'impact des pratiques de charge et d'acheminement sur le vieillissement des batteries des VE, des coûts de dégradation sont associés aux opérations de charge et aux itinéraires. Le chapitre 3 décrit comment ces coûts sont obtenus. L'objectif du MP-E-VRP est de déterminer, pour chaque période, un ensemble d'itinéraires visitant tous les clients et de programmer les opérations de charge des VE tout en minimisant les coûts de dégradation. Le MP-E-VRP intègre le routage des VE et la programmation de la recharge au dépôt, et comporte des contraintes de couplage entre les jours. Ces caractéristiques font du MP-E-VRP un problème complexe à résoudre. Nous fournissons une formulation PLNE en temps continu en utilisant des variables de suivi basées sur les arcs. Notre formulation utilise des modèles de flot pour tenir compte des contraintes de capacité du réseau électrique et de l'infrastructure de charge, et des modèles de combinaison convexe pour représenter le coût d'usure cumulé et les fonctions de charge. Nous présentons ensuite la procédure que nous avons suivie pour générer des instances pour le MP-E-VRP. Les résultats des calculs indiquent que, généralement, le modèle ne peut pas être utilisé directement pour résoudre des cas réalistes. En effet, un solveur commercial MILP est incapable de résoudre de manière optimale les petites instances generées (3 périodes et 10 clients par période) après 3 heures, et l'écart par rapport aux bornes supérieures les plus connues est encore très important. Cette formulation MILP nous permet d'avoir une idée de la difficulté du problème et de la pertinence de concevoir des stratégies plus complexes. Le chapitre 5 rend compte des différentes stratégies mises en œuvre pour résoudre le MP-E-VRP.

## 4.1 Introduction

In this chapter we introduce the Multi-period Electric Vehicle Routing Problem (MP-E-VRP). The MP-E-VRP integrates routing and depot charging scheduling over a planning horizon of several periods. We present the problem in Section 4.2 and a numerical example in Section 4.3. Afterwards, in Section 4.4, we provide a mixed integer linear programming (MILP) formulation using arc-based tracking variables. We perform computational experiments in small-size instances of the MP-E-VRP to test the performance of the MILP formulation. Results are shown in Section 4.5.

Notice that all the main notations used throughout this chapter are summarized in Appendix A.

## 4.2 Problem statement

We define the MP-E-VRP as follows. Let $\mathcal{P} = \{0, \ldots, P_{max} - 1\}$ be the set of periods within the planning horizon. Let $\mathcal{I}$ be the set of customer nodes and 0 a node representing the depot. Each node $i \in \mathcal{I}$ represents a customer with a service time $\delta_i > 0$ and a period $p_i \in \mathcal{P}$ in which the service must take place. A finite set of homogeneous EVs denoted by $\mathcal{K}$ is available to visit the nodes in $\mathcal{I}$. Each EV $k \in \mathcal{K}$ has a battery capacity $Q$ (in kWh). Travelling from one location $i$ (the depot or a visit node) to another location $j$ incurs a driving time $t_{ij} \geq 0$ (in hours) and an energy consumption $e_{ij} \geq 0$ (in kWh). The triangular inequality holds for driving times and energy consumptions. At period $p \in \mathcal{P}$, an EV cannot leave the depot before $E_p$ or return after $L_p$ (with $L_p > E_p$). In other words, time interval $[E_p, L_p]$ corresponds to the opening hours of the depot for period $p \in \mathcal{P}$. The time interval $[L_{p-1}, E_p]$ is called *intershift window*; it corresponds to the closing hours of the depot between periods $p-1$ and $p$, with $p \in \mathcal{P} \setminus \{0\}$. For period 0, the *intershift window* is the time interval $[0, E_0]$. We denote $T = L_{P_{max}-1}$ the ending time of the planning horizon.

At the beginning of the planning horizon each EV $k \in \mathcal{K}$ has an energy $Q_0^k$ (in kWh). The EVs can be fully or partially recharged at the depot at any time. There is no possibility to recharge an EV outside of the depot. The EVs can only perform one route per period and they are allowed to be recharged only once between two routes. Multiple chargers are available at the depot. Each charger is associated with a charging mode (e.g., slow, fast, moderate) belonging to set $\mathcal{M}$. The depot has $A_m$ available chargers for each charging mode $m \in \mathcal{M}$ (usually, but not necessarily, $\sum_{m \in \mathcal{M}} A_m < |\mathcal{K}|$). During a charging operation, a charger of mode $m$ consumes a power $v_m$ (in kW) from the grid. An EV can be recharged using any available charger, but at any time the power grid capacity $PW_{max}$ must not be exceeded. For instance, if the depot has only one charging mode $m$ (with $A_m >> 3$) requiring a power of 11 kW and the power grid capacity $PW_{max}$ is 42 kW, only three EVs can be simultaneously charged. Moreover, it is forbidden to switch the charging mode while charging an EV. Charging operations are also non-preemptive (i.e. they cannot be interrupted and resumed later). Each charging mode is associated with a fixed cost per charge $u_m$ and a charging function $g_m(\Delta)$. The fixed cost per charge $u_m$ represents the influence of the charging mode on the battery degradation, as it is explained

in Section 3.4.1.

$g_m(\Delta)$ maps, for an empty battery, the time $\Delta$ spent charging with a charger of mode $m$ to the final SOC of the battery. We refer to the SOC of a battery as the SOC of the EV that is equipped with that battery. If $SOC_{ini}$ is the SOC of an EV, then the SOC of this EV upon finishing charging during a time equal to $\Delta$ is given by $g_m(\Delta + g_m^{-1}(SOC_{ini}))$. Following the conventions in the literature (Montoya et al., 2017), we assume that $g_m(\Delta)$ is a concave piecewise linear function. Charging function $g_m(\Delta)$ has an ordered set of breakpoints $B_m = \{0, \ldots, b_m\}$. Let $c_b$ and $a_b$ be the charging time and the SOC of breakpoint $b \in B_m$. Fig. 4.1 depicts the piecewise linear approximation of the charging function for a charger yielding a power of 11 kW and charging an EV equipped with a 16 kWh-battery. The battery pack consists of several 3.2 volts-40 Ah li-ion battery cells. The nonlinear charging function is modelled using the considerations presented in Pelletier et al. (2017) and data taken from Marra et al. (2012).

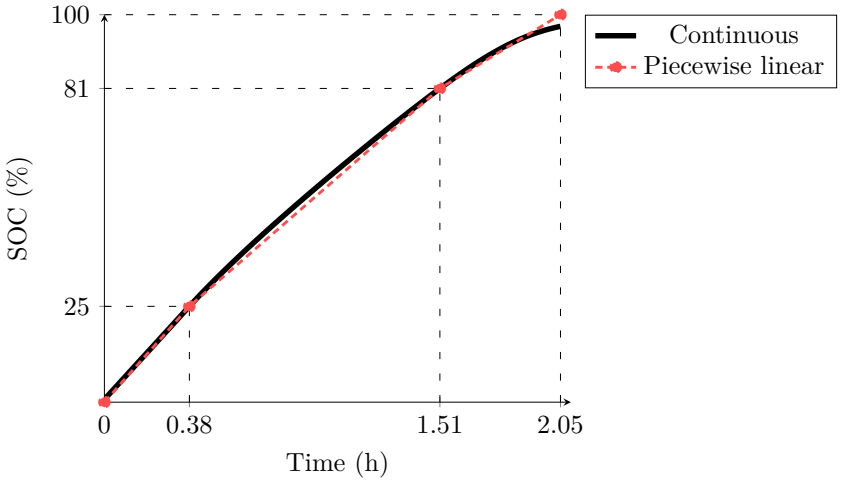


**Fig. 4.1.** Nonlinear charging function vs. piecewise linear approximation for a charger yielding a power of 11 kW charging a 16 kWh li-ion battery. Data taken from Marra et al. (2012).

$\mathcal{W}(\xi)$ is a cumulative wear cost function associated with charging operations and routes (see Section 3.4.2 for the procedure to obtain this function). When an EV is recharged from an initial SOC $\xi_{ini}$ to a final SOC $\xi_{final}$, a cumulative wear cost $\mathcal{W}(\xi_{final}) - \mathcal{W}(\xi_{ini})$ is incurred. Similarly, when an EV performs a route, discharging the battery from an initial SOC $\xi'_{ini}$ to a final SOC $\xi'_{final}$, a cumulative wear cost $\mathcal{W}(\xi'_{ini}) - \mathcal{W}(\xi'_{final})$ is incurred. We approximate $\mathcal{W}(\xi)$ by a piecewise linear function with an ordered set of breakpoints $\Pi = \{0, \ldots, \beta\}$. Let $l_\beta$ and $n_\beta$ be the SOC and the cumulative wear cost of breakpoint $\beta \in \Pi$. Let $\zeta_\beta$ be the slope of the segment between $l_{\beta-1}$ and $l_\beta$ (i.e. $\zeta_\beta = (n_\beta - n_{\beta-1})/(l_\beta - l_{\beta-1})$).

Feasible solutions to the MP-E-VRP satisfy the following conditions: 1) each node $i \in \mathcal{I}$ is visited by a single EV in period $p_i$, 2) each route starts and ends at the depot, 3) each EV can perform one route per period, 4) when an EV starts a route, it must have

enough energy to complete it (no mid-route charging is allowed), 5) no more than $|\mathcal{K}|$ EVs are used on a single period, 6) EVs visit nodes in $\mathcal{I}$ in period $p_i \in \mathcal{P}$ only during time window $[E_{p_i}, L_{p_i}]$, 7) the power consumed by all chargers at any time does not exceed the maximum power $PW_{max}$, and 8) no more than $A_m$ EVs simultaneously charge at the depot using mode $m \in \mathcal{M}$.

The objective of the MP-E-VRP is to determine for each period a set of routes visiting all the customers and to schedule the charging operations of the EVs while minimizing the cost of battery degradation. This cost is defined as the sum of the fixed costs of all charging operations and the cumulative wear costs associated with all charging operations and routes.

## 4.3 Example

Fig. 4.2 provides a numerical example illustrating the MP-E-VRP. The figure shows the planning of the routes and the charging operations of two 8-hour working shifts for an EV with a 16 kWh li-ion battery visiting 4 customers per shift. The *intershift window* between shifts is zero for each working shift. The depot is equipped with two chargers of different modes: a charger of slow mode with charging power of 6 kW and fixed cost of \$1.22, and a charger of moderate mode with charging power of 11 kWh and fixed cost of \$1.42. The piecewise linear cumulative wear cost function for the battery is the one presented in Fig. 3.1. Fig. 4.2a shows the routes performed by the EV, along with the driving time (in hours) and the energy consumed (in kWh) when travelling from one location (a customer, the depot) to another. Fig. 4.2b presents the evolution of the EV's SOC through the working shifts. Horizontal lines indicate a service time in each visited customer. Table 4.2c describes the different costs associated with the battery degradation. In this example, the EV performs two charging operations, each one with a different charger. The EV starts with an initial energy of 4.8 kWh, corresponding to a SOC of 30%, and is charged with the slow mode charger up to 96%, incurring a fixed cost of \$1.22 and an cumulative wear cost of \$3.47. Then, it performs a route visiting customers of the first shift and arrives at the depot with a SOC of 26%. In this route the EV incurs a cumulative wear cost of \$3.65. Then, it is charged with the moderate mode charger up to 87%, incurring a fixed cost of \$1.42 and an cumulative wear cost of \$3.10. Finally, it performs a route visiting customers of the second shift and arrives at the depot with $\epsilon \approx 0\%$ of the battery. In this route the EV incurs a cumulative wear cost of \$4.25. The sum of the fixed costs of the charging operations is \$2.64 and the sum of the cumulative wear costs associated with the charging operations and routes is \$14.48, yielding a total cost of battery degradation of \$17.12.

## 4.4 MILP formulation

The MP-E-VRP is defined on a multigraph $\mathcal{G} = (\mathcal{V}, \mathcal{A})$, where $\mathcal{V}$ is the set of nodes and $\mathcal{A}$ is the set of arcs connecting the nodes. The set $\mathcal{V}$ contains the set of visit nodes $\mathcal{I}$, a set of depot nodes $\mathcal{D}$ and a set of charging nodes $\mathcal{C}$. Let $\mathcal{I}_p$ be the set of visit nodes in each period $p \in \mathcal{P}$ ($\mathcal{I}_p = \{i \in \mathcal{I} : p_i = p\}$ and $\mathcal{I} = \bigcup_{p \in \mathcal{P}} \mathcal{I}_p$). The set of depot nodes $\mathcal{D}$ is

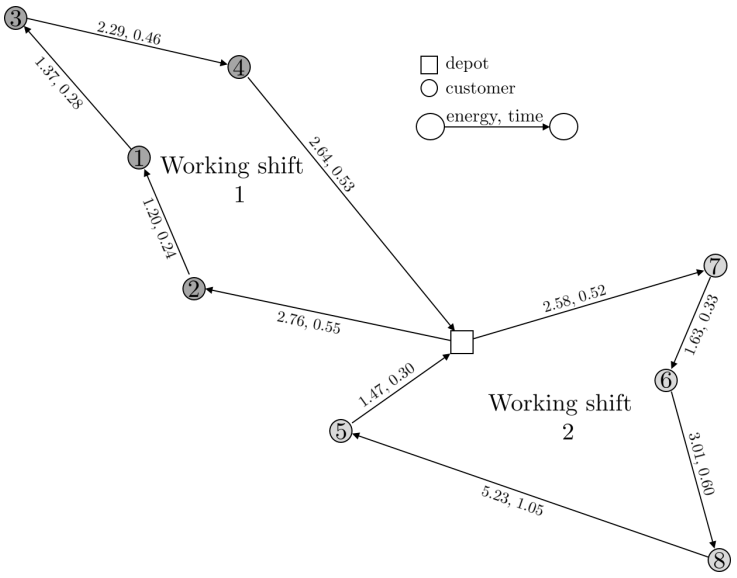


(a) Routes performed by the EV during the planning horizon

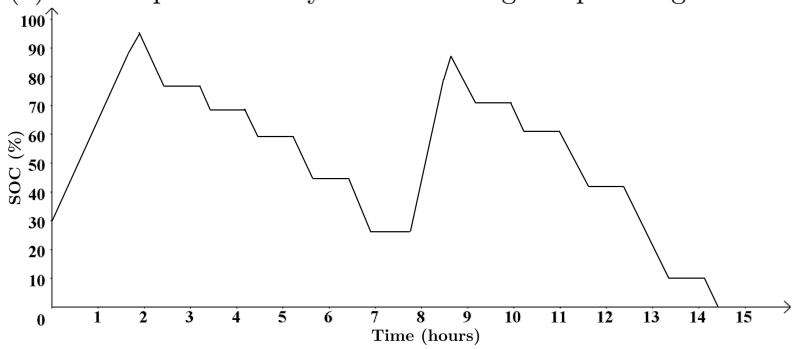


(b) Evolution of the SOC of the EV through the planning horizon

| | Charging operation 1 | Route 1 | Charging operation 2 | Route 2 | Total ($) |
|---|---|---|---|---|---|
| Fixed cost ($) | 1.22 | - | 1.42 | - | 2.64 |
| Cumulative wear cost ($) | 3.47 | 3.65 | 3.10 | 4.25 | 14.48 |
| Total ($) | 4.69 | 3.65 | 4.52 | 4.25 | 17.12 |

(c) Computation of the objective function

**Fig. 4.2.** Illustration of the charging process and the computation of the costs associated with battery degradation for an EV with a 16 kWh battery performing two 4-customers routes in two 8-hour working shifts.

composed of a set of starting depots $\mathcal{D}^{start}$ and a set of ending depots $\mathcal{D}^{end}$ that represent the depot at the beginning and end of each period. Specifically, we denote $d_p^{start} \in \mathcal{D}^{start}$ the starting depot node for period $p \in \mathcal{P}$ and $d_p^{end} \in \mathcal{D}^{end}$ the ending depot node for period $p \in \mathcal{P} \cup \{-1\}$. The number of charges an EV can perform during the time horizon is limited by $P_{max}$ since an EV can charge at most once between two routes and only one route can be performed by period. Let $\mathcal{H} = \{0, \ldots, P_{max} - 1\}$ be a totally ordered set that enumerates the charging operations an EV can perform during the time horizon. Let $\mathcal{C}_h$ be a set that contains $|\mathcal{M}|$ charging nodes associated with charge $h \in \mathcal{H}$ (each charging node is associated with a charge number and a mode). The set of charging nodes $\mathcal{C}$ is defined as the union of sets $\mathcal{C}_h$. Each EV $k$ has a related set of arcs $\mathcal{A}_k$ such that $\mathcal{A} = \cup_{k \in \mathcal{K}} \mathcal{A}_k$. At the risk of abusing notation, every arc $(i,j)^k \in \mathcal{A}_k$ has an associated driving time $t_{ij}$ and an energy consumption $e_{ij}$, related with the values presented in Section 4.2. We formally define $\mathcal{A}_k$ as presented in Table 4.1.

Table 4.1: Definition of the arcs in $\mathcal{A}_k \subset \mathcal{A}$, $k \in \mathcal{K}$, in $\mathcal{G} = (\mathcal{V}, \mathcal{A})$ for the MP-E-VRP

| Definition | Driving time ($t_{ij}$) | Energy consumption ($e_{ij}$) |
|---|---|---|
| $(i,j)^k : p \in \mathcal{P}, i,j \in \mathcal{I}_p, i \neq j$ | $t_{ij}$ | $e_{ij}$ |
| $(d_p^{start}, i)^k : p \in \mathcal{P}, i \in \mathcal{I}_p$ | $t_{0i}$ | $e_{0i}$ |
| $(i, d_p^{end})^k : p \in \mathcal{P}, i \in \mathcal{I}_p$ | $t_{i0}$ | $e_{i0}$ |
| $(d_{p-1}^{end}, d_p^{start})^k : p \in \mathcal{P}$ | 0 | 0 |
| $(d_{p-1}^{end}, d_p^{end})^k : p \in \mathcal{P}$ | 0 | 0 |
| $(d_p^{end}, l)^k : p \in (\mathcal{P} \setminus \{P_{max} - 1\}) \cup \{-1\}, l \in \bigcup_{h \leq p+1} \mathcal{C}_h$ | 0 | 0 |
| $(l, d_p^{start})^k : p \in \mathcal{P}, l \in \bigcup_{h \leq p} \mathcal{C}_h$ | 0 | 0 |

For illustrative purposes, Fig. 4.3 shows the graph $\mathcal{G}$ obtained for an instance associated with the example described in Fig. 4.2, with one EV. Charging mode *slow* represents the 6 kW charger and charging mode *moderate* represents the 11 kW charger. Different types of nodes are represented by different shapes. Nodes belonging to different periods are portrayed in grayscale. Charging nodes present both the associated charging mode (*slow*, *moderate*) and the charge number.

We now introduce a MILP formulation for the MP-E-VRP.

Binary variable $x_{ij}^k$ is equal to 1 if EV $k$ travels on arc $(i,j)^k \in \mathcal{A}_k$, and 0 otherwise. Let $\mathcal{O}$ be the set of all charging operations that can be performed within the planning horizon. Charging operation $o \in \mathcal{O}$ is associated with an EV and a charging node (i.e. with a charge number and a charging mode). Continuous variable $\gamma_o$ accounts for the cumulative wear cost for charging operation $o \in \mathcal{O}$. Continuous variable $\varepsilon_p^k$ accounts for the cumulative wear cost for the route performed by EV $k$ in period $p$. The objective function (4.1) seeks to minimize the cost of battery degradation. This cost is composed of the fixed costs related to the charging operations and the cumulative wear cost associated with charging operations and routes.

$$\text{Minimize} \sum_{k \in \mathcal{K}} \sum_{i \in \mathcal{C}} \sum_{(i,j)^k \in \mathcal{A}_k} u_{m(i)} x_{ij}^k + Q \sum_{o \in \mathcal{O}} \gamma_o + Q \sum_{p \in \mathcal{P}} \sum_{k \in \mathcal{K}} \varepsilon_p^k \tag{4.1}$$

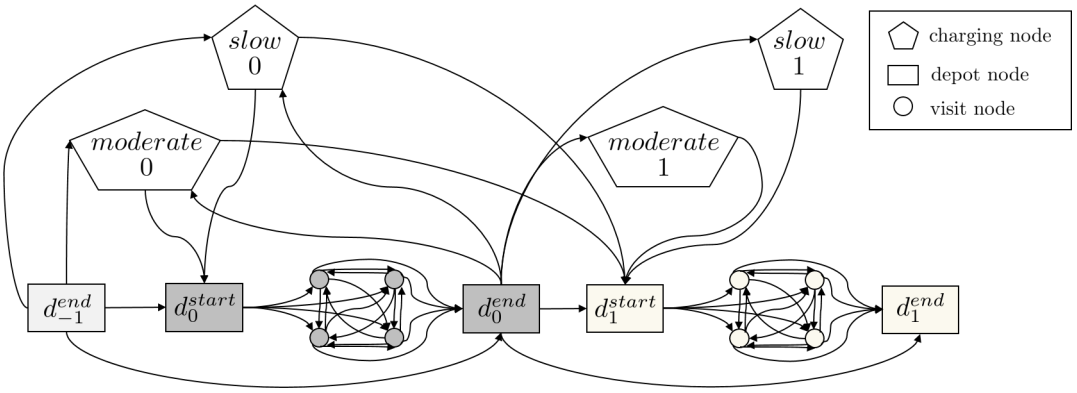


**Fig. 4.3.** An example of the multigraph $\mathcal{G}$ obtained for one particular instance to the MP-E-VRP with one EV.

Now, let us start by defining the sequencing decisions. Continuous variables $y_{ij}^k$ and $\tau_{ij}^k$ represent the energy and the time when EV $k$ departs from node $i \in \mathcal{V}$ to travel on arc $(i,j)^k \in \mathcal{A}_k$. Constraints (4.2) ensure that each node in $\mathcal{I}$ is visited once by a single EV during its period of visit. Constraints (4.3) impose the flow conservation conditions. Constraints (4.4) avoid mid-route charging in every period. Specifically, it restricts the ending depot of each period to be visited only once by every EV. Let node $j(m,h) \in \mathcal{C}$ be the charging node related with charging mode $m \in \mathcal{M}$ and charge $h \in \mathcal{H}$. Constraints (4.5) force the use of only one charging mode for each charge of an EV. For example, in the graph of Fig. 4.3 this means that charging nodes $(slow, 0)$ and $(moderate, 0)$ cannot be both visited by an EV. Constraints (4.6) impose that EV $k$ undergoes charge $h$ only if it has previously undergone charge $h-1$.

$$\sum_{k \in \mathcal{K}} \sum_{(i,j)^k \in \mathcal{A}_k} x_{ij}^k = 1 \qquad \forall i \in \mathcal{I} \tag{4.2}$$

$$\sum_{(j,i)^k \in \mathcal{A}_k} x_{ji}^k - \sum_{(i,j)^k \in \mathcal{A}_k} x_{ij}^k = 0 \qquad \forall i \in \mathcal{V} \setminus \{d_{-1}^{end}, d_{P_{max}-1}^{end}\}, \forall k \in \mathcal{K} \tag{4.3}$$

$$\sum_{(i,j)^k \in \mathcal{A}_k} x_{ij}^k \leq 1 \qquad \forall j \in \mathcal{D} \setminus \{d_{-1}^{end}\}, \forall k \in \mathcal{K} \tag{4.4}$$

$$\sum_{m \in \mathcal{M}} \sum_{(i,j(m,h))^k \in \mathcal{A}_k} x_{i,j(m,h)}^k \leq 1 \qquad \forall h \in \mathcal{H}, \forall k \in \mathcal{K} \tag{4.5}$$

$$\sum_{m \in \mathcal{M}} \sum_{(i,j(m,h))^k \in \mathcal{A}_k} x_{i,j(m,h)}^k \leq \sum_{m \in \mathcal{M}} \sum_{(i,j(m,h-1))^k \in \mathcal{A}_k} x_{i,j(m,h-1)}^k \qquad \forall h \in \mathcal{H} \setminus \{0\}, \forall k \in \mathcal{K} \tag{4.6}$$

Then, we present the energy tracking constraints. Constraints (4.7) couple the variables $x_{ij}^k$ and $y_{ij}^k$. Constraints (4.8) state that if an EV traverses arc $(i,j)^k \in \mathcal{A}_k$, then its energy

when leaving $i$ must be sufficient to traverse the arc and then reach the depot. Constraints (4.9) assign the initial energy to each EV at the beginning of the time horizon. Constraints (4.10) state the energy when departing from each depot and visit node.

$$y_{ij}^k \leq (Q - e_{0i})\, x_{ij}^k \qquad \forall k \in \mathcal{K}, \forall (i,j)^k \in \mathcal{A}_k \tag{4.7}$$

$$y_{ij}^k \geq (e_{ij} + e_{j0})\, x_{ij}^k \qquad \forall k \in \mathcal{K}, \forall (i,j)^k \in \mathcal{A}_k \tag{4.8}$$

$$\sum_{(d_{-1}^{end},j)^k \in \mathcal{A}_k} y_{d_{-1}^{end},j}^k = Q_0^k \qquad \forall k \in \mathcal{K} \tag{4.9}$$

$$\sum_{(i,j)^k \in \mathcal{A}_k} \left( y_{ij}^k - e_{ij} x_{ij}^k \right) = \sum_{(j,l)^k \in \mathcal{A}_k} y_{jl}^k \qquad \forall j \in \mathcal{I} \cup \mathcal{D} \setminus \{d_{-1}^{end}, d_{P_{max}-1}^{end}\}, \forall k \in \mathcal{K} \tag{4.10}$$

Next, we describe how we model the charging scheduling decisions. Let $o_{mh}^k \in \mathcal{O}$ be the charging operation associated with EV $k \in \mathcal{K}$, charging mode $m \in \mathcal{M}$ and charge $h \in \mathcal{H}$. With a slight abuse of notation, let $m(j)$, and $h(j)$ refer to the charging mode and the charge associated with the charging node $j \in \mathcal{C}$ and $m(o)$, $h(o)$, and $k(o)$ refer to the charging mode, the charge and the EV associated with the charging operation $o$. The piecewise linear charging function is represented using a convex combination model. Continuous variables $\underline{q}_o$ and $\overline{q}_o$ represent the energy of an EV upon starting and after completing charging operation $o \in \mathcal{O}$. Continuous variables $\underline{s}_o$ and $\overline{s}_o$ are the starting and ending time of charging operation $o$. Continuous variable $\Delta_o$ represents the duration of charging operation $o$. Binary variables $\underline{\theta}_{ob}$ and $\overline{\theta}_{ob}$ are equal to 1 if the energy of an EV upon starting and after completing charging operation $o$ is between $a_{m(o),b-1}$ and $a_{m(o),b}$ in the charging function. Continuous variables $\underline{\rho}_{ob}$ and $\overline{\rho}_{ob}$ are the coefficients associated with the breakpoint $(c_{m(o),b}, a_{m(o),b})$ in the charging function, when an EV starts and ends charging operation $o$ respectively. The variables $\underline{\rho}_{ob}$ enable the expression of $(\underline{s}_o, \underline{q}_o)$ as a convex combination of the breakpoints $(c_{m(o),b}, a_{m(o),b})$, where $b \in B_m$. Similarly, the variables $\overline{\rho}_{ob}$ enable the expression of $(\overline{s}_o, \overline{q}_o)$ as a convex combination of the breakpoints $(c_{m(o),b}, a_{m(o),b})$, where $b \in B_m$. Constraints (4.11) and (4.12) track the energy when arriving at and leaving each charging node. Constraints (4.13) couple the energy of an EV when arriving and leaving each charging node. For every charging operation $o$, constraints (4.14)-(4.19) define the energy of the EV upon starting charging and the time associated to it in the piecewise linear charging function. Similarly, constraints (4.20)-(4.25) define the energy of the EV after completing it and the time associated to it in the piecewise linear charging function. Constraints (4.26) define the time spent charging.

$$\sum_{(i,j)^k \in \mathcal{A}_k} y_{ij}^k = \underline{q}_{o_{m(j),h(j)}^k} \qquad \forall j \in \mathcal{C}, \forall k \in \mathcal{K} \tag{4.11}$$

$$\sum_{(j,i)^k \in \mathcal{A}_k} y_{ji}^k = \overline{q}_{o_{m(j),h(j)}^k} \qquad \forall j \in \mathcal{C}, \forall k \in \mathcal{K} \tag{4.12}$$

$$\underline{q}_o \leq \overline{q}_o \qquad \forall o \in \mathcal{O} \tag{4.13}$$

$$\underline{q}_o = Q \sum_{b \in B_{m(o)}} \underline{\rho}_{ob} a_{m(o),b} \qquad \forall o \in \mathcal{O} \tag{4.14}$$

$$\sum_{b \in B_{m(o)}} \underline{\rho}_{ob} = \sum_{b \in B_{m(o)} \setminus \{0\}} \underline{\theta}_{ob} \qquad \forall o \in \mathcal{O} \tag{4.15}$$

$$\sum_{b \in B_{m(o)} \setminus \{0\}} \underline{\theta}_{o^k_{m(j),h(j)},b} = \sum_{(i,j)^k \in \mathcal{A}_k} x^k_{ij} \qquad \forall j \in \mathcal{C}, \forall k \in \mathcal{K} \tag{4.16}$$

$$\underline{\rho}_{o0} \leq \underline{\theta}_{o1} \qquad \forall o \in \mathcal{O} \tag{4.17}$$

$$\underline{\rho}_{ob} \leq \underline{\theta}_{ob} + \underline{\theta}_{o,b+1} \qquad \forall o \in \mathcal{O}, \forall b \in B_{m(o)} \setminus \{0, b_m\} \tag{4.18}$$

$$\underline{\rho}_{o,b_m} \leq \underline{\theta}_{o,b_m} \qquad \forall o \in \mathcal{O} \tag{4.19}$$

$$\overline{q}_o = Q \sum_{b \in B_{m(o)}} \overline{\rho}_{ob} a_{m(o),b} \qquad \forall o \in \mathcal{O} \tag{4.20}$$

$$\sum_{b \in B_{m(o)}} \overline{\rho}_{ob} = \sum_{b \in B_{m(o)} \setminus \{0\}} \overline{\theta}_{ob} \qquad \forall o \in \mathcal{O} \tag{4.21}$$

$$\sum_{b \in B_{m(o)} \setminus \{0\}} \overline{\theta}_{o^k_{m(j),h(j)},b} = \sum_{(i,j)^k \in \mathcal{A}_k} x^k_{ij} \qquad \forall j \in \mathcal{C}, \forall k \in \mathcal{K} \tag{4.22}$$

$$\overline{\rho}_{o0} \leq \overline{\theta}_{o1} \qquad \forall o \in \mathcal{O} \tag{4.23}$$

$$\overline{\rho}_{ob} \leq \overline{\theta}_{ob} + \overline{\theta}_{o,b+1} \qquad \forall o \in \mathcal{O}, \forall b \in B_{m(o)} \setminus \{0, b_m\} \tag{4.24}$$

$$\overline{\rho}_{o,b_m} \leq \overline{\theta}_{o,b_m} \qquad \forall o \in \mathcal{O} \tag{4.25}$$

$$\Delta_o = \sum_{b \in B_{m(o)}} \left( \overline{\rho}_{ob} - \underline{\rho}_{ob} \right) c_{m(o),b} \qquad \forall o \in \mathcal{O} \tag{4.26}$$

To model the power grid and charging modes capacity constraints, we use a flow-based formulation. The power grid capacity and the number of chargers of each charging mode $m \in \mathcal{M}$ are considered as cumulative resources. They can be used by several charging operations in parallel, provided that the resource capacities are not exceeded at any time. Let us introduce the flow network that we use. Let $\varphi^+$ and $\varphi^-$ be two dummy

charging operations (acting as the source and the sink of the flows). The characteristics of these charging operations are fixed such that, for every operation $o$, $h(\varphi^+) < h(o)$, $k(\varphi^+) \neq k(o)$, $h(\varphi^-) > h(o)$ and $k(\varphi^-) \neq k(o)$. Let $\mathcal{O}^-(o)$ be the set containing the charging operations that can be performed before charging operation $o$ and $\mathcal{O}^+(o)$ be the set containing the charging operations that can be performed after this charging operation. Let $o \in \mathcal{O} \cup \{\varphi^-\}$ be a charging operation, then $\mathcal{O}^-(o) = \{o' \in \mathcal{O} : k(o') \neq k(o) \vee (k(o') = k(o) \wedge h(o') < h(o))\} \cup \{\varphi^+\}$. Similarly, let $o \in \mathcal{O} \cup \{\varphi^+\}$ be a charging operation, then $\mathcal{O}^+(o) = \{o' \in \mathcal{O} : k(o') \neq k(o) \vee (k(o') = k(o) \wedge h(o) < h(o'))\} \cup \{\varphi^-\}$. For the sake of clarity, Fig. 4.4 presents the flow network associated with the graph depicted in Fig. 4.3 and two EVs. This figure focuses on the subgraph induced by charging operation $o^2_{slow,0}$, and sets $\mathcal{O}^-(o^2_{slow,0})$ and $\mathcal{O}^+(o^2_{slow,0})$. Charging operations belonging to set $\mathcal{O}^-(o^2_{slow,0})$, $\mathcal{O}^+(o^2_{slow,0})$ or both are presented in yellow, blue or green.

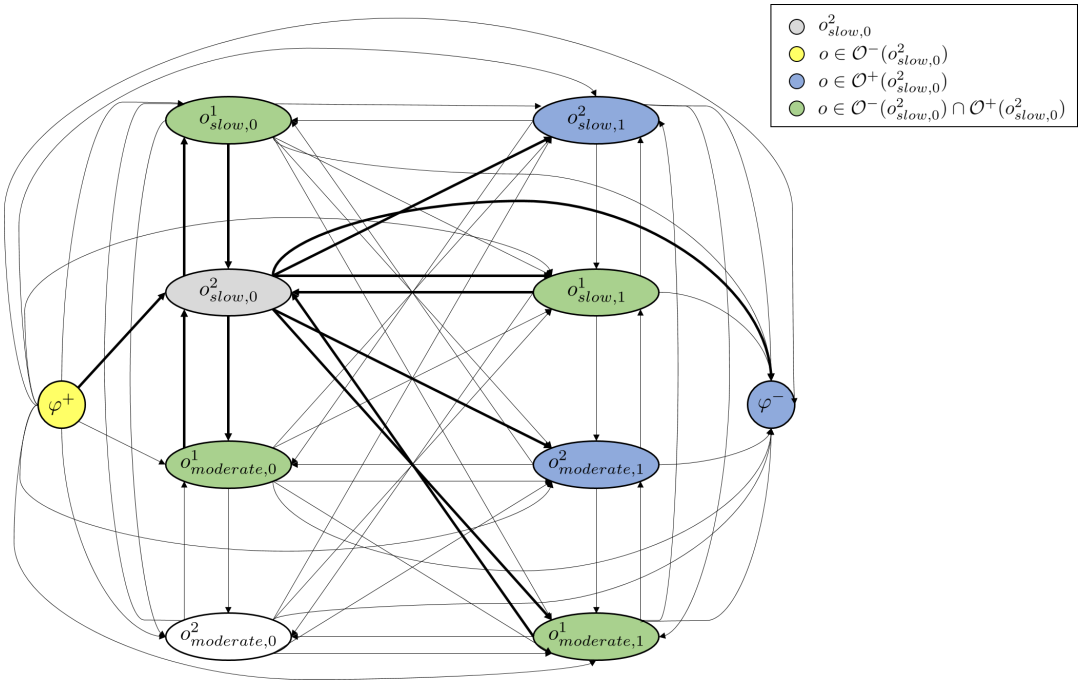


**Fig. 4.4.** Structure of the flow network for one particular instance to the MP-E-VRP with two EVs. For charging operation $o^2_{slow,0}$, charging operations belonging to sets $\mathcal{O}^-(o^2_{slow,0})$, $\mathcal{O}^+(o^2_{slow,0})$ or both are portrayed in different colors.

Binary variable $w_{oo'}$ is equal to 1 if charging operation $o' \in \mathcal{O}^+(o)$ starts after completing charging operation $o \in \mathcal{O} \cup \{\varphi^+\}$, and 0 otherwise. Constraints (4.27) are disjunctive constraints coupling the start time of charging operations $o$ and $o'$ to $w_{oo'}$. Constraints (4.28) express the transitivity of the precedence relations between charging operations. The constraint is active when $w_{oo'} = 1$ and, in that case, it enforces the precedence relation between $o'$ and $o''$ (i.e., $o'$ cannot start before the completion of $o''$).

$$\underline{s}_{o'} - \overline{s}_o \geq \left(T - \min_{i \in \mathcal{I}_{P_{max}-1}} (t_{0i} + t_{i0})\right)(w_{oo'} - 1) \qquad \forall o \in \mathcal{O}, \forall o' \in \mathcal{O}^+(o) \setminus \{\varphi^-\} \quad (4.27)$$

$$w_{o''o'} \geq w_{o''o} + w_{oo'} - 1 \qquad \forall o, o', o'' \in \mathcal{O} : o' \in \mathcal{O}^+(o), o \in \mathcal{O}^+(o'') \quad (4.28)$$

Continuous flow variable $z_{oo'}$ represents the quantity of power transferred from charging operation $o \in \mathcal{O} \cup \{\varphi^+\}$ to charging operation $o' \in \mathcal{O}^+(o)$. Constraints (4.29) state that the power associated with the charging mode of a charging operation has to be allocated to it if the charging operation's EV reaches the corresponding node. Constraints (4.30)-(4.32) ensure the power flow conservation. Constraints (4.33) couple the power flow variables to the sequence variables.

$$\sum_{o' \in \mathcal{O}^-(o^k_{m(j),h(j)})} z_{o',o^k_{m(j),h(j)}} = v_{m(j)} \sum_{(i,j)^k \in \mathcal{A}_k} x^k_{ij} \qquad \forall j \in \mathcal{C}, \forall k \in \mathcal{K} \quad (4.29)$$

$$\sum_{o' \in \mathcal{O}^-(o)} z_{o'o} - \sum_{o' \in \mathcal{O}^+(o)} z_{oo'} = 0 \qquad \forall o \in \mathcal{O} \quad (4.30)$$

$$PW_{max} - \sum_{o \in \mathcal{O}^+(\varphi^+)} z_{\varphi^+,o} = 0 \quad (4.31)$$

$$\sum_{o \in \mathcal{O}^-(\varphi^-)} z_{o,\varphi^-} - PW_{max} = 0 \quad (4.32)$$

$$z_{oo'} \leq \min(v_{m(o)}, v_{m(o')}) w_{oo'} \qquad \forall o \in \mathcal{O}, \forall o' \in \mathcal{O}^+(o) \setminus \{\varphi^-\} \quad (4.33)$$

Let $\mathcal{O}_m$ be the set of charging operations associated with charging mode $m \in \mathcal{M}$. Let $\mathcal{O}^-_m(o)$ be the set of charging operations associated with charging mode $m$ that can be performed before charging operation $o$ and set $\mathcal{O}^+_m(o)$ be the set of charging operations associated with charging mode $m$ that can be performed after this charging operation. Then, for charging mode $m \in \mathcal{M}$ and charging operation $o \in \mathcal{O}_m \cup \{\varphi^-\}$, $\mathcal{O}^-_m(o) = (\mathcal{O}^-(o) \cap \mathcal{O}_m) \cup \{\varphi^+\}$ . Similarly, for charging mode $m \in \mathcal{M}$ and charging operation $o \in \mathcal{O}_m \cup \{\varphi^+\}$, $\mathcal{O}^+_m(o) = (\mathcal{O}^+(o) \cap \mathcal{O}_m) \cup \{\varphi^-\}$. For example, for the graph portrayed in Fig. 4.4, Fig. 4.5 presents the subgraph induced by the charging operations related with charging mode *slow* and Fig. 4.6 presents the subgraph induced by the charging operations related with charging mode *moderate*.

Continuous flow variable $f_{oo'}$ denotes the number of chargers of charging mode $m(o) \in \mathcal{M}$ transferred from charging operation $o \in \mathcal{O}_m \cup \{\varphi^+\}$ to charging operation $o' \in \mathcal{O}^+_m(o)$. Constraints (4.34) state that a charger has to be allocated to a charging operation if EV $k$ reaches the corresponding charging node. Constraints (4.35)-(4.37) ensure the chargers' flow conservation. Constraints (4.38) couple flow variables associated with the chargers to the sequence variables. Specifically, the charger used by operation $o$ can be directly transferred for charging operation $o'$ if $o$ finishes before $o'$.

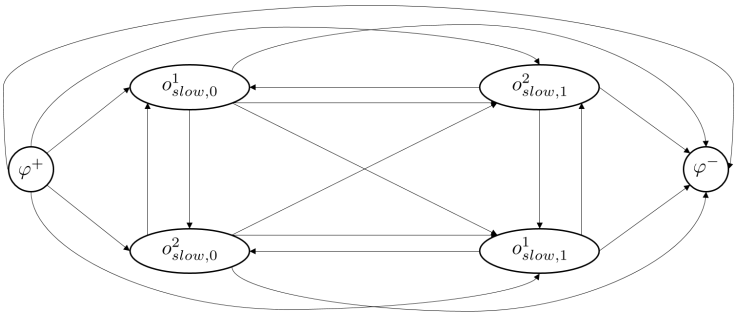


**Fig. 4.5.** Structure of the subgraph induced by the charging operations related with charging mode *slow* in the graph of Fig. 4.4.

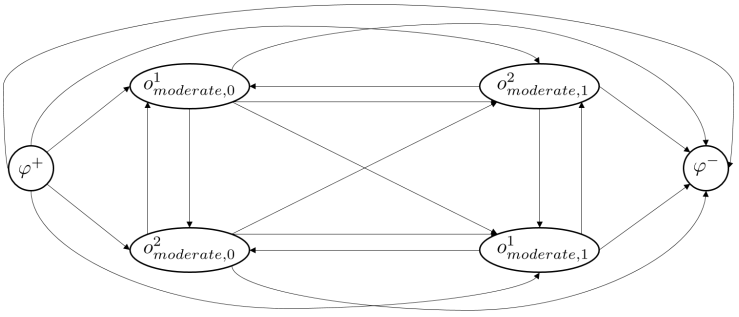


**Fig. 4.6.** Structure of the subgraph induced by the charging operations related with charging mode *moderate* in the graph of Fig. 4.4.

$$\sum_{o' \in \mathcal{O}^-_m(o^k_{m(j),h(j)})} f_{o',o^k_{m(j),h(j)}} = \sum_{(i,j)^k \in \mathcal{A}_k} x^k_{ij} \qquad \forall j \in \mathcal{C}, \forall k \in \mathcal{K} \tag{4.34}$$

$$\sum_{o' \in \mathcal{O}^-_m(o)} f_{o'o} - \sum_{o' \in \mathcal{O}^+_m(o)} f_{oo'} = 0 \qquad \forall m \in \mathcal{M}, \forall o \in \mathcal{O}_m \tag{4.35}$$

$$A_m - \sum_{o \in \mathcal{O}^+_m(\varphi^+)} f_{\varphi^+,o} = 0 \qquad \forall m \in \mathcal{M} \tag{4.36}$$

$$\sum_{o \in \mathcal{O}^-_m(\varphi^-)} f_{o,\varphi^-} - A_m = 0 \qquad \forall m \in \mathcal{M} \tag{4.37}$$

$$f_{oo'} \leq w_{oo'} \qquad \forall m \in \mathcal{M}, \forall o \in \mathcal{O}_m, \forall o' \in \mathcal{O}^+_m(o) \setminus \{\varphi^-\} \tag{4.38}$$

Afterwards, we present the time tracking constraints. Constraints (4.39) and (4.40) couple the variables $x^k_{ij}$ and $\tau^k_{ij}$. Without loss of generality, we restrict waiting times to occur only at the ending depot nodes and the charging nodes. Constraints (4.41)-(4.43) track the departure time from the depot and visit nodes. The inequality in constraint (4.43)

accounts for the waiting time for EV $k$ before performing a route or a charging operation. Constraints (4.44) and (4.45) track the starting and ending time of each charging operation. Constraints (4.46) track the waiting time between the end of a charging operation and the departure to the visit nodes. Constraints (4.47) and (4.48) impose, for every period $p$, the earliest time to leave the depot to go to the visit nodes to be larger than or equal to $E_p$ and the latest time to come back to the depot to be smaller than or equal to $L_p$. Constraints (4.49) break symmetries by imposing that for every EV $k$, if it undergoes charge $h-1$ and charge $h$, charge $h-1$ must occur first.

$$\tau_{ij}^k \leq T x_{ij}^k \qquad \forall k \in \mathcal{K}, \forall (i,j)^k \in \mathcal{A}_k : i \in \mathcal{C} \cup \mathcal{D}^{end} \tag{4.39}$$

$$\tau_{ij}^k \leq L_p x_{ij}^k \qquad \forall p \in \mathcal{P}, \forall k \in \mathcal{K}, \forall (i,j)^k \in \mathcal{A}_k : i \in \mathcal{I}_p \cup \{d_p^{start}\} \tag{4.40}$$

$$\sum_{(i,j)^k \in \mathcal{A}_k} \left(\tau_{ij}^k + t_{ij} x_{ij}^k\right) + \delta_j = \sum_{(j,l)^k \in \mathcal{A}_k} \tau_{jl}^k \qquad \forall j \in \mathcal{I}, \forall k \in \mathcal{K} \tag{4.41}$$

$$\sum_{(i,j)^k \in \mathcal{A}_k} \tau_{ij}^k = \sum_{(j,l)^k \in \mathcal{A}_k} \tau_{jl}^k \qquad \forall j \in \mathcal{D}^{start}, \forall k \in \mathcal{K} \tag{4.42}$$

$$\sum_{(i,j)^k \in \mathcal{A}_k} \left(\tau_{ij}^k + t_{ij} x_{ij}^k\right) \leq \sum_{(j,l)^k \in \mathcal{A}_k} \tau_{jl}^k \qquad \forall j \in \mathcal{D}^{end} \setminus \{d_{-1}^{end}, d_{P_{max}-1}^{end}\}, \forall k \in \mathcal{K} \tag{4.43}$$

$$\sum_{(i,j)^k \in \mathcal{A}_k} \tau_{ij}^k = \underline{s}_{o^k_{m(j),h(j)}} \qquad \forall j \in \mathcal{C}, \forall k \in \mathcal{K} \tag{4.44}$$

$$\underline{s}_o + \Delta_o = \overline{s}_o \qquad \forall o \in \mathcal{O} \tag{4.45}$$

$$\overline{s}_{o^k_{m(j),h(j)}} \leq \sum_{(j,i)^k \in \mathcal{A}_k} \tau_{ji}^k, \qquad \forall j \in \mathcal{C}, \forall k \in \mathcal{K} \tag{4.46}$$

$$\sum_{j \in \mathcal{I}_p} \tau_{d_p^{start},j}^k \geq E_p \sum_{j \in \mathcal{I}_p} x_{d_p^{start},j}^k \qquad \forall p \in \mathcal{P}, \forall k \in \mathcal{K} \tag{4.47}$$

$$\sum_{i \in \mathcal{I}_p} \left(\tau_{i,d_p^{end}}^k + t_{i,d_p^{end}} x_{i,d_p^{end}}^k\right) \leq L_p \sum_{i \in \mathcal{I}_p} x_{i,d_p^{end}}^k \qquad \forall p \in \mathcal{P}, \forall k \in \mathcal{K} \tag{4.48}$$

$$\begin{aligned} \sum_{m \in \mathcal{M}} \sum_{(i,j(m,h))^k \in \mathcal{A}_k} \tau_{i,j(m,h)}^k \; - \; & \sum_{m \in \mathcal{M}} \sum_{(i,j(m,h-1))^k \in \mathcal{A}_k} \tau_{i,j(m,h-1)}^k \\ \geq \; & T \left( \sum_{m \in \mathcal{M}} \sum_{(i,j(m,h))^k \in \mathcal{A}_k} x_{i,j(m,h)}^k - 1 \right) \\ & \forall h \in \mathcal{H} \setminus \{0\}, \forall k \in \mathcal{K} \end{aligned} \tag{4.49}$$

We now focus on the modeling of the cumulative wear costs. We consider a piecewise linear cumulative wear cost function such as the one presented in Fig. 3.1. We take advantage of its convexity to derive the formulation. Notice that other shapes of the piecewise linear cumulative wear cost function can be incorporated to the MILP using a convex combination model. We first introduce the modeling of the cumulative wear costs associated with the charging operations. Continuous variable $\alpha_{o\beta}$ specifies the percentage of energy charged on the segment that lies between points $(l_{\beta-1}, n_{\beta-1})$ and $(l_\beta, n_\beta)$ in the cumulative wear cost function for charging operation $o$, and binary variable $\sigma_{o\beta}$ is equal to 1 if and only if the charging operation involves the segment between those two points. Fig. 4.7 illustrates the definition of these variables.

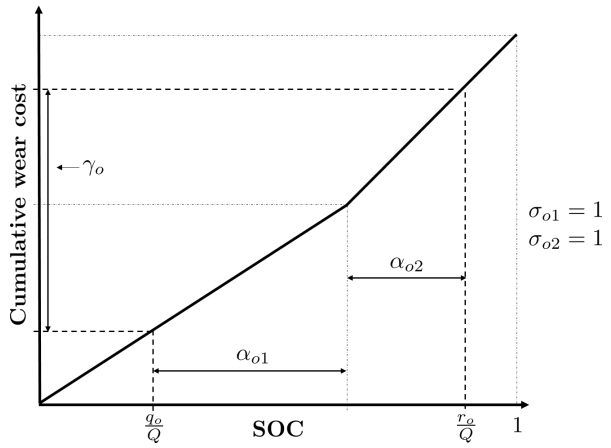


**Fig. 4.7.** Illustration of the definition of variables used for modeling the cumulative wear costs associated with charging operations.

Constraints (4.50) restrict the segments in the cumulative wear cost function on which EVs can charge depending on the energy they have upon arrival at charging nodes. Constraints (4.51) restrict the percentage of energy that can be charged on each segment. Constraints (4.52) impose the activation of at least one segment whenever EV $k$ visits the corresponding charging node. Similarly, constraints (4.53) ensure that a segment is activated only if EV $k$ visits the corresponding charging node. Constraints (4.54) define the energy after a charging operation by summing up the corresponding amounts charged on the relevant segments. Constraints (4.55) define the cumulative wear cost associated with every charging operation.

$$\frac{q_o}{Q} + \alpha_{o\beta} \leq l_\beta \sigma_{o\beta} + (1 - \sigma_{o\beta}) \qquad \forall o \in \mathcal{O}, \forall \beta \in \Pi \setminus \{0\} \tag{4.50}$$

$$\alpha_{o\beta} \leq (l_\beta - l_{\beta-1})\sigma_{o\beta} \qquad \forall o \in \mathcal{O}, \forall \beta \in \Pi \setminus \{0\} \tag{4.51}$$

$$\sum_{\beta \in \Pi \setminus \{0\}} \sigma_{o^k_{m(j),h(j)},\beta} \geq \sum_{(i,j)^k \in \mathcal{A}_k} x^k_{ij} \qquad \forall j \in \mathcal{C}, \forall k \in \mathcal{K} \tag{4.52}$$

$$\sigma_{o^k_{m(j),h(j)},\beta} \leq \sum_{(i,j)^k \in \mathcal{A}_k} x^k_{ij} \qquad \forall j \in \mathcal{C}, \forall \beta \in \Pi \setminus \{0\}, \forall k \in \mathcal{K} \tag{4.53}$$

$$\frac{\overline{q}_o}{Q} = \frac{q_o}{Q} + \sum_{\beta \in \Pi \setminus \{0\}} \alpha_{o\beta} \qquad \forall o \in \mathcal{O} \tag{4.54}$$

$$\gamma_o = \sum_{\beta \in \Pi \setminus \{0\}} \zeta_\beta \alpha_{o\beta} \qquad \forall o \in \mathcal{O} \tag{4.55}$$

We now present the modeling of the cumulative wear costs associated with the energy discharged from an EV when it performs routes. Continuous variable $\eta^k_{p\beta}$ denotes the percentage of energy discharged on the segment that lies between points $(l_{\beta-1}, n_{\beta-1})$ and $(l_{\beta-1}, n_{\beta-1})$ in the cumulative wear cost function for the route of EV $k$ in period $p$, and binary variable $\phi^k_{p\beta}$ is equal to 1 if and only if the discharge includes the segment between those two points. Fig. 4.8 illustrates the definition of these variables.

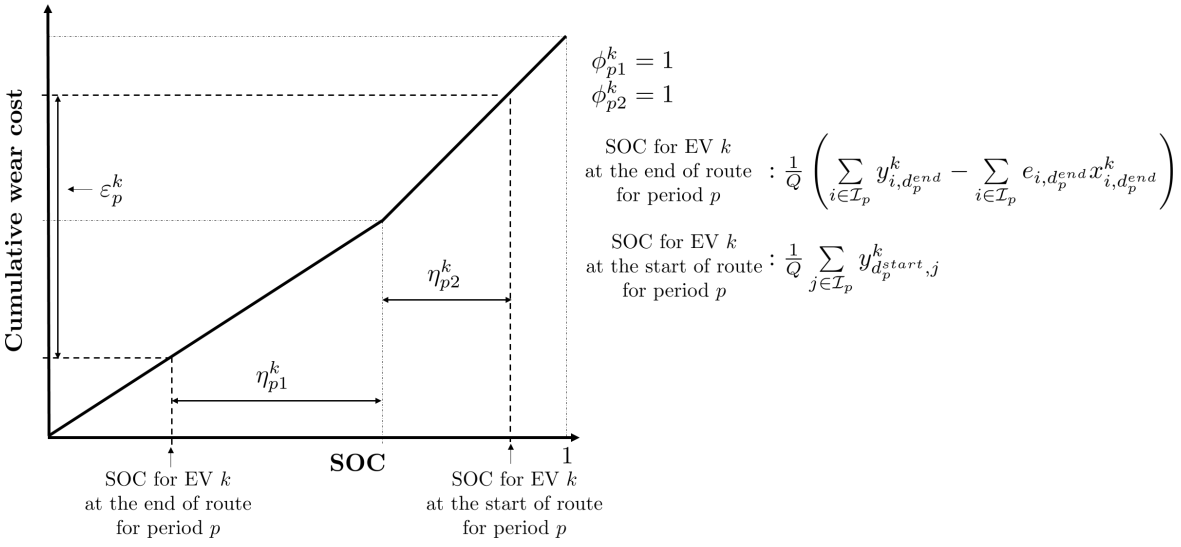


**Fig. 4.8.** Illustration of the definition of variables used for modeling the cumulative wear costs associated with routes.

According to the energy EVs have upon arrival at ending depot nodes, constraints (4.56) delimit the segments in the cumulative wear cost function on which they can discharge. Constraints (4.57) restrict the percentage of energy that can be discharged on each segment. Constraints (4.58) impose the activation of one segment whenever EV $k$ performs a route in the corresponding period. Similarly, constraints (4.59) ensure that a segment is activated only if EV $k$ performs a route in the corresponding period (i.e., goes to at least one visit node). Constraints (4.60) define the energy before performing a route by summing up the corresponding amounts discharged on the relevant segments. Constraints (4.61) define for every EV the cumulative wear cost incurred during each period.

$$\frac{1}{Q}\left(\sum_{i\in\mathcal{I}_p} y^k_{i,d_p^{end}} - \sum_{i\in\mathcal{I}_p} e_{i,d_p^{end}} x^k_{i,d_p^{end}}\right) + \eta^k_{p\beta} \leq l_\beta \phi^k_{p\beta} + (1-\phi^k_{p\beta}) \qquad \forall p \in \mathcal{P}, \forall \beta \in \Pi\backslash\{0\}, \forall k \in \mathcal{K} \tag{4.56}$$

$$\eta^k_{p\beta} \leq (l_\beta - l_{\beta-1})\phi^k_{p\beta} \qquad \forall p \in \mathcal{P}, \forall \beta \in \Pi \setminus \{0\}, \forall k \in \mathcal{K} \tag{4.57}$$

$$\sum_{\beta\in\Pi\backslash\{0\}} \phi^k_{p\beta} \geq \sum_{i\in\mathcal{I}_p} x^k_{i,d_p^{end}} \qquad \forall p \in \mathcal{P}, \forall k \in \mathcal{K} \tag{4.58}$$

$$\phi^k_{p\beta} \leq \sum_{i\in\mathcal{I}_p} x^k_{i,d_p^{end}} \qquad \forall p \in \mathcal{P}, \forall \beta \in \Pi \setminus \{0\}, \forall k \in \mathcal{K} \tag{4.59}$$

$$\frac{1}{Q}\sum_{j\in\mathcal{I}_p} y^k_{d_p^{start},j} = \frac{1}{Q}\sum_{i\in\mathcal{I}_p}\left(y^k_{i,d_p^{end}} - e_{i,d_p^{end}} x^k_{i,d_p^{end}}\right) + \sum_{\beta\in\Pi\backslash\{0\}} \eta^k_{p\beta} \qquad \forall p \in \mathcal{P}, \forall k \in \mathcal{K} \tag{4.60}$$

$$\varepsilon^k_p = \sum_{\beta\in\Pi\backslash\{0\}} \zeta_\beta \eta^k_{p\beta} \qquad \forall p \in \mathcal{P}, \forall k \in \mathcal{K} \tag{4.61}$$

Finally, constraints (4.62)–(4.70) define the domain of the decision variables.

$$x^k_{ij} \in \{0,1\}, \tau^k_{ij} \geq 0, y^k_{ij} \geq 0 \qquad \forall k \in \mathcal{K}, \forall (i,j)^k \in \mathcal{A}_k \tag{4.62}$$

$$\underline{q}_o \geq 0, \overline{q}_o \geq 0, \underline{s}_o \geq 0, \overline{s}_o \geq 0, \Delta_o \geq 0, \gamma_o \geq 0 \qquad \forall o \in \mathcal{O} \tag{4.63}$$

$$\underline{\rho}_{ob} \geq 0, \overline{\rho}_{ob} \geq 0 \qquad \forall o \in \mathcal{O}, \forall b \in B_{m(o)} \tag{4.64}$$

$$\underline{\theta}_{ob} \in \{0,1\}, \overline{\theta}_{ob} \in \{0,1\} \qquad \forall o \in \mathcal{O}, \forall b \in B_{m(o)} \setminus \{0\} \tag{4.65}$$

$$w_{oo'} \in \{0,1\}, z_{oo'} \geq 0 \qquad \forall o \in \mathcal{O} \cup \{\varphi^+\}, o' \in \mathcal{O}^+(o) \tag{4.66}$$

$$f_{oo'} \geq 0 \qquad \forall m \in \mathcal{M}, \forall o \in \mathcal{O}_m \cup \{\varphi^+\}, o' \in \mathcal{O}^+_m(o) \tag{4.67}$$

$$\alpha_{o\beta} \geq 0, \sigma_{o\beta} \in \{0,1\} \qquad \forall o \in \mathcal{O}, \forall \beta \in \Pi \setminus \{0\} \tag{4.68}$$

$$\eta^k_{p\beta} \geq 0, \phi^k_{p\beta} \in \{0,1\} \qquad \forall p \in \mathcal{P}, \forall k \in \mathcal{K}, \forall \beta \in \Pi \setminus \{0\} \tag{4.69}$$

$$\varepsilon^k_p \geq 0 \qquad \forall p \in \mathcal{P}, \forall k \in \mathcal{K} \tag{4.70}$$

We refer to equations (4.1)-(4.70) as formulation $[F^1]$.

## 4.5 Computational experiments

In this section, we present the computational experiments for the $[F^1]$. We used Gurobi Optimizer (version 8.0.1) to solve $[F^1]$. We used a single thread with 15 GB. The experiments were carried out on a Compute Canada's high-performance computing facility (see Appendix B for characteristics). In all tables, the CPU time is rounded to the nearest integer. We ran $[F^1]$ with a time limit of three hours. Section 4.5.1 provides information on the test instances for the MP-E-VRP. Section 4.5.2 presents the results of the experiments.

### 4.5.1 Instance generation for the MP-E-VRP

Since the problem introduced in this thesis is new to E-VRPs literature, no publicly available benchmark exists. Moreover, adapting existing benchmarks related to specific E-VRPs is a complex task that does not seem to be appropriate since the characteristics of this problem are very different from the existing E-VRPs. We therefore have taken advantage of some insights provided by companies using EVs to get inside knowledge on how real-data for the problem look like. Based on this knowledge, we built an instance generator that we believe captures reality with a good degree of accuracy.

We consider three periods representing three 8 hours working shifts and an *intershift window* between shifts of zero for each period ($E_0 = 0, L_0 = E_1 = 8, L_1 = E_2 = 16$, and $L_2 = 24$). We generated sets of customer locations. We located the customers in a geographic space of approximately 45×45 km using a random uniform distribution. We chose this geographic space to represent an urban operation in which routes from the depot to each customer are energy feasible, thus there is no need for mid-route charging. Service time is fixed to 0.75 hours for all customers.

We included two types of charging mode: *slow* (with a power of 6 kW and a charging rate of 0.25 C-rate) and *moderate* (with a power of 11 kW and a charging rate of 0.5 C-rate). We consider the *slow* mode as referring to the charger included in the EV and the *moderate* mode as referring to the charging equipment installed at the depot. Then, the number of available *slow* chargers is equal to the number of EVs while the number of available *moderate* chargers is approximately 1/5 of the number of EVs. We considered instances with only one charging mode, *slow*, and instances with two charging modes, *slow* and *moderate*. The power grid capacity is adjusted depending on the number of EVs, so that all chargers of both charging modes cannot be used at the same time.

We assume the EVs have an energy consumption rate of 0.125 kWh/km and batteries of 16 kWh. In addition, we fixed the batteries' price to $6560 based on the assumption of a battery cost of $410/kWh (Nykvist and Nilsson, 2015). The initial energy for all EVs is fixed to 8 kWh or 12.8 kWh. For each pair $(i, j)$ of locations (customers or depot), the energy consumption $e_{ij}$ to travel from $i$ to $j$ is assumed to be equal to the comsumption rate of the EV multiplied by the driving time $t_{ij}$. Using the procedure presented in Section 3.4.1, the calculation of the fixed cost for the EVs yields $1.22 for *slow* mode and $1.42 for *moderate* mode. The piecewise linear approximations of the charging functions are derived from the model presented in Pelletier et al. (2018) using data from Marra et al. (2012). For the cumulative wear cost function, we use the piecewise linear approximation

presented in Fig. 3.1 which is derived from the data of Han et al. (2014).

#### 4.5.1.1 G1 testbed

We generated 100 small size instances to the MP-E-VRP. We denote this testbed as G1. We generated instances with 5, 10, or 15 customers in each period. For each number of customers per period we generated 5 sets of customer locations. We adjusted the number of EVs depending on the number of customers per period. Table 4.2 summarizes the parameter setting of testbed G1. Additionally, Table 4.3 provides the number of variables and constraints in the MILP formulation. This figure allows the reader to assess the size of the instances.

Table 4.2: Parameter setting for testbed G1 (5 instances for each number of customers per period)

| Parameters | Values | | |
|---|---|---|---|
| Periods | 3 | | |
| Customers/$p$ | 5 | 10 or 15 | |
| EVs | 2 | 4 | 5 |
| Power grid capacity | 15 kW | 30 kW | 35 kW |
| Initial energy | 8 kWh or 12.8 kWh | | |
| Charging mode | one (*slow*) or two (*slow* and *moderate*) | | |

Customers/$p$: customers per period

Table 4.3: Size of instances for testbed G1 with $[F^1]$

| | | Number of charging modes | | | |
|---|---|---|---|---|---|
| | | 1 | | 2 | |
| Customers/period | EVs | Number of variables | Number of constraints | Number of variables | Number of constraints |
| 5 | 2 | 920 | 1219 | 1329 | 2063 |
| 10 | 4 | 4934 | 6574 | 6255 | 14812 |
| | 5 | 6302 | 9289 | 8268 | 26516 |
| 15 | 4 | 9614 | 11449 | 10935 | 19687 |
| | 5 | 12152 | 15379 | 14118 | 32606 |

### 4.5.2 Results for the MILP formulation

Table 4.4 reports for each number of customers per period (Customers/$p$) the number of instances reaching the time limit without finding any feasible solution (#NoSol), the number of instances with a feasible solution not proven to be optimal (#Feas), the number of instances with a feasible solution proven to be optimal (#Opt), the average CPU time in seconds for instances in (#Opt), (Time), and the average gap for instances in #Feas (Gap). All gaps reported in the manuscript are computed as

$$\frac{ObjVal - ObjBound}{ObjVal} \tag{4.71}$$

where $ObjVal$ is the objective function of the computed solution (i.e., the incumbent solution objective) and $ObjBound$ is the lower bound retrieved by the solver or the objective function of the best (minimal) upper bound, as appropriate. As can be seen from the table, the model has difficulty finding optimal solutions for instances from 10 customers per period. To obtain insights on the characteristics of the MP-E-VRP that makes $[F^1]$ difficult to solve, we present in Table 4.5 the average gap for instances in (#Feas) with 10 and 15 customers per period, differentiated by number of EVs, number of charging modes and initial energy. This table suggests that $[F^1]$ is more difficult to solve when the number of EVs and charging modes increases and when the initial energy is larger. The increase in difficulty related with the number of EVs and charging modes may come from the fact that increasing the number of EVs and charging modes leads to a larger number of variables. Concerning the initial energy, the result is somewhat counterintuitive. A possible explanation for this might be that diminishing the initial energy reduces the search space (the decision to charge before the first route may be obvious if the initial energy is reduced). This in turn makes the model easier to solve.

Table 4.4: Computational results for $[F^1]$ on instances to the MP-E-VRP

| Customers/$p$ | #NoSol | #Feas | #Opt | Time (s) | Gap |
|---|---|---|---|---|---|
| 5 | 0 | 0 | 20 | 8 | - |
| 10 | 0 | 40 | 0 | - | 18.01% |
| 15 | 10 | 30 | 0 | - | 26.61% |

Table 4.5: Gap for instances to the MP-E-VRP in (#Feas)

| | Gap | | | | | |
|---|---|---|---|---|---|---|
| | Number of EVs | | Number of charging modes | | Initial energy | |
| Customers/$p$ | 4 | 5 | 1 | 2 | 8 kWh | 12.8 kWh |
| 10 | 15.25% | 20.78% | 17.43% | 18.59% | 16.24% | 19.79% |
| 15 | 25.20% | 28.03% | 25.46% | 27.76% | 23.93% | 28.17% |

# Chapter 5

# Decomposition methods for solving the MP-E-VRP

Dans ce chapitre, nous présentons une stratégie de décomposition pour aborder le MP-E-VRP. Le premier sous-problème à résoudre consiste à concevoir un ensemble de routes réalisables de bonne qualité et diversifiées. Le deuxième sous-problème concerne la sélection des routes à effectuer, l'affectation des VE à ces routes et la programmation des opérations de chargement qui rendent cette affectation possible. Nous proposons trois méthodes qui suivent cette stratégie de décomposition. Elles utilisent toutes une heuristique existante pour échantillonner l'espace des routes réalisables. Pour résoudre le second sous-problème, nous proposons une heuristique constructive, une formulation MILP et une approche basée sur « local branching ». L'heuristique constructive, bien que simple, permet de trouver une solution réalisable en peu de temps. Pour chaque période, l'heuristique attribue la route ayant la plus grande consommation d'énergie au VE ayant la plus grande énergie disponible et poursuit l'attribution jusqu'à ce que toutes les routes de la période soient attribuées. En outre, l'heuristique vérifie la satisfaction des contraintes de l'infrastructure de recharge. La solution obtenue peut alors être fournie pour accélérer le processus de recherche dans les autres stratégies de décomposition. La formulation MILP est construite sur la base de la formulation MILP présentée pour le MP-E-VRP. Peu de modifications sont nécessaires pour formuler le nouveau problème concernant l'affectation des VE aux routes et la programmation des opérations de chargement. Enfin, l'approche basée sur « local branching » est basée sur la formulation MILP présentée dans ce chapitre et consiste à ajouter des inégalités linéaires à cette formulation, pour explorer l'espace de solution en effectuant des recherches locales sur des voisinages définis en vue de trouver des solutions de bonne qualité. La définition du voisinage et la stratégie de diversification sont modifiées pour tenir compte des caractéristiques du MP-E-VRP. Les résultats expérimentaux nous permettent d'identifier cette méthode comme la meilleure pour trouver des solutions pour des instances de grande taille.

## 5.1 Introduction

It is common knowledge that directly solving MILP formulations is frequently computationally intractable for medium-sized and especially for large-sized instances. The results in Chapter 4 shows the limitation of solving $[F^1]$ with a MILP solver to provide good-quality solutions to the MP-E-VRP in a reasonable amount of time. Only small instances with 5 customers per period were solved to optimality and gaps for larger instances are considerable. Therefore, we propose to decompose the MP-E-VRP in two subproblems to be solved sequentially, following a route-first assemble-second approach. The first subproblem is the route generation for the MP-E-VRP. This consists of finding a pool of routes that are feasible for the MP-E-VRP. The second subproblem concerns the selection the routes to be performed and the assignment of EVs to them while scheduling the recharging operations. We introduce it as the Multi-period Electric Vehicle Route Assignment and Charging Scheduling Problem (MP-E-VRACSP). In this chapter we present our decomposition strategy along with three methods to tackle it. All three methods use the same route generator. We adapt an existing matheuristic to generate a pool of high-quality routes. For solving the MP-E-VRACSP, we propose a constructive heuristic, a MILP formulation and a local branching based approach. The later is based on solving small MILP formulations to perform local searches in defined neighborhoods. The constructive heuristic, for its part, can itself be used to obtain an initial solution for both the MILP formulation and the local branching heuristic.

This chapter is organized as follows. Section 5.2 provides more information regarding the decomposition strategy. Section 5.3 presents the matheuristic we propose to tackle the route generation. Section 5.4 describes the constructive heuristic we developed for finding a feasible solution to the MP-E-VRACSP. Section 5.5 provides the MILP formulation for the MP-E-VRACSP. Section 5.6 presents the local branching based approach. We perform computational experiments in instances of different sizes. Results are shown in Section 5.7. Finally, Section 5.8 concludes.

## 5.2 Decomposition strategy

In this section, we define in more detail the two subproblems in which we decompose the MP-E-VRP, in order to solve larger size instances. It follows a route-first assemble-second approach, which has shown to be a successful strategy for solving several hard VRPs, such as the VRP with time windows (Alvarenga et al., 2007), the truck and trailer routing problem (Villegas et al., 2013), and the E-VRP-NL (Montoya et al., 2017). Generally, the second phase of the route-first assemble-second approach consists on building the best possible solution by solving a set partitioning (SP) model over the pool of routes. The problems where this approach is typically used do not have route coupling constraints. The MP-E-VRP has several characteristics that make the second problem not so easy to solve. The MP-E-VRP integrates routing and depot charging scheduling over a planning horizon of several days. Both routing and charging scheduling decisions depend upon each other, so they cannot be solved separately. Therefore, we propose to transform the routing problem into an assignment problem, in which EVs must be assigned to routes already fixed. With

regard to the routes, they are chosen from a high-quality and diverse pool. Consequently, the first subproblem concerns the creation of the pool of routes. The second subproblem focuses on selecting routes and assigning EVs to them while scheduling the recharging operations, depending on the depot charging infrastructure capacity constraints.

### 5.2.1 Route generation for the MP-E-VRP

The first subproblem consist of building a high-quality and diverse pool $\Omega$ of routes that are both time and energy feasible. Time feasibility signifies that, for period $p \in \mathcal{P}$, routes in $\Omega_p \subset \Omega$ are performed only during time window $[E_p, L_p]$. Energy feasibility, on the other hand, means that the energy consumption of a route cannot be greater than the battery capacity of EVs, $Q$. $\Omega$ is, however, a subset of the set $\mathcal{R}$ of all feasible routes. This leads to the reduction of the solution space for the MP-E-VRP to the solutions containing the routes belonging to $\Omega$. To generate $\Omega$, we use a matheuristic that works in two phases developed per period $p \in \mathcal{P}$: sampling and assembling. In the sampling phase it builds a pool of routes $\Omega_p$ via a set of randomized route-first cluster-second heuristics. In the assembling phase and per integer parameter $\varkappa$, $\varkappa \in \{1, \ldots, |\mathcal{K}|\}$, the approach uses the routes stored in $\Omega_p$ to select a set of routes $\Omega_{p\varkappa}$ minimizing energy consumption, such that $|\Omega_p| = \varkappa$. The energy consumption of a route is used as a proxy of the cumulative wear cost incurred when an EV performs it. This cost would be really revealed when an EV is assigned to the route, taking into account the EV's energy at the beginning of the route. Regarding parameter $\varkappa$, it is used to fix the number of routes that must be performed per period. Finally, $\Omega$ is obtained as follows:

$$\Omega = \bigcup_{p \in \mathcal{P}, \varkappa \in \{1,\ldots,|\mathcal{K}|\}} \Omega_{p\varkappa} \tag{5.1}$$

### 5.2.2 The Multi-period Electric Vehicle Route Assignment and Charging Scheduling Problem (MP-E-VRACSP)

The second subproblem arises when transforming the MP-E-VRP's routing problem into a problem concerning the assignment of EVs to routes. In this case routes are assumed to be given. Due to the charging infrastructure capacity constraints, this subproblem also comprises the charging scheduling, to be solved jointly with the assignment problem. We call it the Multi-period Electric Vehicle Route Assignment and Charging Scheduling Problem (MP-E-VRACSP) and we define it in more detail as follows. The MP-E-VRACSP consists in assigning a fleet of EVs to service a given set of routes over a planning horizon of several periods. EVs are charged at the depot at any time, subject to the charging infrastructure capacity constraints. We define the MP-E-VRACSP using the parameters introduced in Section 4.2 for the MP-E-VRP. Only set $\mathcal{I}$ is modified. Each node $i \in \mathcal{I}$ represents a route with duration $t_i \geq 0$ (in hours), energy consumption $e_i \geq 0$ (in kWh) and period $p_i \in \mathcal{P}$. All the routes start and end at the depot. Feasible solutions to the MP-E-VRACSP satisfy conditions 1)-8) presented for the MP-E-VRP (Section 4.2). The objective of this problem is to assign the EVs to the routes in each period and to schedule the charging operations of the EVs while minimizing the cost of battery degradation.

Notice that the charging scheduling problem resembles a multi-mode Resource Constrained Project Scheduling Problem (MRCPSP) with renewable resources (see Hartmann and Briskorn (2010) for an overview of RCPSP variants and extensions). The RCPSP is itself a strongly NP-hard problem, as shown by Blazewicz et al. (1983). In the the charging scheduling problem, charging modes correspond to the multiple modes in which an activity (i.e., a charging operation) can be performed, consuming a certain amount of power of the grid and using a charger of the mode in consideration (the renewable resources). Additionally, there are time lags between charging operations of the same EV, as the EV can be recharged only once between two routes. Nonetheless, the charging scheduling problem differs from problems in the MRCPSP literature in the extent that the duration of each charging operation and the number of charging operations to be performed in each mode are decision variables. Moreover, they are subject to the assignment of EVs to routes and vice versa. As far as we know, this case has never been addressed in the RCPSP literature. We propose to modify $[F^1]$, the MILP formulation for the MP-E-VRP, to obtain a model to solve this problem. This formulation is presented in Section 5.5. Solving this model using a commercial solver allows us to address instances with larger size than the one solved with $[F^1]$. However, the size of the instances may still be reduced as it is an exact method. Therefore, we propose in addition a local branching based approach, that performs local searches in neighborhoods obtained by adding cuts to a MILP formulation. Section 5.6 describes our local branching based matheuristic. Furthermore, we provide a constructive heuristic for finding feasible solutions to the MP-E-VRACSP. This solution can be supplied to both methods to speed up the search. Section 5.4 details this heuristic.

The MP-E-VRACSP assumes that the set of routes to be performed is already known, but finding such a feasible set of routes could be a difficult task. Taking that into account, we propose a modification to the MP-E-VRACSP denoted as MP-E-VRACSPm. MP-E-VRACSPm considers selecting the routes from a pool of routes. This pool of routes is intended to be diverse so it would allow to select a set of routes that leads to feasible solutions for this problem. Section 5.2.2.1 presents the MP-E-VRACSPm.

#### 5.2.2.1 The modified MP-E-VRACSP (MP-E-VRACSPm)

We consider a fleet of EVs that must service a set of customers over a planning horizon of several periods. Routes to be performed by the fleet of EVs must be selected from a pool of feasible routes in such a way all customers are visited. The modified MP-E-VRACSP (MP-E-VRACSPm) consists in selecting the set of routes from the pool, assigning the fleet of EVs to service the routes and scheduling the charging operations of the EVs at the depot, subject to the charging infrastructure capacity constraints. We define the MP-E-VRACSPm using the same parameters previously presented for the MP-E-VRACSP. We include the set of customers $\mathcal{J}$. Parameter $\psi_{ni} \in \{0, 1\}$ is equal to 1 if customer $n \in \mathcal{J}$ is served in route $i \in \mathcal{I}$, and 0 otherwise. Feasible solutions to this problem satisfy conditions 1)-8) presented for the MP-E-VRP (see Section 4.2). Additionally, they satisfy the condition that each customer $n \in \mathcal{J}$ is served by one route $i \in \mathcal{I}$ such that $\psi_{ni} = 1$. The objective of this problem is to select the routes for each period from the pool of routes and assign the EVs to them, and to schedule the charging operations while minimizing the cost of battery degradation. This cost has the same definition of the one given in Section

4.2.

## 5.3 RouteGenerator

### 5.3.1 Introduction

We have developed a route generator which is based on the multi-space sampling heuristic (MSH). MSH is a heuristic originally proposed by Mendoza and Villegas (2013) for the vehicle routing problem with stochastic demands. It has shown to be competitive for solving other routing problems such as the VRP with stochastic travel and service times (Gómez et al., 2016), the Green VRP (Montoya et al., 2016), and the combined maintenance and routing problem (Fontecha et al., 2020). MSH is a multi-space search strategy with two phases. In the first phase (sampling) it samples multiple solution representation spaces via a set of randomized route-first cluster-second heuristics, while in the second phase (assembling), it uses the sampled elements to assemble a solution to the problem. The route-first cluster-second approach (Beasley, 1983; Prins et al., 2014) followed by the randomized heuristics consists on using a TSP heuristic to select a tour in the set $\mathcal{T}$ of TSP-like tours (i.e., giant tours visiting all customers that start and end at the depot) and splitting it into feasible routes. Then, this set of routes is used to map the selected tour to a solution in the set of all feasible solutions to the problem $\mathcal{S}$. In MSH the solution is obtained by solving a set partitioning problem on the set of routes sampled in the first phase. Finding a solution to the MP-E-VRP requires the assignment of the EVs to the routes and the scheduling of the charging operations. Consequently, our route generator only handles the construction of the pool of routes to be used as input for the other methods.

### 5.3.2 Detailed algorithm description

Our route generator works in two phases: sampling and assembling. In the sampling phase the algorithm uses a set $\mathcal{U}$ of randomized TSP heuristics to obtain a set of TSP-like tours. Then, RouteGenerator extracts every feasible route that can be obtained without altering the order of the customers of each TSP tour. RouteGenerator uses these routes to build a set $\Omega \subset \mathcal{R}$, where $\mathcal{R}$ is the set of all feasible routes. In the assembling phase RouteGenerator obtains a subset of $\Omega$ by solving a set partitioning formulation on it.

#### 5.3.2.1 General structure

Algorithm 1 describes the routes generator general structure. The procedure works per period $p \leq |\mathcal{P}| - 1$. Let $\mathcal{V}_p^* = \mathcal{I}_p \cup \{0\}$ and $\mathcal{V}^* = \bigcup_{p \in \mathcal{P}} \mathcal{V}_p^*$. `RouteGenerator` starts by entering the sampling phase (lines 8-20). At each iteration $n \leq N$, the algorithm selects a sampling heuristic from a set $\mathcal{U}$ (line 11) and uses it to build a TSP tour $tsp^{pn}$ starting from the depot and visiting the customers that must be serviced in that period ($\forall i \in \mathcal{V}_p^*$). Then, the algorithm uses a tour splitting procedure (known as `Split`) to retrieve a set of routes added to the set of routes for period $p$, $\Omega_p \in \mathcal{R}$. Routes in $\Omega_p$ respect the maximum duration, related with the opening hours of the depot ($L_p - E_p$),

and the maximum energy consumption, $Q$. `Split` also retrieves $s_p^n$, the best set of routes that can be obtained from $\Omega_p^n$ visiting all customers in period $p$ while minimizing the energy consumption. $s_p^n$ is used to update an upper bound $f(s_p^*)$ on the objective function of the set partitioning formulation solved in line 23 (see lines 15-18). Then the algorithm enters the assembling phase (lines 22-26). Per $\varkappa \in \{1, \ldots, |\mathcal{K}|\}$, the algorithm calls procedure `SetPartitioning` to solve a set partitioning formulation over $\Omega_p$ using $f(s_p^*)$ as upper bound. The solution to this problem, $\Omega_{p\varkappa}$ is such that $|\Omega_{p\varkappa}| = \varkappa$. If the set partitioning is infeasible, `SetPartitioning` returns an empty set. $\Omega_{p\varkappa}$ is stored in $\Omega$ and is used as an input in subsequent solution methods.

#### 5.3.2.2 Sampling heuristic

RouteGenerator use randomized versions of four TSP constructive heuristics to sample $\mathcal{U}$, the set of TSP-like tours. The strategies adopted are those presented by Mendoza and Villegas (2013), which are described here for the sake of completeness.

Let $tsp^{pn}$ be an ordered set of vertices representing the TSP tour being built by a given sampling heuristic at iteration $n$ for period $p$, $\mathcal{B}_p$ the set of vertices visited by $tsp^{pn}$, and $\mathcal{F}_p = \mathcal{V}_p^* \setminus \mathcal{B}_p$ an ordered set of non-routed vertices. With the aim of simplifying, we assume that sets $\mathcal{B}_p$ and $\mathcal{F}_p$ are updated every time a vertex is added to $tsp^{pn}$. Let $\iota$ be a random integer in $\{1, \ldots, \min\{U, |\mathcal{F}_p|\}\}$, where parameter $Z$ denotes the randomization factor of each heuristic. Let $\mathcal{F}_p^\iota$ be the $\iota$-th element in the ordered set $\mathcal{F}_p$. Table 5.1 provides the functioning of the four sampling heuristics.

#### 5.3.2.3 Split

To extract $\langle \Omega_p^n, s_p^n \rangle$ from $tsp^{pn}$ (line 13 in Algorithm 1), we adapt the optimal splitting procedure for the VRP introduced by Prins (2004). Given the giant tour $tsp^{pn} = (0, \nu_1, \nu_1, \ldots, \nu_i, \ldots, \nu_{|\mathcal{I}_p|}, 0)$ where $\nu_i$ represents the customer in the $i$-th position, the splitting procedure builds a directed acyclic graph $\mathcal{G}_p^n = (\mathcal{V}_p^n, \mathcal{A}_p^n)$ composed of the ordered vertex set $\mathcal{V}_p^n$ and the arc set $\mathcal{A}_p^n$. $\mathcal{V}_p^n$ contains an auxiliary vertex $\nu_0 = 0$ and $|\mathcal{I}_p|$ nodes numbered from 1 to $|\mathcal{I}_p|$, where node $i$ represents customer $\nu_i$ (that is, the customer in $i$-th position in $tsp^{pn}$). $\mathcal{A}_p^n$ contains arc $(i-1, j)$ if and only if route $r_{ij} = (0, \nu_i, \ldots, \nu_j, 0)$, with duration $t_{r_{ij}}$ and energy consumption $e_{r_{ij}}$, is feasible. Our heuristic obtains $\Omega_p^n$ by adding to it one route for each arc in $\mathcal{A}_p^n$. Furthermore, to obtain $s_p^n$, the procedure finds the shortest path connecting 0 and $\nu_{|\mathcal{I}_p|}$ in $\mathcal{G}_p^n$. The arcs along this shortest path represent the routes chosen, guaranteeing that each customer is visited exactly once. It should be pointed out that since $\mathcal{G}_p^n$ is directed and acyclic, building the graph and finding the shortest path can be done simultaneously (Prins, 2004).

Algorithm 2 shows the tour splitting procedure based on the one developed for the capacitated VRP (Prins, 2004). First, `Split` initializes the shortest path labels (lines 2–6). Then, it enters the exterior loop (lines 7–34). This starts by setting the tail of an arc and initializing an empty route (lines 8–12). After that, it enters the interior loop to scan all the arcs sharing the same tail node (lines 13–33). At each iteration of the interior loop, a new arc is explored by adding the next customer to the route (line 16). Next, `Split` computes the weight and time of the arc (lines 17–23). For the MP-E-VRP,

**Algorithm 1:** Route generator: general structure

```
1  Function RouteGenerator(P, V*, K, M, U, N)
2      Ω ⟵ ∅
3      for ϰ ← 1 to |K| do
4          Ω_ϰ ⟵ ∅
5      end
6      n ⟵ 1
7      for p ← 0 to |P| − 1 do
8          Ω_p ⟵ ∅
9          while n ≤ N do
10             for l ← 1 to |U| do
11                 h ⟵ U_l            // selects a sampling heuristic
12                 tsp^pn ⟵ h(V*_p) // builds a TSP tours visiting customers in
                    I_p
13                 ⟨Ω^n_p, s^n_p⟩ ⟵Split (V*_p, tsp^pn)       // splits the TSP tours to
                    retrieve routes
14                 Ω_p ⟵ Ω_p ∪ Ω^n_p
15                 if n = 1 then
16                     s*_p ⟵ s^n_p
17                 else if f(s^n_p) < f(s*_p) then
18                     s*_p ⟵ s^n_p
19                 n ⟵ n + 1
20             end
21         end
22         for ϰ ← 1 to |K| do
23             Ω_pϰ ⟵ SetPartitioning (V*_p, Ω_p, s*_p, ϰ)
24             Ω_ϰ ⟵ Ω_ϰ ∪ Ω_pϰ
25             Ω ⟵ Ω ∪ Ω_pϰ
26         end
27     end
28     Ω_K ⟵ ∅
29     for ϰ ← 1 to |K| do
30         Ω_K ⟵ Ω_K ∪ {Ω_ϰ};
31     end
32     return ⟨Ω, Ω_K⟩
33 End
```

Table 5.1: Sampling heuristics for RouteGenerator

| Heuristic | Initialization | At each iteration | Stopping criterion |
|---|---|---|---|
| RNN | $tsp^{pn} = (0), v = 0$ | -identify vertex $v'$ that is the $\iota$-th nearest vertex to $v$<br>-append $v'$ to $tsp^{pn}$<br>-set $v = v'$ | $\lvert\mathcal{F}_p\rvert = 0$<br>-append 0 to $tsp^{pn}$ to complete the tour |
| RNI | $tsp^{pn}$ is a tours starting at the depot and performing a round trip to a randomly selected customer | -sort $\mathcal{F}_p$ in nondecreasing order of $e_{min}(v')\star$<br>-insert $v' = \mathcal{F}_p^{\iota}$ in the best possible position in the tour $tsp^{pn}$ $\star\star$ | $\lvert\mathcal{F}_p\rvert = 0$ |
| RBI | $tsp^{pn}$ is a tours starting at the depot and performing a round trip to a randomly selected customer | -sort $\mathcal{F}_p$ in nondecreasing order of $\mu_{min}(v')$ $\star\star\star$<br>-insert $v' = \mathcal{F}_p^{\iota}$ in the best possible position in the tour $tsp^{pn}$ $\star\star$ | $\lvert\mathcal{F}_p\rvert = 0$ |
| RFI | $tsp^{pn}$ is a tours starting at the depot and performing a round trip to a randomly selected customer | -sort $\mathcal{F}_p$ in nondecreasing order of $e_{max}(v')$ $\star\star\star\star$<br>-insert $v' = \mathcal{F}_p^{\iota}$ in the best possible position in the tour $tsp^{pn}\star$ | $\lvert\mathcal{F}_p\rvert = 0$ |

RNN: randomized nearest neighbor
RNI: randomized nearest insertion
RBI: randomized best insertion
RFI: randomized farthest insertion
$\star e_{min}(v') = \min\{e_{v,v'} | v' \in \mathcal{B}_p\}$
$\star\star$ the position generating the smallest increment in the cost of the tour
$\star\star\star \mu_{min}(v') = \min\{e_{v,v'} + e_{v',v''} - e_{v,v''} | (v, v'') \in tsp^{pn}\}$
$\star\star\star\star\ e_{max}(v') = \max\{e_{v,v'} | v' \in \mathcal{B}_p\}$

these two measures correspond to the total energy consumption $e_r$ and total time $t_r$ of the associated route. Then, the algorithm checks for the feasibility of the route associated to the arc by means of function `CheckFeasibility` and stores the result in a boolean variable $feas_r$ (line 24). `CheckFeasibility` validates if route $r$ can be part of a solution to the MP-E-VRP, that is, with respect to its energy consumption ($e_r \leq Q$) and duration ($t_r \leq L_p - E_p$, where $p$ is the period in which route $r$ is performed). Additionally, if $p = 0$ and $e_r > Q_0^k, \forall k \in \mathcal{K}$, `CheckFeasibility` also checks the possibility to charge an EV before performing the route. For this, the function checks if the route duration, $t_r$, allows for charging the most charged EV with the fastest mode and performing the route before $L_p$. If the route is feasible, the corresponding arc is added to the graph. If the shortest path label of the head node of arc $(i, j)$ can be improved (i.e., $label_{i-1} + e_r \leq label_j$ ), `Split` updates the shortest path label and the predecessor information (lines 28–31). Then, the algorithm starts the next interior-loop iteration or exits the loop. After completing the exterior loop `Split` retrieves the best set of routes that can be obtained using the tour $tsp^{pn}$ and the predecessor labels (for an algorithm to retrieve this set of routes we refer the reader to Prins (2004)).

Fig. 5.1 illustrates the tour splitting procedure. Fig. 5.1a shows the TSP tour and the relevant information. Fig. 5.1b depicts the auxiliary graph.

#### 5.3.2.4 Set partitioning

In the assembly phase, RouteGenerator finds a subset of routes $\Omega_{p\varkappa}$ from set $\Omega_p$ by solving a set partitioning

$$\min_{\Omega_{p\varkappa} \subseteq \Omega_p} \left\{ \sum_{r \in \Omega_{p\varkappa}} e_r : \cup_{r \in \Omega_{p\varkappa}} = \mathcal{V}_p^*; |\Omega_{p\varkappa}| = \varkappa; r_i \cap r_j = 0 \ \forall r_i, r_j \in \Omega_{p\varkappa} \right\} \tag{5.2}$$

The set partitioning is intended to select the best set of routes from $\Omega_p$ that minimizes energy consumption while guaranteeing that each customer will be visited by exactly one route. The cardinality of this set must be equal to $\varkappa$. We use a commercial optimizer to solve the set partitioning.

## 5.4 DM-C: a constructive heuristic for the MP-E-VRP

### 5.4.1 Introduction

The methodologies we propose to solve the MP-E-VRACSPm are all based on solving MILPs. In consequence, we can be faced to the difficulty of finding a solution, especially for larger instances. Therefore, we propose a constructive heuristic for computing an initial solution to the MP-E-VRACSPm by focusing on the solution space associated to the MP-E-VRACSP. Our constructive heuristic, defined as DM-C, takes as input a set of routes $\Omega_\varkappa$, with $\varkappa \in \{1, ..., |\mathcal{K}|\}$. For each period, the heuristic assigns the route with the highest energy consumption to the EV with the most available energy and continues the assignment until all routes of the period are assigned. In addition, the heuristic checks for

**Algorithm 2:** Split

**Function** `Split`$(\mathcal{V}_p^*, tsp^{pn})$
  $label_0 \longleftarrow 0$ // *label*: shortest path labels
  **for** $i \leftarrow 1$ **to** $|\mathcal{I}_p|$ **do**
    $label_i \longleftarrow +\infty$
    $pred_i \longleftarrow 0$ // *pred*: predecessor labels
  **end**
  **for** $i \leftarrow 1$ **to** $|\mathcal{I}_p|$ **do**
    $r \longleftarrow (0)$ // initialize route $r$
    $e_r \longleftarrow 0$ // initialize total energy consumption $e_r$
    $t_r \longleftarrow 0$ // initialize total time $t_r$
    $j \longleftarrow i$
    $continue \longleftarrow true$
    **while** $j \leq |\mathcal{I}_p|$ **and** $continue = true$ **do**
      $\nu \longleftarrow tsp_j^{pn}$ // get customer in position $j$ of $tsp^{pn}$
      $\nu' \longleftarrow tsp_{j-1}^{pn}$ // get customer in position $j-1$ of $tsp^{pn}$
      $r \longleftarrow r \cup \{\nu\}$
      **if** $j = 1$ **then**
        $e_r \longleftarrow e_{0,\nu} + e_{\nu,0}$ // update total energy consumption
        $t_r \longleftarrow t_{0,\nu} + t_{\nu,0} + \delta_\nu + \delta_0$ // update total time
      **else**
        $e_r \longleftarrow e_r - e_{\nu',0} + e_{\nu',\nu} + e_{\nu,0}$ // update total energy consumption
        $t_r \longleftarrow t_r - t_{\nu',0} + t_{\nu',\nu} + t_{\nu,0} + \delta_\nu$ // update total time
      **end**
      $feas_r \longleftarrow$ `CheckFeasibility`$(r)$ // evaluate route feasibility
      **if** $feas_r = false$ **then**
        $continue \longleftarrow false$
      **end**
      **if** $label_{i-1} + e_r \leq label_j$ **and** $continue = true$ **then**
        $label_j \longleftarrow label_{i-1} + e_r$ // update label
        $pred_j \longleftarrow i - 1$ // update predecessor
      **end**
      $j \longleftarrow j + 1$
    **end**
  **end**
  $s \longleftarrow RetrieveRoutes(pred, tsp^{pn})$
  **return** $s$;
**End**

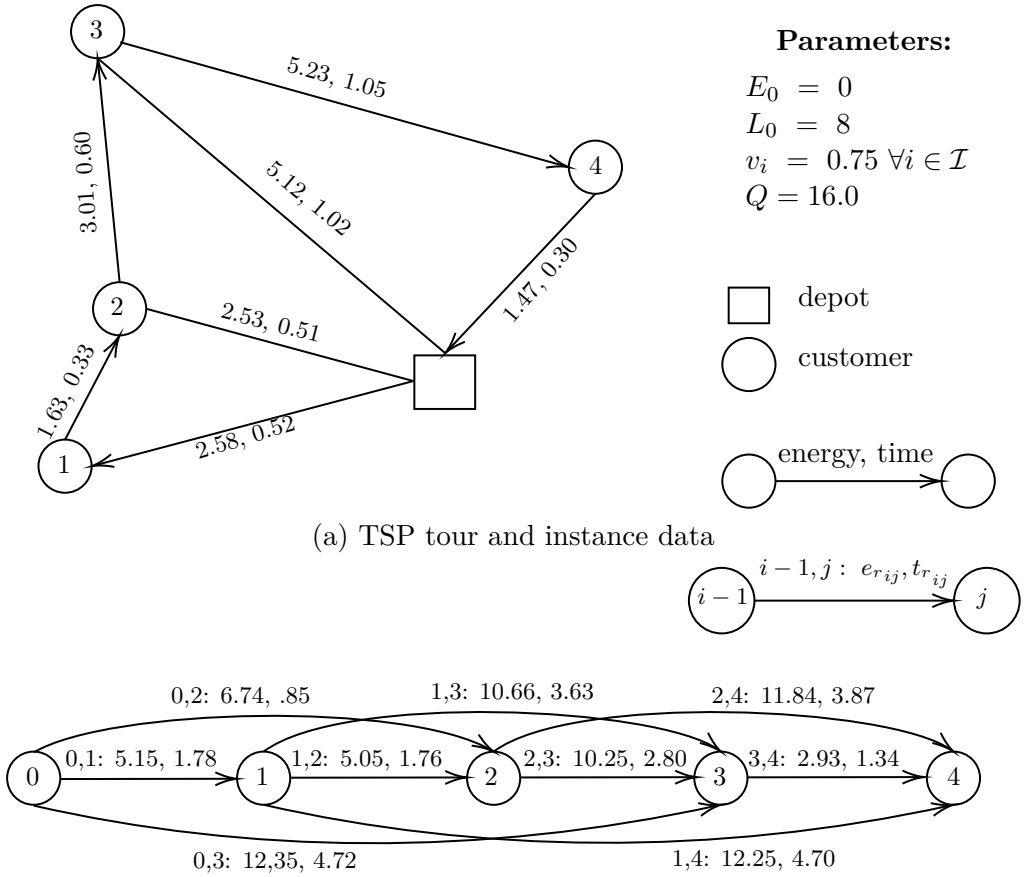


(a) TSP tour and instance data

(b) Auxiliary graph

**Fig. 5.1.** An example of the splitting procedure

the satisfaction of the charging infrastructure capacity constraints. This heuristic, though simple, allows for speeding up the search process in solving the MP-E-VRACSPm by using the methods developed in Sections 5.5 and 5.6.

### 5.4.2 Detailed algorithm description

DM-C is a constructive algorithm that assigns EVs to routes sequentially, recharging EVs if needed. For each period $p \in \mathcal{P}$, the heuristic creates set $unassigned\Omega_{p\varkappa} \subseteq \Omega_{p\varkappa}$ to pick routes from, in decreasing order of energy consumption. After selecting route $i \in \Omega_{p\varkappa}$, DM-C creates a set $avail\mathcal{K} \subseteq \mathcal{K}$ to choose the EV to be assigned to $i$. Then, DM-C evaluates the feasibility of assigning an EV from $avail\mathcal{K}$ by considering the EVs one by one in decreasing order of energy availability. The first EV for which the assignment is feasible is considered the EV chosen for route $i$. This process is repeated until all routes to be performed in the current period have their EV assigned. Additionally, if there are EVs not assigned, they are not charged.

Aiming at the feasibility of the EV-to-route assignment in subsequent periods, DM-C recharges the EV to the maximum energy possible in the current period. However, it checks with the charging modes in increasing order of consumed power value. This to reduce both the fixed cost per charge and the chance of exceeding the power grid capacity. DM-C verifies that the assignment is energy and time feasible. Besides, it checks for the satisfaction of the charging infrastructure capacity constraints. When an EV is to be recharged, the algorithm creates a charging operation $o$. DM-C checks if it incurs in a constraint violation if it includes $o$ in the set of already fixed charging operations $\mathcal{O}$. If such is the case, $o$'s starting time is shifted for later in the planning horizon. The assignment is again checked for energy and time feasibility. If it is feasible, $o$ is added to $\mathcal{O}$ and the EV is assigned to the route.

Algorithm 3 presents the general structure of DM-C which uses auxiliary functions presented in Algorithm 4. Among the parameters introduced by the algorithm, we provide the definition of the following, as they require further explanation:

- $t_i$: duration of route $i$
- $\mathcal{O}$: set of charging operations
- $e_k$: available energy on EV $k$
- $availTimeCharge_{k,p}$: time remaining in period $p-1$ that can be used to charge EV $k$ in period $p$
- $unassigned\Omega_{p\varkappa} \subseteq \Omega_{p\varkappa}$: routes still not assigned to a EV in period $p$
- $e_{\Omega_{p\varkappa}} = \{e_i : p \in \mathcal{P} \wedge i \in \Omega_{p\varkappa}\}$: energy consumption of routes to be performed in period $p$
- $avail\mathcal{K} \subseteq \mathcal{K}$: set of EVs available to be assigned to a route in the current period
- $maxRT$: charging time available to charge an EV in the current period

- $avail\mathcal{M} \subseteq \mathcal{M}$: set of charging modes still not considered to charge an EV in the current period
- $v_{\mathcal{M}} = \{v_m : m \in \mathcal{M}\}$: power consumption of charging modes
- $m(o)$: charging mode of charging operation $o$

In addition to auxiliary functions in Algorithm 4, the procedure uses the following functions:

- `RechargingTime`$(k, i, m)$: time to recharge EV $k$ to perform route $i$ with mode $m$
- `Max`$(set, criterion)$: draw from $set$ an element with maximum value of attribute in set $criterion$
- `Min`$(set, criterion)$: draw from $set$ an element with minimum value of attribute in set $criterion$
- `Update`$(\lambda)$: update solution $\lambda$ with new information
- `Update`$(e_k)$: update available energy on EV $k$
- `CreateCharOper`$(k, m, t)$: creates a charging operation in which EV $k$ is recharged to the maximum energy possible during time $t$ using charging mode $m$
- `Start`$(o)$: start time of charging operation $o$
- `End`$(o)$: end time of charging operation $o$
- `ShiftCharOper`$(o, \mathcal{O})$: shifts charging operation $o$ based on charging operations on set $\mathcal{O}$

Procedure `DM-C` receives as input the pool of routes $\Omega_{\varkappa}$ and sets $\mathcal{P}, \mathcal{K}$ and $\mathcal{M}$, and returns a solution to the MP-E-VRP. The procedure starts by initializing the relevant information (lines 2-7). Next, it enters the main for-loop to assign EVs to the routes in $\Omega_{\varkappa}$ (lines 8-39). For each period $p \in \mathcal{P}$ the heuristic selects the route with the highest energy consumption $i$ (line 12). Then, it enters a while-loop that is iterated until either an EV has been assigned to route $i$ or no EV can perform the route (lines 14-30). The algorithm selects the EV with the most available energy $k$. If $k$ is not charged to its maximum capacity $Q$, `DM-C` checks if it can be recharged to the maximum energy possible taking into account the time needed to recharge. It starts checking with the charging mode with minimum power $m$. If it is feasible, the algorithm calls procedure `RechargeAssignEV`. This function recharges EV $k$ and assigns it to route $i$ if the charging operation is feasible. If it is not feasible, a different charging mode is chosen and the process is repeated (lines 20-26). If $k$ was already charged to its maximum capacity, it is assigned to $i$ directly (see function `AssignEV` in line 28). If no EV can be recharged to perform the route, a warning message is printed. The process followed with route $i$ is repeated for all the routes to be assigned in period $p$ (lines 11-31). Finally, if there are any EVs left unassigned in period $p$, the solution $\lambda$ is updated with this information (lines 32-38).

As shown in Algorithm 4, `RechargeAssignEV` uses function `CheckCharOperFeas` to check if it is feasible to recharge EV $k$ with mode $m$ during time $maxRT$ to perform route $i$. The result is stored in a boolean variable $charOperFeasibility$. If the value of $charOperFeasibility$ is `true`, the EV is assigned and solution $\lambda$ is updated. In more detail, `CheckCharOperFeas` creates charging operation $o$ and checks if the introduction of $o$ leads to the violation of the charging infrastructure constraints (regarding the maximum power to be consumed by all chargers at any time and the number of chargers available for mode $m$). If so, the starting time of the charging operation is shifted for later in the planning horizon, when it starts to be feasible. The energy charged on $k$ and the start of the route are adjusted accordingly. If EV $k$ can still perform the route, charging operation $o$ is added to the set $\mathcal{O}$ and $charOperFeasibility$ is set to `true`.

In theory, this method can obtain infeasible solutions, because the assignment of EVs to routes and the execution of charging operations are considered fixed after finding a feasible match. However, in the computational experiments we performed we could obtain feasible solutions for all the instances.

## 5.5 DM-M: a MILP formulation for the MP-E-VRACSP

We define the MP-E-VRACSP on a multigraph $\mathcal{G} = (\mathcal{V}, \mathcal{A})$ similar to the one for the MP-E-VRP (see Section 4.2). We associate a driving time and an energy consumption to every arc $(i, j)^k \in \mathcal{A}_k$. Table 5.2 summarizes how these values are set.

Fig. 5.2 shows the graph $\mathcal{G}$ obtained for an instance with one EV, two periods, two routes per period and two charging modes (*slow* and *moderate*), following the same conventions of Fig. 4.3.

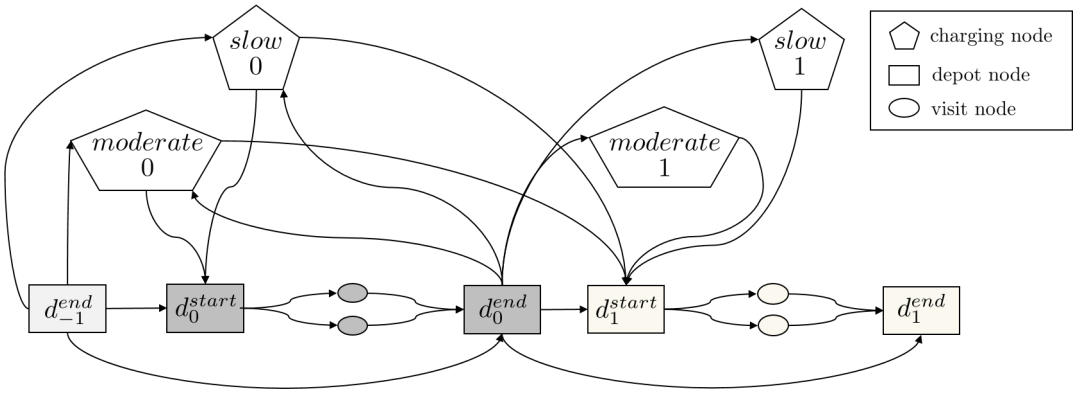


**Fig. 5.2.** An example of the multigraph $\mathcal{G}$ obtained for one particular instance to the MP-E-VRACSP with one EV.

The MILP formulation for the MP-E-VRACSP is a modified version of formulation $[F^1]$. This formulation, denoted as $[F^2]$, is obtained by replacing constraints (4.7), (4.8) and (4.41) with the following constraints:

**Algorithm 3:** DM-C: general structure

**Function** DM-C($\Omega_{\varkappa}, \mathcal{P}, \mathcal{K}, \mathcal{M}$)
  $\lambda \leftarrow undefined$
  $\mathcal{O} \longleftarrow \emptyset$
  **for** $k \in \mathcal{K}$ **do**
    $e_k \leftarrow kWh_0^k$
    $availTimeCharge_{k,-1} \leftarrow 0$
  **end**
  **for** $p \leftarrow 0$ **to** $|\mathcal{P}| - 1$ **do**
    $unassigned\Omega_{p\varkappa} \leftarrow \Omega_{p\varkappa}$
    $avail\mathcal{K} \leftarrow \mathcal{K}$
    **while** $unassigned\Omega_{p\varkappa} \neq \emptyset$ **do**
      $i \leftarrow$Max($unassigned\Omega_{p\varkappa}, e_{\Omega_{p\varkappa}}$)
      $assignedEVtoRoute \leftarrow false$
      **while** $assignedEVtoRoute = false$ **and** $avail\mathcal{K} \neq \emptyset$ **do**
        $k \leftarrow$Max($avail\mathcal{K}, e_{\mathcal{K}}$)
        **if** $e_k < Q$ **then**
          $maxRT \leftarrow availTimeCharge_{k,p-1} + (L_p - t_i - L_{p-1})$
          $chargingModeNotFound \leftarrow true$
          $avail\mathcal{M} \leftarrow \mathcal{M}$
          **while** $chargingModeNotFound = true$ **and** $avail\mathcal{M} \neq \emptyset$ **do**
            $m \leftarrow$Min($avail\mathcal{M}, v_{\mathcal{M}}$)
            $neededRT \leftarrow$ RechargingTime($k$,$i$,$m$)
            **if** $neededRT \leq maxRT$ **then**
              RechargeAssignEV($k, i, m, maxRT$)
            **end**
          **end**
        **else**
          AssignEV($k, i$)
        **end**
      **end**
    **end**
    **while** $avail\mathcal{K} \neq \emptyset$ **do**
      $k \leftarrow$Max($avail\mathcal{K}, e_{\mathcal{K}}$)
      Update($\lambda$)
      **if** $p < |\mathcal{P}|$ **then**
        $availTimeCharge_{k,p} \leftarrow L_p - E_p$
      **end**
    **end**
  **end**
  **return** $\lambda$
**End**

**Algorithm 4:** DM-C: auxiliary functions

**Function** `RechargeAssignEV`$(k, i, m, maxRT)$
  $\{charOperFeasibility, endTimeRoute\} \leftarrow$ `CheckCharOperFeas`$(k, i, m, p, maxRT)$;
  **if** $charOperFeasibility = true$ **then**
    `Update`$(\lambda)$;
    `Update`$(e_k)$;
    $availTimeCharge_{k,p} \leftarrow L_p - endTimeRoute$;
    $chargingModeNotFound \leftarrow false$;
    $assignedEVtoRoute \leftarrow true$;
  **end**
**End**
**Function** `AssignEV`$(k, i, m, maxRT)$
  `Update`$(\lambda)$;
  `Update`$(e_k)$;
  $availTimeCharge_{k,p} \leftarrow L_p - t_i$;
  $assignedEVtoRoute \leftarrow true$;
**End**
**Function** `CheckCharOperFeas`$(k, i, m, p, maxRT)$
  $\{o, energyCharged, endTimeRoute\} \leftarrow$`CreateCharOper`$(k, m, maxRT)$;
  $powerCons \leftarrow v_m$;
  $chargersCount \leftarrow 1$;
  **for** $o' \in \mathcal{O}$ **do**
    **if** `End`$(o')$>`Start`$(o)$ **then**
      $powerCons \leftarrow powerCons + v_{m(o')}$;
      **if** $m(o') = m$ **then**
        $chargersCount \leftarrow chargersCount + 1$;
      **end**
    **end**
  **end**
  **if** $powerCons > PW_{max}$ **or** $chargersCount > A_m$ **then**
    $\{o, energyCharged, endTimeRoute\} \leftarrow$`ShiftCharOper`$(o, \mathcal{O})$;
  **end**
  **if** $e_k + energyCharged \geq e_i$ **and** $endTimeRoute \leq L_{p_i}$ **then**
    $\mathcal{O} \leftarrow \mathcal{O} \cup \{o\}$;
    $chargingModeNotFound \leftarrow false$;
    $assignedEVtoRoute \leftarrow true$;
    $charOperFeasibility \leftarrow true$;
  **else**
    $charOperFeasibility \leftarrow false$;
  **end**
  **return** $\{charOperFeasibility, endTimeRoute\}$;
**End**

Table 5.2: Definition of the arcs in $\mathcal{A}_k \subset \mathcal{A}$, $k \in \mathcal{K}$, in $\mathcal{G} = (\mathcal{V}, \mathcal{A})$ for the MP-E-VRACSP

| Definition | Driving time ($t_{ij}$) | Energy consumption ) ($e_{ij}$) |
|---|---|---|
| $(d_p^{start}, i)^k : p \in \mathcal{P}, i \in \mathcal{I}_p$ | $t_i$ | $e_i$ |
| $(i, d_p^{end})^k : p \in \mathcal{P}, i \in \mathcal{I}_p$ | 0 | 0 |
| $(d_{p-1}^{end}, d_p^{start})^k : p \in \mathcal{P}$ | 0 | 0 |
| $(d_{p-1}^{end}, d_p^{end})^k : p \in \mathcal{P}$ | 0 | 0 |
| $(d_p^{end}, l)^k : p \in (\mathcal{P} \setminus \{P_{max} - 1\}) \cup \{-1\}, l \in \bigcup_{h \leq p+1} \mathcal{C}_h$ | 0 | 0 |
| $(l, d_p^{start})^k : p \in \mathcal{P}, l \in \bigcup_{h \leq p} \mathcal{C}_h$ | 0 | 0 |

$$y_{ij}^k \leq Q x_{ij}^k \qquad \forall k \in \mathcal{K}, \forall (i,j)^k \in \mathcal{A}_k \tag{5.3}$$

$$y_{ij}^k \geq e_{ij} x_{ij}^k \qquad \forall k \in \mathcal{K}, \forall (i,j)^k \in \mathcal{A}_k \tag{5.4}$$

$$\sum_{(i,j)^k \in \mathcal{A}_k} \left( \tau_{ij}^k + t_{ij} x_{ij}^k \right) = \sum_{(j,l)^k \in \mathcal{A}_k} \tau_{jl}^k \qquad \forall j \in \mathcal{I}, \forall k \in \mathcal{K} \tag{5.5}$$

The MILP formulation for the modified version of the MP-E-VRACSP is based on formulation $[F^2]$. We only replace constraints (4.2) with the following constraints:

$$\sum_{k \in \mathcal{K}} \sum_{i \in \mathcal{I}} \sum_{(i,j)^k \in \mathcal{A}_k} \psi_{ni} x_{ij}^k = 1 \qquad \forall n \in \mathcal{J} \tag{5.6}$$

This formulation is denoted as $[F^{2m}]$.

## 5.6 DM-LB: a local branching approach for the MP-E-VRP

### 5.6.1 Introduction

Local branching is a heuristic proposed by Fischetti and Lodi (2003) that performs local searches in neighborhoods obtained by adding linear inequalities to a MILP formulation. Starting with an initial solution, it defines the neighrborhood surrounding it by adding cuts, called local branching constraints. Then, it explores the neighborhood using a MILP solver to find better solutions. The algorithm prevents being trapped in a local optimum by applying a diversification strategy in the sense of local search metaheuristics. Local branching is intended to obtain earlier and more often updates of the incumbent solution, accelerating the global search. This algorithm has been used to solve many optimization problems obtaining very good results. Among them we can find the capacitated fixed-charge network design problem (Rodríguez-Martín and Salazar-González, 2010), the train formation plan (Yaghini et al., 2013), the quay crane scheduling problem (Legato and Trunfio, 2014), the yard template planning (Zhen et al., 2016), the open pit mine

production scheduling problem (Samavati et al., 2017), the capacitated ring tree problem (Hill and Voß, 2018), the Graph Edit Distance Problem (Darwiche et al., 2019) and the vehicle routing problem with stochastic demands (Hernandez et al., 2019). For solving the MP-E-VRACSP, we adapt the neighborhood definition and the diversification strategy to consider the problem-dependent information.

### 5.6.2 The DM-LB framework

We consider the MILP formulation $[F^{2m}]$. In their general framework, Fischetti and Lodi (2003) define the neighborhood based on the set of all binary variables of the underlying MILP formulation. We focus, instead, only on variables $x_{ij}^k \in \{0,1\}$. They represent the path followed by the vehicles, visiting customers and recharging at the different chargers available at the depot. The remaining binary variables, $\omega_{ob}$ and $w_{oo'}$, that model charging operations sequencing, can be inferred by the model based on variables $x_{ij}^k$.

The local branching cuts are implemented as follows. Given a solution $s^n$ of $[F^{2m}]$, let $S^n := \{i,j \in \mathcal{V}, k \in \mathcal{K} : x_{ij}^k = 1\}$. For positive integer parameter $\kappa$, the $\kappa$-opt neighborhood $\mathcal{N}(s^n,\kappa)$ of $s^n$ corresponds to the set of the feasible solutions of $[F^{2m}]$ that meet the additional local branching constraint

$$\Delta(s,s^n) := \sum_{(i,j,k)\in S^n} (1 - x_{ij}^k) + \sum_{(i,j,k)\notin S^n} x_{ij}^k \leq \kappa \tag{5.7}$$

ensuring that the number of variables $x_{ij}^k$ changing their value with respect to $s^n$ is $\kappa$ at most (i.e., that the Hamming distance between $s$ and $s^n$ is maximum $\kappa$). Local branching bifurcates the solution space associated to $s^n$ by adding to the current MILP formulation the local branching constraint (5.8), corresponding to the left branch, or $\Delta(s,s^n) \geq \kappa + 1$, corresponding to the right branch.

The procedure followed by the local branching algorithm is illustrated in Fig. 5.3. This figure presents the different cases that may arise during the execution of the algorithm. Starting with an initial solution $s^0$ at node 1, local branching defines the neighborhood $\mathcal{N}(s^0,\kappa)$ by adding the local branching constraint $\Delta(s,s^0) \leq \kappa$. The resulting formulation is solved using the MILP solver in order to find the best solution in $\mathcal{N}(s^0,\kappa)$ within a time limit, called *node_time_limit* and fixed to all nodes. This corresponds to node 2 in Fig. 5.3. The *node_time_limit* is imposed to avoid consuming the computing time in hard-to-solve nodes. If a new solution $s^1$ is found within the *node_time_limit* and it is optimal in $\mathcal{N}(s^0,\kappa)$, the constraint $\Delta(s,s^0) \leq \kappa$ is replaced by $\Delta(s,s^0) \geq \kappa + 1$ and the right branch from node 1 is explored. This guarantees that the subsequencing neighborhoods to be explored will not contain the neighborhood previously visited. A new left branch is created to explore the neighborhood $\mathcal{N}(s^1,\kappa)$ associated with solution $s^1$, by adding constraint $\Delta(s,s^1) \leq \kappa$ (see node 4 in Fig. 5.3). This time, a feasible but suboptimal solution $s^2$ is found within the *node_time_limit*. In this case, the constraint $\Delta(s,s^1) \leq \kappa$ is deleted and a new local branching constraint $\Delta(s,s^2) \leq \kappa$ is added. As the neighborhood $\mathcal{N}(s^1,\kappa)$ was not completely explored, replacing the constraint $\Delta(s,s^1) \leq \kappa$ with $\Delta(s,s^1) \geq \kappa + 1$ would eliminate the possibility of exploring a (possibly) promising region of this neighborhood. Following, the exploration of the neighborhood $\mathcal{N}(s^2,\kappa)$ does

not lead to a feasible solution (see node 5 in Fig. 5.3). In that case, constraint $\Delta(s, s^2) \leq \kappa$ is replaced by $\Delta(s, s^2) \leq \kappa/2$, in order to visit a smaller neighborhood and increase the possibility to find an improved solution. If doing so results in not finding a feasible solution again (node 6 in Fig. 5.3), then a diversification step is applied to explore a different region of the search space (as it will be explained in what follows). The algorithm continues until either a *total_time_limit* or a maximum number of diversifications (*dv_max*) is exceeded.

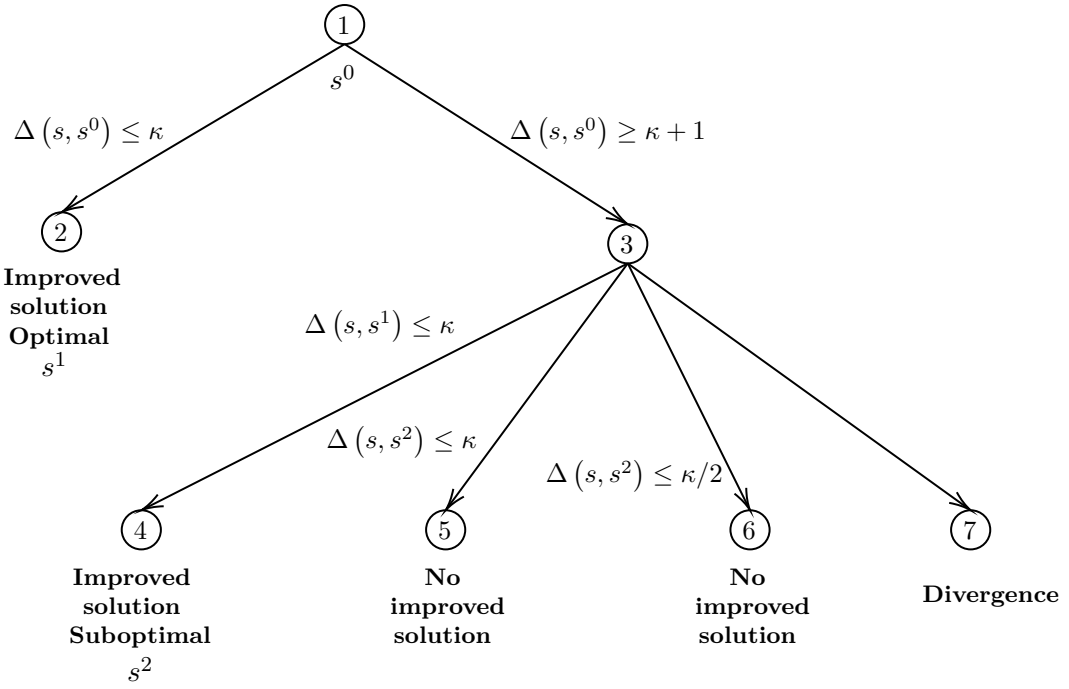


**Fig. 5.3.** DM-LB flow

Our diversification strategy consists on changing a certain percentage of routes, in order to explore a different region of the search space. The routes are the component of the problem that influences the most the objective function. The diversification constraint is then

$$\Delta_{div}(s, s^n) := \sum_{(i,j,k) \in S^n_{route}} (1 - x^k_{ij}) + \sum_{(i,j,k) \notin S^n_{route}} x^k_{ij} \geq \kappa_{dv} \tag{5.8}$$

where $S^n_{route} := \{i, j \in \mathcal{V}, i \vee j \in \mathcal{I}, k \in \mathcal{K} : x^k_{ij} = 1\}$ and $\kappa_{dv}$ is the minimum percentage of routes to be changed.

We define $\kappa_{dv}$ as

$$\kappa_{dv} = \max\{minChangedRoutes, percRoutesChange \times nRoutes\} \tag{5.9}$$

where parameters *minChangedRoutes* and *percRoutesChange* are the minimum number of routes to be changed and the percentage of routes to be changed. The actual number

of routes to be changed depends on the relation between $minChangedRoutes$ and $nRoutes$, the number of routes in the current solution.

#### 5.6.2.1 Detailed algorithm description

Algorithm 5 provides the general structure of DM-LB which uses auxiliary functions presented in Algorithm 6. Function `LocBra` receives as input the neighborhood size ($\kappa$), the maximum execution time ($total\_time\_limit$), the time limit for each branch explored ($node\_time\_limit$), the maximum number of diversifications allowed ($dv\_max$), the minimum number of routes to be changed when performing a diversification $minChangedRoutes$ and the percentage of routes to be changed $percRoutesChange$. The function returns as output the best solution obtained $s^*$. The algorithm starts by retrieving an initial feasible solution using the function `FirstSol` and adding the local branching constraint related to this solution; the time for branching is also updated (lines 5-8). This first solution can be obtained by solving the MILP formulation within a time limit or by any other method. Then, `LocBra` enters in a while loop that will be exploring the branches of the tree search until any of the conditions is met: the maximum execution time is achieved or the maximum number of diversifications allowed is reached (lines 9-24). At each iteration, the function `MILPSolver` is called to solve a new MILP problem using a solver (line 11). This function receives as input the time for branching ($tl$), the upper bound ($UB$) used as a cut-off for the optimization process, the current solution ($\tilde{s}$), and the flag $first\_sol$ to be set to true for terminating the optimization when the first feasible solution is found. Moreover, DM-LB uses flag $mod\_dv$ to force a diversification in the next iteration if certain conditions are met.

Depending on the solver optimization *status*, different cases emerge:

- An **optimal solution** is found (lines 14-16). If the new solution is better than the one saved, the function `NewReferenceSol` is called to replace the last local branching constraint, add a new local branching constraint, and update the current and best solutions. The latter, if the new solution is better than the best one saved. If the new solution is equal to the best one already saved, `Diversify` is called to omit the current neighborhood and jump to a different region of the search space. By forcing to change a certain percentage of the routes chosen in current solution, `Diversify` allows the algorithm to skip the current neigborhood. Additionally, `Diversify` resets $UB$ to $+\infty$ and sets $first\_sol = true$ in order to terminate the next optimization when finding the first feasible solution, no matter if it is worst that the best one known.
- A **feasible solution** is found but its optimality could not be proven. This because of the time limit or because $first\_sol = true$, so the optimization was terminated after finding the first feasible solution (lines 17-19). The function `NewReferenceSol` is called to delete the last local branching constraint, add a new local branching constraint, and update the best solution (if the new solution is better than the one saved). Recall that replacing the last local branching constraint with its right-branch counterpart, as it is done in the previous case, would lead to excluding a (possibly) promising region of this neighborhood

- **No feasible solution** is found (lines 20-22). If flag $mode\_dv = false$, the function `ReduceNeighborhood` is called to replace $\kappa$ by $\kappa/2$ in the last local branching constraint, so as to reduce the current neighborhood and facilitate the search. Additionally, $mode\_dv$ is set to *true* to force a diversification in the next iteration, if again no feasible solution is found. If a diversification was done in the previous iteration, a new diversification is carried out.

- The MILP being solved is **infeasible** (line 23). This means that the current MILP is proven to have no feasible solution of cost strictly less than the input upper bound $UB$. Hence, the function `Diversify` is called to search in a new region in the search space.

**Algorithm 5:** *LocBra* algorithm

```
1  Function LocBra(κ, total_time_limit, node_time_limit,
       dv_max, dv_cons_max, minChangedRoutes, percRoutesChange)
2      bestUB, UB ← ∞; s*, s̄, s̃ ← undefined
3      time_limit, elapsed_time, dv, dv_cons, κ_current, κ_div, nRoutes ← 0
4      mode_dv ← false; first_sol ← false
5      elapsed_time ← FirstSol()
6      κ_current ← κ
7      NewReferenceSol()
8      time_limit ← node_time_limit  // Set the time for branching
9      while elapsed_time < total_time_limit and dv ≤ dv_max and dv_cons ≤ dv_cons_max do
10         time_limit ← min{time_limit, total_time_limit − elapsed_time}
11         ⟨status, nRoutes⟩ ← MILPSolver(time_limit, UB, s̃)
12         time_limit ← node_time_limit
13         κ_div ← max{minChangedRoutes, percRoutesChange × nRoutes}
14         if status = "opt_sol_found" then
15             if s̃ ≠ s̄ then NewReferenceSol() else Diversify()
16         end
17         if status = "feasible_sol_found" then
18             NewReferenceSol()
19         end
20         if status = "no_feasible_sol_found" then
21             if mode_dv = false then ReduceNeighborhood() else Diversify()
22         end
23         if status = "infeasible" then Diversify()
24         elapsed_time ← elapsed_time + time_limit
25     end
26     return s*
27 End
```

**Algorithm 6:** *LocBra* auxiliary functions

**Function** `NewReferenceSol()`
  **if** *first_sol* = *false* **and** $\bar{s} \neq undefined$ **then**
    **if** *status* $\neq$ "$feasible\_sol\_found$" **then** replace last added constraint $\Delta(s, \bar{s}) \leq \kappa\_current$ by $\Delta(s, \bar{s}) \geq \kappa\_current + 1$
    **else** delete last added constraint $\Delta(s, \bar{s}) \leq \kappa\_current$
  **end**
  $\bar{s} \leftarrow \tilde{s}$; $UB \leftarrow f(\tilde{s})$; $mode\_dv \leftarrow false$; $dv\_cons \leftarrow 0$
  $\kappa\_current \leftarrow \kappa$; $first\_sol \leftarrow false$
  add new constraint $\Delta(s, \bar{s}) \leq \kappa\_current$
  **if** $UB < bestUB$ **then** $s^* \leftarrow \tilde{s}$; $bestUB \leftarrow f(\tilde{s})$
**End**

**Function** `Diversify()`
  **if** *status* = $no\_feasible\_sol\_found$ **then**
    delete last added constraint $\Delta(s, \bar{s}) \leq \kappa\_current$
  **else**
    replace last constraint $\Delta(s, \bar{s}) \leq \kappa\_current$ with $\Delta(s, \bar{s}) \geq \kappa\_current + 1$
  **end**
  add new constraint $\Delta_{div}(s, \bar{s}) \geq \kappa\_div$
  $UB, time\_limit \leftarrow \infty$; $dv \leftarrow dv + 1$; $mode\_dv, first\_sol \leftarrow true$
  $dv\_cons \leftarrow dv\_cons + 1$
  $\kappa\_current \leftarrow \kappa$
**End**

**Function** `ReduceNeighborhood()`
  replace last added constraint $\Delta(s, \bar{s}) \leq \kappa\_current$ by $\Delta(s, \bar{s}) \leq \lceil \kappa\_current/2 \rceil$
  $\kappa\_current \leftarrow \lceil \kappa\_current/2 \rceil$
  $mode\_dv \leftarrow true$; $first\_sol \leftarrow false$; $dv\_cons \leftarrow 0$
**End**

## 5.7 Computational experiments

We performed computational experiments to compare the performance of the decomposition methods presented in this chapter. We implemented the algorithms in Java (jre V.1.8.0) and used Gurobi Optimizer (version 8.0.1) to solve the MILP formulations through its Java API. We used a single thread with 15 GB. The experiments were carried out on a Compute Canada's high-performance computing facility (see Appendix B for characteristics). We set a 3-hour time limit, and CPU times are reported in seconds and rounded to the nearest integer. We performed our tests on testbed G1 (see Section 4.5.1.1), contaning small-sized instances, and on a 120-instances testbed, denoted G2, containing medium-sized instances. Gaps are computed using Equation 4.71. Section 5.7.1 provides information on testbed G2.

### 5.7.1 G2 testbed

Instances of testbed G2 follow the same considerations provided on Section 4.5.1. We generated instances with 15, 25, 30, 45, 50, and 60 customers per period. For each number of customers per period (Customer/$p$), we generated 5 sets of customers locations. We adjusted the number of EVs depending on the number of customers per period. Furthermore, this adjustment tries to capture the level of difficulty added by adding more EVs. For that reason the number of EVs does not increase at the same pace as the number of customers per period. Table 5.3 summarizes the parameter setting of testbed G2.

Table 5.3: Parameter setting for testbed G2 (5 instances for each number of customers per period)

| Parameters | Values | | | | | |
|---|---|---|---|---|---|---|
| Periods | 3 | | | | | |
| Customers/$p$ | 15 | 25 | 30 | 45 | 50 | 60 |
| EVs | 5 | 6 | 11 | 15 | 11 | 21 |
| Power grid capacity | 35 | 41 | 71 | 95 | 71 | 131 |
| Initial energy | 8 kWh or 12.8 kWh | | | | | |
| Charging mode | one (*slow*) or two (*slow* and *moderate*) | | | | | |

### 5.7.2 Experimentation settings

All parameters are set based on preliminary tests. Table 5.4 presents the values given to the parameters for each method. Besides, Tables 5.5 and 5.6 provide the size of model $[F^{2m}]$ for instances in testbeds G1 and G2, with the pool of routes $\Omega$ as obtained with RouteGenerator. This allows the reader to assess the size of the model to be solved. Some details are to be made according to the method:

- RouteGenerator: values for the sampling heuristic parameters are chosen based on the original version of MSH (Mendoza and Villegas, 2013)

- DM-C: we conducted an experiment to select the minimum value for $\varkappa$ for which a feasible solution can be obtained using DM-C. This value depends on the instance. We obtained feasible solutions for all the instances in G1 and G2
- DM-M: we tested for using the solution obtained by DM-C as an initial solution to speed up the search process. Such method is then called DM-C-M
- DM-LB: to be certain we have a feasible solution in a timely manner, we chose to use the solution obtained by DM-C as the first solution. Moreover, although this would not represent a decomposition method per se, we tested for using $[F^1]$ as a base MILP formulation. We denote this method as DM-LB-$[F^1]$. DM-LB is then modified to use this formulation. Notice that $dv\_max$ is set to $+\infty$, which means that these algorithms will run until reaching the $total\_time\_limit$

Table 5.4: Parameter setting for decomposition methods

| Method | Parameter | Value |
|---|---|---|
| RouteGenerator | $N$ | 500 |
| | $Z_{RNN}$ | 3 |
| | $Z_{RNI}$ | 6 |
| | $Z_{RFI}$ | 6 |
| | $Z_{RBI}$ | 6 |
| DM-C | $\Omega_{\varkappa}$ | Pool of fixed routes from RouteGenerator |
| | $\varkappa$ | Minimum number of routes per period leading to a feasible solution (same number for all periods) |
| DM-M | $\Omega$ | Pool of routes from RouteGenerator |
| DM-LB | $s^0$ | Solution obtained with DM-C |
| | $\kappa$ | 25 (Customers/$p$: 5-25)<br>10 (Customers/$p$: 30-50)<br>5 (Customers/$p$: 60) |
| | $\kappa\_div$ | 10% |
| | $dv\_div$ | $+\infty$ |
| | node_time_limit | 600s |
| | total_time_limit | 10800s (3h) |
| DM-LB-$[F^1]$ | $s^0$ | Solution obtained with DM-C |
| | $\kappa$ | 20 (Customers/$p$: 5-25)<br>5 (Customers/$p$: 30-60) |
| | $\kappa\_div$ | 10% |
| | $dv\_div$ | $+\infty$ |
| | node_time_limit | 600s |
| | total_time_limit | 10800s (3h) |

In conclusion, we compare the performance of the following methods: DM-M, DM-C-M, DM-LB, and DM-LB-$[F^1]$.

Table 5.5: Size of instances for testbed G1 with $[F^{2m}]$

| | | Number of charging modes | | | |
|---|---|---|---|---|---|
| | | 1 | | 2 | |
| Customers/$p$ | EVs | Avg. number of variables | Avg. number of constraints | Avg. number of variables | Avg. number of constraints |
| 5 | 2 | 485.6 | 693.8 | 894.6 | 1513.8 |
| | 4 | 1446.8 | 2812.4 | 2767.8 | 11002.4 |
| 10 | 5 | 2141 | 4851 | 4107 | 22018 |
| | 4 | 1367.6 | 2721.8 | 2688.6 | 10911.8 |
| 15 | 5 | 2063 | 4762 | 4029 | 21929 |

Table 5.6: Size of instances for testbed G2 with $[F^{2m}]$

| | | Number of charging modes | | | |
|---|---|---|---|---|---|
| | | 1 | | 2 | |
| Customers/$p$ | EVs | Avg. number of variables | Avg. number of constraints | Avg. number of variables | Avg. number of constraints |
| 15 | 5 | 2057 | 4754 | 4023 | 21921 |
| 25 | 6 | 2770.4 | 7532.2 | 5514.6 | 38725.8 |
| 30 | 11 | 9103.4 | 40906.2 | 17552.4 | 257421.2 |
| 45 | 15 | 16418 | 99472 | 31899 | 670899 |
| 50 | 11 | 8463.2 | 40112.6 | 17044.2 | 256803.6 |
| 60 | 21 | 32308.4 | 266216.2 | 61717.8 | 1883558.4 |

### 5.7.3 Results in testbed G1

All methods find feasible solutions for the instances in G1. We first checked for the convenience of including an initial solution to speed up the optimization process for DM-M, that is, we compare the performance of DM-M and DM-C-M. Both methods find the optimal solution for all instances with $[F^{2m}]$. Table 5.7 shows the average solution time (Time) for both methods, for each value of customers per period and EVs. This time includes the computing time for RouteGenerator. It is apparent from this table that using the first feasible solution provided by DM-C slows down the optimization process. In fact, an inspection of the instances allowed us to see that in more than 70% of the instances DM-M is faster than DM-C-M. Therefore, we excluded DM-C-M for the following analyses in testbed G1.

Table 5.7: Average solution time for DM-M and DM-C-M for testbed G1

| | | Time | |
|---|---|---|---|
| Customers/$p$ | EVs | DM-M | DM-C-M |
| 5 | 2 | 3 | 3 |
| | 4 | 27 | 28 |
| 10 | 5 | 639 | 791 |
| | 4 | 48 | 48 |
| 15 | 5 | 506 | 390 |

We report on Table 5.8 the average gap with respect to (wrt) the best MILP solution obtained (using $[F^1]$) and on Table 5.9 the average gap with respect to the best lower bound found for $[F^1]$, both for each number of customers per period. For easy of reading, we also provide the average gap for $[F^1]$ relative to the best lower bound found for this model. We only report results on instances with feasible solutions for $[F^1]$. From Table 5.8, we can see that from the three methods considered, DM-LB-$[F^1]$ is the one producing better improvements in relation to the solutions obtained by optimizing $[F^1]$. This improvements reaches up to 4% for instances with 15 customers per period. This conclusion is supported by results on Table 5.9, in which we can see that the gap with reference to the best lower bound is reduced by using DM-LB-$[F^1]$.

On the other hand, DM-M and DM-LB have average positive gaps for instances with 10 customers per period. Recall that both methods have $[F^{2m}]$ as base formulation. Moreover, as stated before, DM-M finds the optimal solution for all instances when solving $[F^{2m}]$. This suggest that, given the pool of routes $\Omega$ obtained by RouteGenerator, the solutions that can be obtained by DM-M and DM-LB are suboptimal. An inspection of the solutions allowed us to identify that, for some instances, some routes belonging to the best solution obtained by solving $[F^1]$ did not belong to the corresponding pool $\Omega$. For example, the solution for an instance included two routes to be performed in the first period, $p = 0$. These two routes do not belong to $\Omega_{02}$, the set of two routes minimizing the energy consumption in $p = 0$. An explanation for this situation is that, when assigning EVs to routes and scheduling the charging operations, the routes that minimize the cost of battery degradation are not necessarily the ones that minimize the energy consumption.

We now report in Table 5.10 the results obtained by comparing the matheuristic meth-

Table 5.8: Computational results for instances in testbed G1: gap wrt to best MILP solution ($[F^1]$)

| | Avg. gap wrt best MILP solution ($[F^1]$) | | |
|---|---|---|---|
| Customers/$p$ | DM-M | DM-LB | DM-LB-$[F^1]$ |
| 5 | 0.00% | 0.00% | 0.00% |
| 10 | 1.53% | 1.53% | -0.08% |
| 15 | -3.10% | -3.05% | -4.10% |

Table 5.9: Computational results for instances in testbed G1: gap wrt best lower bound for $[F^1]$

| | Avg. gap wrt best lower bound for $[F^1]$ | | | |
|---|---|---|---|---|
| Customers/$p$ | $[F^1]$ | DM-M | DM-LB | DM-LB-$[F^1]$ |
| 5 | 0.00% | 0.00% | 0.00% | 0.00% |
| 10 | 18.01% | 19.29% | 19.29% | 17.95% |
| 15 | 26.61% | 24.59% | 24.59% | 23.93% |

ods with each other. For each number of customers per period, we report the number of best known solutions (BKSs), the average gap to the BKS considering all the instances (Gap), and the average gap to the BKS considering only the instances for which the solution is different from the BKS (Gap$^*$). From this table, we can see that, even DM-LB-$[F^1]$ is the best method for instances in G1, the decomposition methods DM-M and DM-LB can still obtain good results, with a gap still under 5% with respect to the BKS obtained among the methods.

Table 5.10: Computational results for instances in testbed G1: methods comparison

| | DM-M | | | DM-LB | | | DM-LB-$[F^1]$ | | |
|---|---|---|---|---|---|---|---|---|---|
| Customers/$p$ | BKS | Gap | Gap$^*$ | BKS | Gap | Gap$^*$ | BKS | Gap | Gap$^*$ |
| 5 | 20 | 0.00% | - | 20 | 0.00% | - | 20 | 0.00% | - |
| 10 | 23 | 1.69% | 3.99% | 23 | 1.69% | 3.99% | 35 | 0.09% | 0.75% |
| 15 | 17 | 1.07% | 1.87% | 15 | 1.13% | 1.80% | 23 | 0.59% | 1.39% |

### 5.7.4 Results in testbed G2

We start by checking the benefits of using DM-C-M instead of DM-M. Table 5.11 shows the average solution time (Time) for both methods and the number of instances for which we obtain a optimal (#Optimal) and a feasible not proven to be optimal (#Feas) solution when solving $[F^{2m}]$. It is apparent from this table that from 30 customers per period, for more than half of the instances DM-M cannot find a feasible solution within three hours. Regarding DM-C-M, this method has a feasible solution for all instances by default (at worst, the one supplied by DM-C). However, it cannot find the optimal solution for the vast majority of instances.

We now present the results obtained with all methods: DM-M, DM-C-M, DM-LB, and DM-LB-$[F^1]$. Table 5.12 only provides the results for instances with feasible solutions for

Table 5.11: Average solution time and instances count for DM-M and DM-C-M for testbed G2

| | DM-M | | | DM-C-M | | |
|---|---|---|---|---|---|---|
| | $[F^{2m}]$ | | | $[F^{2m}]$ | | |
| Customers/$p$ | #Feas | #Optimal | Time | #Feas | #Optimal | Time |
| 15 | 0 | 20 | 506 | 0 | 20 | 390 |
| 25 | 4 | 16 | 3678 | 4 | 16 | 4300 |
| 30 | 12 | 0 | 3h | 20 | 0 | 3h |
| 45 | 9 | 0 | 3h | 20 | 0 | 3h |
| 50 | 9 | 1 | 3h | 20 | 0 | 3h |
| 60 | 3 | 0 | 3h | 20 | 0 | 3h |

DM-M. For each number of customers per period, we report the number of BKSs, the average gap to the BKS considering all the instances (Gap), and the average gap to the BKS considering only the instances for which the solution is different from the BKS (Gap$^*$). As we can see, DM-LB-$[F^1]$ does not seem to be the best alternative for large instances and DM-C-M seem to have the best overall performance. This figure can, however, be a distortion of reality, as not all instances are considered. Therefore, Table 5.13 provides the results for all instances, and so it only compares DM-C-M, DM-LB, and DM-LB-$[F^1]$. According to this table, DM-LB is now the method with best overall results for instances in G2.

Table 5.12: Computational results for instances in testbed G2: all instances with feasible solutions in DM-M

| | DM-M | | | DM-C-M | | | DM-LB | | | DM-LB-$[F^1]$ | | |
|---|---|---|---|---|---|---|---|---|---|---|---|---|
| Customers/$p$ | BKS | Gap | Gap* | BKS | Gap | Gap* | BKS | Gap | Gap* | BKS | Gap | Gap* |
| 15 | 10 | 1.06% | 2.12% | 10 | 1.06% | 2.12% | 9 | 1.13% | 2.06% | 9 | 0.82% | 1.49% |
| 25 | 18 | 0.02% | 0.21% | 17 | 0.05% | 0.33% | 11 | 0.34% | 0.76% | 2 | 3.09% | 3.43% |
| 30 | 7 | 0.50% | 1.38% | 11 | 0.00% | - | 2 | 1.22% | 1.49% | 0 | 8.23% | 8.23% |
| 45 | 4 | 1.93% | 3.87% | 7 | 0.01% | 0.11% | 0 | 3.88% | 3.88% | 0 | 7.78% | 7.78% |
| 50 | 7 | 0.03% | 0.11% | 7 | 0.07% | 0.32% | 2 | 0.95% | 1.22% | 0 | 11.57% | 11.57% |
| 60 | 3 | 0.00% | - | 3 | 0.00% | - | 0 | 1.40% | 1.40% | 0 | 20.45% | 20.45% |

Table 5.13: Computational results for instances in testbed G2: without DM-M

| | DM-C-M | | | DM-LB | | | DM-LB-$[F^1]$ | | |
|---|---|---|---|---|---|---|---|---|---|
| Customers/$p$ | BKS | Gap | Gap* | BKS | Gap | Gap* | BKS | Gap | Gap* |
| 15 | 10 | 1.06% | 2.12% | 9 | 1.13% | 2.06% | 9 | 0.82% | 1.49% |
| 25 | 17 | 0.05% | 0.31% | 11 | 0.34% | 0.75% | 3 | 3.09% | 3.63% |
| 30 | 13 | 2.02% | 5.77% | 9 | 1.07% | 1.94% | 3 | 5.34% | 6.28% |
| 45 | 12 | 2.58% | 6.46% | 9 | 1.69% | 3.08% | 3 | 3.82% | 4.49% |
| 50 | 9 | 1.35% | 2.46% | 12 | 0.42% | 1.06% | 1 | 5.85% | 6.16% |
| 60 | 4 | 7.53% | 9.41% | 17 | 0.21% | 1.40% | 7 | 7.42% | 11.41% |

## 5.8 Conclusions

In this chapter, we have presented a decomposition strategy to tackle the MP-E-VRP. The first subproblem to be solved consists on designing a high-quality and diverse pool of feasible routes. The second subproblem refers to selecting the routes to be performed, assigning EVs to them, and scheduling the charging operations that make this assignment feasible.

We have proposed three methods following this decomposition strategy. All of them use an existing heuristic to sample the space of feasible routes. To solve the second subproblem, we propose a constructive heuristic, a MILP formulation, and a local branching based approach. The constructive heuristic, yet simple, allows to find a feasible solution in short time. This solution can be provided to speed up the search process in the other decomposition strategies. The MILP formulation is built upon the MILP formulation presented for the MP-E-VRP (see Chapter 4). Finally, the local branching based approach is based in the MILP formulation presented in this chapter and lies in adding linear inequalities to this formulation, to explore the solution space by performing local searches on defined regions looking for good quality solutions.

With respect to the results of the computational experiments, two conclusions can be drawn. First, results allow to have insights in the difficulty of solving the MP-E-VRP. The pool of routes to be built must be of good quality and diverse enough to increase the possibility of finding the optimal routes, but having large pools makes the second subproblem more difficult to solve. Moreover, as the real degradation costs are revealed when assigning the EVs to the routes and scheduling the charging operations (that is, solving the second subproblem), the criterion used to select the routes to be included in the pool would then underestimate the cost related to a route. Second, the local branching based method allows for finding, in general, better results subject to the base MILP formulation. We were allowed to solve instances of up to 60 customers per period.

# Chapter 6

# General conclusions and perspectives

## 6.1 English version

This research has explored the optimization of the multi-period electric vehicle routing problem.

First, we have reviewed the OR literature in this topic. Starting from the classical VRP and its most important variants, we have identified a new stream of research concerned by the environmental impact of transportation activities, called green vehicle routing problems. Among them, the Electric Vehicle Routing problems (E-VRPs) extend classical routing problems by considering the limited driving range and long charging durations of electric vehicles (EVs). We have studied the E-VRP literature emphasizing on modeling rather than solution methods, to focus on how real-life characteristics have been incorporated. We have pointed out how improvements in battery technology entail a new line of E-VRPs based on depot charging rather than en route recharging. Moreover, we have stressed the importance of considering battery degradation concerns in transportation planning. From this analysis, we have identified the lack in the literature of E-VRPs coupling routing and charging scheduling over multiple days, to address battery aging properly.

Second, in view of the importance of battery degradation in transportation planning, we have presented a background on degradation of li-ion batteries, the preferred technology for EVs. We have emphasized on the economical and environmental issues related to battery degradation, as well as its effect on the distribution operations with EVs. We have summarized the most representative battery degradation models found in the literature. Given that battery degradation modeling is very complex (as it involves non-linear functions, interactions between variables, multiple parameters), their inclusion in optimization strategies is a challenging task. For this reason, we have approximated the battery degradation function as battery degradation costs that can be easily included to E-VRPs. These cost can be computed with readily available data, provided by battery manufacturers or relative to the operations themselves.

Third, we have defined a new E-VRP that addresses the gap found in the literature concerning the coupling of routing and charging scheduling over several days, to mitigate battery degradation in the long term. We have introduced this problem as the Multi-period Electric Vehicle Routing Problem (MP-E-VRP). Some of the special features of this problem are the consideration of depot charging infrastructure capacity constraints (e.g., grid constraints, the maximum number of available chargers), a realistic charging process and battery degradation costs associated with charging operations and routes. The objective is to determine for each period a set of routes visiting all the customers to be serviced and to schedule the charging operations of the EVs while minimizing the cost of battery degradation. This objective has not yet been widely used in E-VRPs. We have provided a mixed integer linear programming formulation (MILP) that integrates EV routing and depot charging scheduling, referred to as $[F^1]$. Unlike most E-VRP models found in the literature, $[F^1]$ models time in a continuous basis. Moreover, $[F^1]$ uses arc-based tracking variables, flow models to account for the power grid and charging infrastructure capacity constraints, and convex combination models to represent the battery degradation costs and charging functions. Since the MP-E-VRP is a new problem in the E-VRP literature, we have presented the procedure we followed to generate instances based on some insights provided by companies using EVs. The direct resolution of $[F^1]$ is computationally intractable for most of the instances, which gives us an idea of the difficulty of the problem and the relevance of designing more complex strategies.

To solve larger instances of the problem, we have decomposed the problem in two subproblems. The first subproblem concerns the generation of a pool of high-quality routes while relaxing the charging infrastructure capacity constraints. The second subproblem selects the routes from the pool, assign EVs to them, and schedule the charging operations. We have proposed three methods following this decomposition strategy. All of them use an existing heuristic to sample the space of feasible routes. To solve the second subproblem (routes selection, assignment of EVs, and scheduling of charging operations), we have proposed a constructive heuristic, a MILP formulation, and a local branching-based approach. The constructive heuristic, yet simple, allows finding a feasible solution in a short time. For each period, the heuristic assigns the route with the highest energy consumption to the EV with the most available energy and continues the assignment until all routes of the period are assigned. In addition, the heuristic checks for the satisfaction of the charging infrastructure capacity constraints. The solution obtained can then be provided to speed up the search process in the other decomposition strategies. We have obtained feasible solutions for all the instances considered, that is, instances with three periods and up to 60 customers per period.

We have built the decomposition method based on a MILP by modifying $[F^1]$, this new formulation is referred to as $[F^{2m}]$. Few modifications were needed to adapt $[F^1]$ to solve the new problem concerning the assignment of EVs to routes and the scheduling of the charging operations. This shows the versatility of the formulation to be adapted to different problems involving EV routing and charging scheduling in a multi-period scheme.

Lastly, we have implemented an adapted version of the local branching heuristic based on $[F^{2m}]$. Local branching is a matheuristic that performs local searches in neighborhoods obtained by adding linear inequalities to a MILP formulation. We have modified the neighborhood definition and the diversification strategy to consider MP-E-VRP fea-

tures. Neighborhoods are determined by considering variables related with EV-flow and the diversification strategy consists on changing a percentage of the routes chosen in the current solution in order to explore a different region of the search space.

In the experiments we conducted comparing the decomposition methods, the local branching-based heuristic proved to be the best method for finding solutions in large-size instances within a 3-hour time limit. This method shows an average gap of lest than 2% with respect to the best known solution and finds the most of best known solutions for the largest instances (with 50 and 60 customers per period in a 3-period planning horizon).

We identify several perspectives to improve this thesis work.

First, the constructive heuristic we have proposed assigns EVs to routes and schedule the charging operations in a sequential manner, fixing the assignment and the execution of the charging operations. This strategy could lead to infeasible instances when none of the EVs available on a period can be assigned to a route or a charging infrastructure capacity constraints violation is incurred and cannot be repaired (by shifting the new charging operation, for example). We could implement a procedure to repair an infeasible solution by reassigning EVs to routes, going backwards starting from the period for which the infeasibility is found.

Regarding the route generator, we could improve the quality of the pool of routes by minimizing the cumulative wear cost associated to the routes instead of the energy consumption in the set partitioning. This together with considering the EVs being initially charged at the start of each period with different energy values. This way, we could approximate the real cost of battery degradation incurred when an EV is assigned to a route with the aim of ameliorating the results obtained by solving the MP-E-VRACSP (i.e., the second subproblem in the decomposition strategy).

For the local branching-based approach, we could implement a method for parameter tuning using the design of experiment approach, as Yaghini et al. (2013) proposed. Accordingly, the solution objective function and CPU time would be the response variables, and the tuning parameters of the heuristic would be the factors, with the different values they can take corresponding to the levels of the factors.

Last, as another decomposition strategy, we could use a Benders' like decomposition of the MP-E-VRACSP, that is, the problem concerning the selection of the routes to be performed, the assignment of EVs to them, and the scheduling of the charging operations. Let a charging-routing sequence for an EV be a complete sequence of routes and charging operations such as the EV performs at most one route per period and the charging operations are scheduled in such a way the sequence is energy-feasible (i.e., when the EV starts a route, it has enough energy to complete it). The Benders' like decomposition would be composed by a charging-routing sequence selection master problem and a charging infrastructure capacity management subproblem. The master problem would consist of selecting a set of charging-routing sequences for the EVs such that every customer is covered exactly by one route. The subproblem would check if the charging infrastructure capacity constraints can be met. Preliminary ideas on how to solve this problem include defining a MILP model for the charging-routing sequence selection problem and a constraint programming model for the charging infrastructure capacity management subproblem. The MILP model would be derived directly from $[F^{2m}]$, by relaxing the charging infrastruc-

ture capacity constraints. Furthermore, as constraint programming has proven to be well suited for solving complex scheduling problems, we could take advantage of its capabilities for solving the subproblem (Baptiste et al., 2012). To this end, the charging and battery wear cost functions must be discretized and all parameters must be integer-valued.

## 6.2 Version française

Cette recherche a permis d'explorer l'optimisation du problème de routage des véhicules électriques à périodes multiples avec prise en compte des coûts liés à la dégradation des batteries.

Nous avons tout d'abord passé en revue la littérature sur la Recherche Opérationnelle dans ce domaine. En partant du problème de tournées de véhicules classique et de ses variantes les plus importantes, nous avons identifié un nouveau courant de recherche concerné par l'impact environnemental des activités de transport, appelé les problèmes de routage des véhicules verts. Parmi ceux-ci, les problèmes de routage des véhicules électriques (E-VRP) étendent les problèmes de routage classiques en prenant en compte l'autonomie limitée et les longues durées de charge des véhicules électriques (VEs). Nous avons étudié la littérature sur les E-VRPs en mettant l'accent sur la modélisation plutôt que sur les méthodes de résolution, pour nous concentrer sur la manière dont les caractéristiques réelles ont été incorporées. Nous avons souligné que les améliorations de la technologie des batteries impliquent un nouveau type de E-VRPs basés sur la recharge au dépôt plutôt que sur la recharge en route. De plus, nous avons souligné l'importance de prendre en compte les problèmes de dégradation des batteries dans la planification des transports. Cette analyse nous a permis d'identifier l'absence dans la littérature d'E-VRPs couplant le routage et la programmation de la charge sur plusieurs jours, afin de traiter correctement le problème du vieillissement des batteries.

Deuxièmement, compte tenu de l'importance de la dégradation des batteries dans la planification des transports, nous avons présenté l'état de l'art des modèles de dégradation des batteries lithium-ion, la technologie privilégiée pour les VEs. Nous avons mis l'accent sur les questions économiques et environnementales liées à la dégradation des batteries, ainsi que sur leurs effets sur les opérations de distribution des VEs. Nous avons résumé les modèles de dégradation des batteries les plus représentatifs trouvés dans la littérature. Étant donné que la modélisation de la dégradation des batteries est très complexe (car elle implique des fonctions non linéaires, des interactions entre variables, des paramètres multiples), leur prise en compte dans les stratégies d'optimisation est une tâche difficile. Pour cette raison, nous avons estimé la fonction de dégradation des batteries comme étant les coûts de dégradation des batteries qui peuvent être facilement inclus dans les E-VRP. Ces coûts peuvent être calculés à l'aide de données facilement disponibles, fournies par les fabricants de batteries ou relatives aux opérations elles-mêmes.

Troisièmement, nous avons défini un nouveau E-VRP qui comble le vide constaté dans la littérature concernant le couplage du routage et de la programmation de la charge sur plusieurs jours, afin d'atténuer la dégradation des batteries à long terme. Nous avons introduit ce problème sous le nom de « Multi-period Electric Vehicle Routing Problem » (MP-E-VRP). Ce problème se caractérise notamment par la prise en compte des contraintes

de capacité des infrastructures de chargement des dépôts (par exemple, les contraintes de réseau, le nombre maximum de chargeurs disponibles), un processus de chargement réaliste et des coûts de dégradation des batteries associés aux opérations de chargement et aux itinéraires. L'objectif est de déterminer pour chaque période un ensemble d'itinéraires visitant tous les clients à desservir et de programmer les opérations de charge des VEs tout en minimisant le coût de la dégradation des batteries. Cet objectif n'a pas encore été largement utilisé dans les E-VRP. Nous avons fourni une formulation de programmation linéaire mixte en nombres entiers (PLNE) qui intègre le routage des VEs et la programmation de la recharge au dépôt, appelée $[F^1]$. Contrairement à la plupart des modèles E-VRP que l'on trouve dans la littérature, le modèle $[F^1]$ fonctionne en continu. En outre, $[F^1]$ utilise des variables de suivi basées sur les arcs, des modèles de flot pour tenir compte des contraintes de capacité du réseau électrique et de l'infrastructure de charge, et des modèles de combinaison convexe pour représenter les coûts de dégradation des batteries et les fonctions de charge. Étant donné que le MP-E-VRP est un nouveau problème dans la littérature sur les E-VRPS, nous avons présenté la procédure que nous avons suivie pour générer des instances en nous basant sur certaines informations fournies par des entreprises utilisant des VEs. La résolution directe de $[F^1]$ est impossible à calculer pour la plupart des cas, ce qui nous donne une idée de la difficulté du problème et de la pertinence de concevoir des stratégies plus complexes.

Pour résoudre des instances de taille plus importante du problème, nous avons décomposé le problème en deux sous-problèmes. Le premier sous-problème concerne la génération d'un pool de routes de bonne qualité tout en assouplissant les contraintes de capacité des infrastructures de tarification. Le second sous-problème consiste à sélectionner les itinéraires du pool, à leur affecter des VEs et à programmer les opérations de recharge. Nous avons proposé trois méthodes suivant cette stratégie de décomposition. Elles utilisent toutes une heuristique existante pour échantillonner l'espace des itinéraires possibles. Pour résoudre le deuxième sous-problème (sélection des routes, affectation des VE et programmation des opérations de chargement), nous avons proposé une heuristique constructive, une formulation PLNE et une approche basée sur « *local branching* ». L'heuristique constructive, bien que simple, permet de trouver une solution réalisable en peu de temps. Pour chaque période, l'heuristique attribue la route ayant la plus grande consommation d'énergie à la VE ayant la plus grande énergie disponible et poursuit l'attribution jusqu'à ce que toutes les routes de la période soient attribuées. En outre, l'heuristique vérifie la satisfaction des contraintes de capacité de l'infrastructure de recharge. La solution obtenue peut alors être fournie pour accélérer le processus de recherche dans les autres stratégies de décomposition. Nous avons obtenu des solutions réalisables pour tous les cas considérés, c'est-à-dire des cas avec trois périodes et jusqu'à 60 clients par période.

Nous avons construit la méthode de décomposition basée sur une PLNE en modifiant $[F^1]$, cette nouvelle formulation est appelée $[F^{2m}]$. Quelques modifications ont été nécessaires pour adapter $[F^1]$ afin de résoudre le nouveau problème concernant l'affectation des VEs aux itinéraires et la programmation des opérations de recharge. Cela montre la polyvalence de la formulation qui peut s'adapter aux différents problèmes concernant l'affectation des VE aux itinéraires et la programmation des opérations de recharge dans un schéma multipériodique.

Enfin, nous avons implémenté une version adaptée de l'heuristique de « *local branching*

» basée sur $[F^{2m}]$. « *Local branching* » est une matheuristique qui effectue des recherches locales dans les voisinages obtenus en ajoutant des contraintes linéaires à une formulation PLNE. Nous avons modifié la définition des voisinages et la stratégie de diversification pour tenir compte des caractéristiques du MP-E-VRP. Les voisinages sont déterminés en tenant compte de variables liées au flot de VE et la stratégie de diversification consiste à modifier un pourcentage des itinéraires choisis dans la solution actuelle afin d'explorer une région différente de l'espace de recherche.

Dans les expériences que nous avons menées pour comparer les méthodes de décomposition, l'heuristique basée sur « *local branching* » s'est avérée être la meilleure méthode pour trouver des solutions dans des cas de grande taille dans un délai de 3 heures. Cette méthode montre un écart moyen de moins de 2 % par rapport à la meilleure solution connue et trouve la plupart des meilleures solutions connues pour les plus grandes instances (avec 50 et 60 clients par période dans un horizon de planification de 3 périodes).

Nous identifions plusieurs perspectives pour améliorer ce travail de thèse.

Premièrement, l'heuristique constructive que nous avons proposée assigne les VEs aux itinéraires et programme les opérations de recharge de manière séquentielle, en fixant l'assignation et l'exécution des opérations de recharge. Cette stratégie pourrait conduire à des cas irréalisables où aucun des VEs disponibles sur une période donnée ne peut être affecté à un itinéraire sans une violation des contraintes de capacité de l'infrastructure de recharge qui ne peut être réparé (en déplaçant la nouvelle opération de recharge, par exemple). Nous pourrions mettre en œuvre une procédure pour réparer une solution irréalisable en réaffectant les VEs aux itinéraires, en remontant dans le temps à partir de la période pour laquelle l'irréalisabilité est constatée.

En ce qui concerne le générateur de routes, nous pourrions améliorer la qualité du pool de routes en minimisant le coût de dégradation cumulé associé aux routes au lieu de la consommation d'énergie dans le « *set partitioning* ». Ceci, tout en considérant les VEs qui sont initialement chargés au début de chaque période avec des valeurs énergétiques différentes. De cette façon, nous pourrions estimer le coût réel de la dégradation des batteries encouru lorsqu'un VE est affecté à une route dans le but d'améliorer les résultats obtenus en résolvant le MP-E-VRACSP (c'est-à-dire le deuxième sous-problème de la stratégie de décomposition).

Pour l'approche basée sur « *Local branching* », nous pourrions mettre en œuvre une méthode de réglage des paramètres en utilisant l'approche du plan d'expérience, comme le propose Yaghini et al. (2013). En conséquence, la fonction objectif de la solution et le temps CPU seraient les variables de réponse, et les paramètres de réglage de l'heuristique seraient les facteurs, les différentes valeurs qu'ils peuvent prendre correspondant aux niveaux des facteurs.

Enfin, comme autre stratégie de décomposition, nous pourrions utiliser une décomposition de type Benders du MP-E-VRACSP, c'est-à-dire le problème concernant la sélection des itinéraires à effectuer, l'affectation des VEs à ceux-ci et la programmation des opérations de chargement. Soit la séquence de chargement-acheminement d'un VE une séquence complète de routes et d'opérations de chargement tel que le VE effectue au maximum une route par période et les opérations de chargement sont programmées de telle sorte que la séquence soit réalisable sur le plan énergétique (c'est-à-dire que lorsque le VE commence

une route, il a suffisamment d'énergie pour la terminer). La décomposition de type Benders serait composée d'un problème de sélection de la séquence de charge-acheminement et d'un sous-problème de gestion de la capacité de l'infrastructure de charge. Le problème principal consisterait à sélectionner un ensemble de séquences de chargement-acheminement pour les VEs de telle sorte que chaque client soit couvert exactement par un itinéraire. Le sous-problème consisterait à vérifier si les contraintes de capacité de l'infrastructure de recharge peuvent être respectées. Des idées préliminaires sur la manière de résoudre ce problème comprennent la définition d'un modèle MILP pour le problème de sélection des séquences de chargement-acheminement et un modèle de programmation par contraintes pour le sous-problème de gestion de la capacité de l'infrastructure de chargement. Le modèle MILP serait dérivé directement de $[F^{2m}]$, en assouplissant les contraintes de capacité de l'infrastructure de recharge. En outre, comme la programmation par contraintes s'est avérée bien adaptée à la résolution de problèmes d'ordonnancement complexes, nous pourrions tirer parti de ses capacités pour résoudre le sous-problème (Baptiste et al., 2012). À cette fin, les fonctions de recharge et du coût de dégradation de la batterie devraient être discrétisées et tous les paramètres doivent avoir une valeur entière.

# Bibliography


K. Abdulla, J. de Hoog, V. Muenzel, F. Suits, K. Steer, A. Wirth, and S. Halgamuge. Optimal operation of energy storage systems considering forecasts and battery degradation. *IEEE Transactions on Smart Grid*, 9(3):2086–2096, 2018.

A. Afroditi, M. Boile, S. Theofanis, E. Sdoukopoulos, and D. Margaritis. Electric vehicle routing problem with industry constraints: trends and insights for future research. *Transportation Research Procedia*, 3:452–459, 2014.

N. Ahmad. A framework for estimating carbon dioxide emissions embodied in international trade of goods. In *Measuring Sustainable Development. Integrated Economic, Environmental and Social Frameworks*, chapter 10. OECD Publishing, Paris, 2004.

G. B. Alvarenga, G. R. Mateus, and G. De Tomi. A genetic and set partitioning two-phase approach for the vehicle routing problem with time windows. *Computers & Operations Research*, 34(6):1561–1584, 2007.

J. Andelmin and E. Bartolini. An exact algorithm for the green vehicle routing problem. *Transportation Science*, 51(4):1288–1303, 2017.

E. Angelelli, M. Grazia Speranza, and M. W. Savelsbergh. Competitive analysis for dynamic multiperiod uncapacitated routing problems. *Networks*, 49(4):308–317, 2007.

O. Arslan, B. Yıldız, and O. E. Karaşan. Minimum cost path problem for plug-in hybrid electric vehicles. *Transportation Research Part E: Logistics and Transportation Review*, 80:123–141, 2015.

I. Baghdadi, O. Briat, J.-Y. Delétage, P. Gyan, and J.-M. Vinassa. Lithium battery aging model based on Dakin's degradation approach. *Journal of Power Sources*, 325(1): 273–285, 2016.

R. Baldacci, M. Battarra, and D. Vigo. Routing a heterogeneous fleet of vehicles. In B. Golden, S. Raghavan, and E. Wasil, editors, *The Vehicle Routing Problem: Latest Advances and New Challenges*, pages 3–27. Springer US, 2008.

P. Baptiste, C. Le Pape, and W. Nuijten. *Constraint-based scheduling: applying constraint programming to scheduling problems*, volume 39. Springer Science & Business Media, 2012.

J. Barco, A. Guerra, L. Muñoz, and N. Quijano. Optimal routing and scheduling of charge for electric vehicles: Case study. *Mathematical Problems in Engineering*, 2017: 1–16, 2017.

J. E. Beasley. Route first—cluster second methods for vehicle routing. *Omega*, 11(4): 403–408, 1983.

T. Bektaş, J. F. Ehmke, H. N. Psaraftis, and J. Puchinger. The role of operational research in green freight transportation. *European Journal of Operational Research*, 274(3):807–823, 2019.

M. B. Benedikt Sobotka. Batteries can power sustainable development. here's how, 01 2019. Retrieved on 25/11/2019 from `https://www.weforum.org/agenda/2019/01/batteries-can-power-sustainable-development-heres-how/`.

J. Betz, D. Werner, and M. Lienkamp. Fleet disposition modeling to maximize utilization of battery electric vehicles in companies with on-site energy generation. *Transportation Research Procedia*, 19(2016):241 – 257, 2016. Transforming Urban Mobility. mobil.TUM 2016. International Scientific Conference on Mobility and Transport. Conference Proceedings.

J. Blazewicz, J. K. Lenstra, and A. Rinnooy Kan. Scheduling subject to resource constraints: classification and complexity. *Discrete Applied Mathematics*, 5(1):11–24, 1983.

C. Bordin, H. O. Anuta, A. Crossland, I. Lascurain Gutierrez, C. J. Dent, and D. Vigo. A linear programming approach for battery degradation analysis and optimization in offgrid power systems with solar energy integration. *Renewable Energy*, 101:417–430, 2017.

U. Breunig, R. Baldacci, R. F. Hartl, and T. Vidal. The electric two-echelon vehicle routing problem. *Computers & Operations Research*, 103:198–210, 2019.

M. Bruglieri, F. Pezzella, O. Pisacane, and S. Suraci. A variable neighborhood search branching for the electric vehicle routing problem with time windows. *Electronic Notes in Discrete Mathematics*, 47:221–228, 2015.

M. Bruglieri, S. Mancini, F. Pezzella, O. Pisacane, and S. Suraci. A three-phase matheuristic for the time-effective electric vehicle routing problem with partial recharges. *Electronic Notes in Discrete Mathematics*, 58:95–102, 2017.

M. Bruglieri, S. Mancini, F. Pezzella, and O. Pisacane. A path-based solution approach for the green vehicle routing problem. *Computers & Operations Research*, 103:109–122, 2019a.

M. Bruglieri, S. Mancini, and O. Pisacane. The green vehicle routing problem with capacitated alternative fuel stations. *Computers & Operations Research*, 112:104759, 2019b.

J.-A. Bühne, D. Gruschwitz, J. Hölscher, M. Klötzke, U. Kugler, and C. Schimeczek. How to promote electromobility for European car drivers? Obstacles to overcome for a broad market penetration. *European Transport Research Review*, 7:30, 2015.

N. Bullard. Electric car price tag shrinks along with battery cost, 04 2019. Retrieved on 21/10/2019 from https://www.bloomberg.com/opinion/articles/2019-04-12/electric-vehicle-battery-shrinks-and-so-does-the-total-cost.

L. C. Casals, E. Martinez-Laserna, B. A. García, and N. Nieto. Sustainability analysis of the electric vehicle use in Europe for CO2 emissions reduction. *Journal of Cleaner Production*, 127:425–437, 2016.

L. C. Casals, B. A. García, F. Aguesse, and A. Iturrondobeitia. Second life of electric vehicle batteries: relation between materials degradation and environmental impact. *The International Journal of Life Cycle Assessment*, 22(1):82–93, 2017.

P. Chandra and M. L. Fisher. Coordination of production and distribution planning. *European Journal of Operational Research*, 72(3):503 – 517, 1994. ISSN 0377-2217.

Y. Choi and H. Kim. Optimal scheduling of energy storage system for self-sustainable base station operation considering battery wear-out cost. *Energies*, 9(6):462, 2016.

N. Christofides and J. E. Beasley. The period routing problem. *Networks*, 14(2):237–256, 1984.

B. Collins. Innolith battery strikes at 'flammable' lithium-ion: Q&A, 5 2019. Retrieved on 19/11/2019 from https://about.bnef.com/blog/innolith-battery-strikes-flammable-lithium-ion-qa/.

R. G. Conrad and M. A. Figliozzi. The recharging vehicle routing problem. In *Proceedings of the 2011 Industrial Engineering Research Conference*, pages 8–15. IISE Norcross, GA, 2011.

Á. Corberán and G. Laporte. *Arc routing: problems, methods, and applications*. SIAM, 2013.

J.-F. Cordeau and G. Laporte. The dial-a-ride problem: models and algorithms. *Annals of Operations Research*, 153(1):29–46, 2007.

T. G. Crainic and G. Laporte. Planning models for freight transportation. *European Journal of Operational Research*, 97(3):409–438, 1997.

G. B. Dantzig and J. H. Ramser. The truck dispatching problem. *Management science*, 6 (1):80–91, 1959.

M. Darwiche, D. Conte, R. Raveaux, and V. T'Kindt. A local branching heuristic for solving a graph edit distance problem. *Computers & Operations Research*, 106:225–235, 2019.

S. T. S. David Pearson. Better place's failure is blow to renault, 05 2013. Retrieved on 10/02/2020 from https://www.wsj.com/articles/SB10001424127887323855804578507263247107312.

R. S. de Campos, A. T. Simon, and F. de Campos Martins. Assessing the impacts of road freight transport on sustainability: A case study in the sugar-energy sector. *Journal of Cleaner Production*, 220:995–1004, 2019.

G. Desaulniers, J. Desrosiers, A. Erdmann, M. Solomon, and F. Soumis. *The VRP with pickup and delivery*, chapter 9. SIAM Monographs on Discrete Mathematics and Applications, 2001.

G. Desaulniers, O. B. Madsen, and S. Ropke. The vehicle routing problem with time windows. In *Vehicle Routing: Problems, Methods, and Applications*, chapter 5, pages 119–159. SIAM, second edition, 2014.

G. Desaulniers, F. Errico, S. Irnich, and M. Schneider. Exact algorithms for electric vehicle-routing problems with time windows. *Operations Research*, 64(6):1388–1405, 2016.

B. Dunn, H. Kamath, and J.-M. Tarascon. Electrical energy storage for the grid: a battery of choices. *Science*, 334(6058):928–935, 2011.

R. Eglese and T. Bektaş. Green vehicle routing. In *Vehicle Routing: Problems, Methods, and Applications*, chapter 15, pages 437–458. SIAM, second edition, 2014.

S. Erdoğan and E. Miller-Hooks. A green vehicle routing problem. *Transportation Research Part E: Logistics and Transportation Review*, 48(1):100–114, 2012.

Eurostat. Greenhouse gas emission statistics - emission inventories, 06 2019. Retrieved on 18/11/2019 from `https://ec.europa.eu/eurostat/statistics-explained/index.php/Greenhouse_gas_emission_statistics#Trends_in_greenhouse_gas_emissions`.

Á. Felipe, M. T. Ortuño, G. Righini, and G. Tirado. A heuristic approach for the green vehicle routing problem with multiple technologies and partial recharges. *Transportation Research Part E: Logistics and Transportation Review*, 71:111–128, 2014.

M. A. Figliozzi. The time dependent vehicle routing problem with time windows: Benchmark problems, an efficient solution algorithm, and solution characteristics. *Transportation Research Part E: Logistics and Transportation Review*, 48(3):616–636, 2012.

M. Fischetti and A. Lodi. Local branching. *Mathematical programming*, 98:23–47, 2003.

J. E. Fontecha, O. O. Guaje, D. Duque, R. Akhavan-Tabatabaei, J. P. Rodríguez, and A. L. Medaglia. Combined maintenance and routing optimization for large-scale sewage cleaning. *Annals of Operations Research*, 286(1):441–474, 2020.

A. Fotouhi, D. J. Auger, K. Propp, S. Longo, and M. Wild. A review on electric vehicle battery modelling: From lithium-ion toward lithium–sulphur. *Renewable and Sustainable Energy Reviews*, 56:1008–1021, 2016.

A. Franceschetti, D. Honhon, G. Laporte, T. Van Woensel, and J. C. Fransoo. Strategic fleet planning for city logistics. *Transportation Research Part B: Methodological*, 95: 19–40, 2017.

FREVUE. FREVUE Factsheet - UPS - Electricity grid infrastructure upgrade, 2016.

A. Froger, J. E. Mendoza, O. Jabali, and G. Laporte. The electric vehicle routing problem with capacitated charging stations. Working paper or preprint, 11 2019a. URL `https://hal.archives-ouvertes.fr/hal-02386167`.

A. Froger, J. E. Mendoza, O. Jabali, and G. Laporte. Improved formulations and algorithmic components for the electric vehicle routing problem with nonlinear charging functions. *Computers & Operations Research*, 104:256 – 294, 2019b.

M. Gendreau, G. Laporte, and R. Séguin. Stochastic vehicle routing. *European Journal of Operational Research*, 88(1):3 – 12, 1996.

D. Goeke and M. Schneider. Routing a mixed fleet of electric and conventional vehicles. *European Journal of Operational Research*, 245(1):81–99, 2015.

M. Goetschalckx and C. Jacobs-Blecha. The vehicle routing problem with backhauls. *European Journal of Operational Research*, 42(1):39–51, 1989.

A. Gómez, R. Mariño, R. Akhavan-Tabatabaei, A. L. Medaglia, and J. E. Mendoza. On modeling stochastic travel and service times in vehicle routing. *Transportation Science*, 50(2):627–641, 2016.

L. Grandinetti, F. Guerriero, F. Pezzella, O. Pisacane, et al. A pick-up and delivery problem with time windows by electric vehicles. *International Journal of Productivity and Quality Management*, 18(2-3):403–423, 2016.

P. Greim, A. Solomon, and C. Breyer. Assessment of lithium criticality in the global energy transition and addressing policy gaps in transportation. *Nature communications*, 11(1): 1–11, 2020.

A. Haghani and S. Jung. A dynamic vehicle routing problem with time-dependent travel times. *Computers & Operations Research*, 32(11):2959–2986, 2005.

S. Han, S. Han, and H. Aki. A practical battery wear model for electric vehicle charging applications. *Applied Energy*, 113:1100–1108, 2014.

S. Hartmann and D. Briskorn. A survey of variants and extensions of the resource-constrained project scheduling problem. *European Journal of Operational Research*, 207(1):1–14, 2010.

F. Hernandez, M. Gendreau, O. Jabali, and W. Rei. A local branching matheuristic for the multi-vehicle routing problem with stochastic demands. *Journal of Heuristics*, 25 (2):215–245, 2019.

G. Hiermann, J. Puchinger, S. Ropke, and R. F. Hartl. The electric fleet size and mix vehicle routing problem with time windows and recharging stations. *European Journal of Operational Research*, 252(3):995–1018, 2016.

G. Hiermann, R. F. Hartl, J. Puchinger, and T. Vidal. Routing a mix of conventional, plug-in hybrid, and electric vehicles. *European Journal of Operational Research*, 272(1): 235–248, 2019.

A. Hill and S. Voß. Generalized local branching heuristics and the capacitated ring tree problem. *Discrete Applied Mathematics*, 242:34–52, 2018.

J. Hof, M. Schneider, and D. Goeke. Solving the battery swap station location-routing problem with capacitated electric vehicles using an AVNS algorithm for vehicle-routing problems with intermediate stops. *Transportation Research Part B: Methodological*, 97: 102–112, 2017.

A. Hoke, A. Brissette, D. Maksimović, A. Pratt, and K. Smith. Electric vehicle charge optimization including effects of lithium-ion battery degradation. In *2011 IEEE Vehicle Power and Propulsion Conference*, pages 1–8. IEEE, 2011.

K. G. Høyer. The history of alternative fuels in transportation: The case of electric and hybrid cars. *Utilities Policy*, 16(2):63–71, 2008.

W. Jie, J. Yang, M. Zhang, and Y. Huang. The two-echelon capacitated electric vehicle routing problem with battery swapping stations: Formulation and efficient methodology. *European Journal of Operational Research*, 272(3):879 – 904, 2019.

M. Keskin and B. Çatay. Partial recharge strategies for the electric vehicle routing problem with time windows. *Transportation Research Part C: Emerging Technologies*, 65:111–127, 2016.

M. Keskin and B. Çatay. A matheuristic method for the electric vehicle routing problem with time windows and fast chargers. *Computers & Operations Research*, 100:172–188, 2018.

M. Keskin, G. Laporte, and B. Çatay. Electric vehicle routing problem with time-dependent waiting times at recharging stations. *Computers & Operations Research*, 107:77–94, 2019.

Ç. Koç and I. Karaoglan. The green vehicle routing problem: A heuristic based exact solution approach. *Applied Soft Computing*, 39:154–164, 2016.

Ç. Koç, O. Jabali, J. E. Mendoza, and G. Laporte. The electric vehicle routing problem with shared charging stations. *International Transactions in Operational Research*, 26 (4):1211–1243, 2018.

A. L. Kok, E. W. Hans, and J. M. Schutten. Vehicle routing under time-dependent travel times: the impact of congestion avoidance. *Computers & Operations Research*, 39(5): 910–918, 2012.

H. Kopfer and B. Vornhusen. Energy vehicle routing problem for differently sized and powered vehicles. *Journal of Business Economics*, 89(7):793–821, 2019.

T. O. Kouider, W. R. Cherif-Khettaf, and A. Oulamara. Constructive heuristics for periodic electric vehicle routing problem. In *Proceedings of the 7th International Conference on Operations Research and Enterprise Systems (ICORES 2018)*, pages 264–271, 2018.

N. D. Kullman, J. Goodson, and J. E. Mendoza. Electric Vehicle Routing with Public Charging Stations. Working paper or preprint, 04 2020. URL `https://hal.archives-ouvertes.fr/hal-01928730`.

L. Lam. A practical circuit-based model for state of health estimation of li-ion battery cells in electric vehicles. Master's thesis, University of Technology Delft, Netherlands, 2011.

G. Laporte. What you should know about the vehicle routing problem. *Naval Research Logistics (NRL)*, 54(8):811–819, 2007.

P. Lebeau, C. De Cauwer, J. Van Mierlo, C. Macharis, W. Verbeke, and T. Coosemans. Conventional, hybrid, or electric vehicles: which technology for an urban distribution centre? *The Scientific World Journal*, 2015, 2015.

P. Lebeau, C. Macharis, and J. Van Mierlo. Exploring the choice of battery electric vehicles in city logistics: A conjoint-based choice analysis. *Transportation Research Part E: Logistics and Transportation Review*, 91:245–258, 2016.

P. Legato and R. Trunfio. A local branching-based algorithm for the quay crane scheduling problem under unidirectional schedules. *4OR*, 12(2):123–156, 2014.

V. Leggieri and M. Haouari. A practical solution approach for the green vehicle routing problem. *Transportation Research Part E: Logistics and Transportation Review*, 104: 97–112, 2017.

J. K. Lenstra and A. R. Kan. Complexity of vehicle routing and scheduling problems. *Networks*, 11(2):221–227, 1981.

C. Li, T. Ding, X. Liu, and C. Huang. An electric vehicle routing optimization model with hybrid plug-in and wireless charging systems. *IEEE Access*, 6:27569–27578, 2018.

H. Li, Y. Lu, J. Zhang, and T. Wang. Trends in road freight transportation carbon dioxide emissions and policies in China. *Energy Policy*, 57:99–106, 2013.

J.-Q. Li, P. B. Mirchandani, and D. Borenstein. Real-time vehicle rerouting problems with time windows. *European Journal of Operational Research*, 194(3):711–727, 2009.

W. Li-ying and S. Yuan-bin. Multiple charging station location-routing problem with time window of electric vehicle. *Journal of Engineering Science & Technology Review*, 8(5): 190–201, 2015.

C.-S. Liao, S.-H. Lu, and Z.-J. M. Shen. The electric vehicle touring problem. *Transportation Research Part B: Methodological*, 86:163 – 180, 2016.

C. Lin, K. L. Choy, G. T. Ho, S. H. Chung, and H. Lam. Survey of green vehicle routing problem: past and future trends. *Expert Systems with Applications*, 41(4):1118–1138, 2014.

J. Lin, W. Zhou, and O. Wolfson. Electric vehicle routing problem. *Transportation Research Procedia*, 12:508–521, 2016.

C. Liu, J. Lin, H. Cao, Y. Zhang, and Z. Sun. Recycling of spent lithium-ion batteries in view of lithium recovery: A critical review. *Journal of Cleaner Production*, 228:801–813, 2019.

W. Lv, Z. Wang, H. Cao, Y. Sun, Y. Zhang, and Z. Sun. A critical review and analysis on the recycling of spent lithium-ion batteries. *ACS Sustainable Chemistry & Engineering*, 6(2):1504–1521, 2018.

G. Macrina, L. D. P. Pugliese, F. Guerriero, and G. Laporte. The green mixed fleet vehicle routing problem with partial battery recharging and time windows. *Computers & Operations Research*, 101:183–199, 2019.

S. Madankumar and C. Rajendran. Mathematical models for green vehicle routing problems with pickup and delivery: A case of semiconductor supply chain. *Computers & Operations Research*, 89:183–192, 2018.

G. Majeau-Bettez, T. R. Hawkins, and A. H. Strømman. Life cycle environmental assessment of lithium-ion and nickel metal hydride batteries for plug-in hybrid and battery electric vehicles. *Environmental Science & Technology*, 45(10):4548–4554, 2011.

F. Marra, G. Y. Yang, C. Træholt, E. Larsen, C. N. Rasmussen, and S. You. Demand profile study of battery electric vehicle under different charging options. In *Power and Energy Society General Meeting, 2012 IEEE*, pages 1–7. IEEE, July 2012.

M. A. Masmoudi, M. Hosny, E. Demir, K. N. Genikomsakis, and N. Cheikhrouhou. The dial-a-ride problem with electric vehicles and battery swapping stations. *Transportation Research Part E: Logistics and Transportation Review*, 118:392 – 420, 2018.

A. McKinnon and M. Piecyk. Measurement of $CO_2$ emissions from road freight transport: A review of UK experience. *Energy Policy*, 37(10):3733–3742, 2009.

M. C. McManus. Environmental consequences of the use of batteries in low carbon systems: The impact of battery production. *Applied Energy*, 93:288–295, 2012.

J. E. Mendoza and J. G. Villegas. A multi-space sampling heuristic for the vehicle routing problem with stochastic demands. *Optimization Letters*, 7:1503–1516, 2013.

C. Middlehurst. New battery tech faces a long road to mass adoption, 7 2019. Retrieved on 18/11/2019 from `https://www.ft.com/content/3324aae6-7d63-11e9-8b5c-33d0560f039c`.

MINING.COM. Li-ion battery demand to grow tenfold by 2029 – report, 06 2020. Retrieved on 17/10/2020 from `https://www.mining.com/li-ion-battery-demand-to-grow-tenfold-by-2029-report/`.

A. Montoya, C. Guéret, J. E. Mendoza, and J. G. Villegas. A multi-space sampling heuristic for the green vehicle routing problem. *Transportation Research Part C: Emerging Technologies*, 70:113–128, 2016.

A. Montoya, C. Guéret, J. E. Mendoza, and J. G. Villegas. The electric vehicle routing problem with nonlinear charging function. *Transportation Research Part B: Methodological*, 103:87–110, 2017.

J. R. Montoya-Torres, J. López Franco, S. Nieto Isaza, H. Felizzola Jiménez, and N. Herazo-Padilla. A literature review on the vehicle routing problem with multiple depots. *Computers & Industrial Engineering*, 79:115–129, 2015.

V. Muenzel, J. de Hoog, M. Brazil, A. Vishwanath, and S. Kalyanaraman. A multi-factor battery cycle life prediction methodology for optimal battery management. In *Proceedings of the 2015 ACM Sixth International Conference on Future Energy Systems*, pages 57–66. ACM, 2015.

V. M. Muggeo. Estimating regression models with unknown break-points. *Statistics in medicine*, 22(19):3055–3071, 2003.

S. Nathan. Tesla research partner claims "million-mile battery" result, 9 2019. Retrieved on 18/11/2019 from `https://www.theengineer.co.uk/tesla-million-mile-battery/`.

M. Nicholas. Estimating electric vehicle charging infrastructure costs across major US metropolitan areas, 2019. Retrieved from the International Council on Clean Transportation, `https://theicct.org/sites/default/files/publications/ICCT_EV_Charging_Cost_20190813.pdf`.

NobelPrize.org. The Nobel prize in chemistry 2019. Popular science background, 10 2019. Retrieved on 21/10/2019 from `https://www.nobelprize.org/uploads/2019/10/popular-chemistryprize2019.pdf`.

D. A. Notter, M. Gauch, R. Widmer, P. Wäger, A. Stamp, R. Zah, and H.-J. Althaus. Contribution of li-ion batteries to the environmental impact of electric vehicles. *Environmental Science & Technology*, 44(17):6550–6556, 2010.

B. Nykvist and M. Nilsson. Rapidly falling costs of battery packs for electric vehicles. *Nature Climate Change*, 5(4):329—-332, 2015.

B. Nykvist, F. Sprei, and M. Nilsson. Assessing the progress toward lower priced long range battery electric vehicles. *Energy policy*, 124:144–155, 2019.

N. Omar, M. Abdel Monem, Y. Firouz, J. Salminen, J. Smekens, O. Hegazy, H. Gaulous, G. Mulder, P. Van den Bossche, T. Coosemans, and J. Van Mierlo. Lithium iron phosphate based battery–assessment of the aging parameters and development of cycle life model. *Applied Energy*, 113:1575–1585, 2014.

Operational Research Society. News and notes. *Journal of the Operational Research Society*, 13(3):279–286, 1962. doi: 10.1057/jors.1962.46. URL `https://doi.org/10.1057/jors.1962.46`.

J. Partyka and R. Hall. Vehicle routing software survey: VR delivers the goods. *OR/MS Today*, 41(1):40–46, 2014.

J. Paz, M. Granada-Echeverri, and J. Escobar. The multi-depot electric vehicle location routing problem with time windows. *International Journal of Industrial Engineering Computations*, 9(1):123–136, 2018.

S. Pelletier, O. Jabali, and G. Laporte. 50th anniversary invited article—Goods distribution with electric vehicles: Review and research perspectives. *Transportation Science*, 50(1):3–22, 2016.

S. Pelletier, O. Jabali, G. Laporte, and M. Veneroni. Battery degradation and behaviour for electric vehicles: Review and numerical analyses of several models. *Transportation Research Part B: Methodological*, 103:158–187, 2017.

S. Pelletier, O. Jabali, and G. Laporte. Charge scheduling for electric freight vehicles. *Transportation Research Part B: Methodological*, 115:246 – 269, 2018.

S. B. Peterson, J. Apt, and J. Whitacre. Lithium-ion battery cell degradation resulting from realistic vehicle and vehicle-to-grid utilization. *Journal of Power Sources*, 195(8): 2385–2392, 2010.

C. Prins. A simple and effective evolutionary algorithm for the vehicle routing problem. *Computers & Operations Research*, 31(12):1985–2002, 2004.

C. Prins, P. Lacomme, and C. Prodhon. Order-first split-second methods for vehicle routing problems: A review. *Transportation Research Part C: Emerging Technologies*, 40:179–200, 2014.

H. N. Psaraftis, M. Wen, and C. A. Kontovas. Dynamic vehicle routing problems: Three decades and counting. *Networks*, 67(1):3–31, 2016.

H. Quak, N. Nesterova, and T. van Rooijen. Possibilities and barriers for using electric-powered vehicles in city logistics practice. *Transportation Research Procedia*, 12:157–169, 2016. Tenth International Conference on City Logistics 17-19 June 2015, Tenerife, Spain.

H. Quak, R. Koffrie, T. Van Rooijen, and N. Nesterova. Validating freight electric vehicles in urban europe. *D3. 2: Economics of EVs for City Logistics–Report. FREVUE*, 2017.

M. Rinaldi, F. Parisi, G. Laskaris, A. D'Ariano, and F. Viti. Optimal dispatching of electric and hybrid buses subject to scheduling and charging constraints. In *2018 21st International Conference on Intelligent Transportation Systems (ITSC)*, pages 41–46. IEEE, Nov 2018.

R. Roberti and M. Wen. The electric traveling salesman problem with time windows. *Transportation Research Part E: Logistics and Transportation Review*, 89:32–52, 2016.

I. Rodríguez-Martín and J. J. Salazar-González. A local branching heuristic for the capacitated fixed-charge network design problem. *Computers & Operations Research*, 37 (3):575–581, 2010.

M. Samavati, D. Essam, M. Nehring, and R. Sarker. A local branching heuristic for the open pit mine production scheduling problem. *European Journal of Operational Research*, 257(1):261–271, 2017.

E. Sarasketa-Zabala, I. Gandiaga, L. Rodriguez-Martinez, and I. Villarreal. Calendar ageing analysis of a LiFePO $_4$/graphite cell with dynamic model validations: Towards realistic lifetime predictions. *Journal of Power Sources*, 272:45–57, 2014.

E. Sarasketa-Zabala, I. Gandiaga, E. Martinez-Laserna, L. Rodriguez-Martinez, and I. Villarreal. Cycle ageing analysis of a LiFePO $_4$/graphite cell with dynamic model validations: Towards realistic lifetime predictions. *Journal of Power Sources*, 275:573–587, 2015.

O. Sassi and A. Oulamara. Electric vehicle scheduling and optimal charging problem: complexity, exact and heuristic approaches. *International Journal of Production Research*, 55(2):519–535, 2017.

O. Sassi, W. R. Cherif-Khettaf, and A. Oulamara. Multi-start iterated local search for the mixed fleet vehicle routing problem with heterogenous electric vehicles. In *European Conference on Evolutionary Computation in Combinatorial Optimization*, pages 138–149. Springer, Springer International Publishing, 2015.

T. Satyavani, A. S. Kumar, and P. S. Rao. Methods of synthesis and performance improvement of lithium iron phosphate for high rate li-ion batteries: A review. *Engineering Science and Technology, an International Journal*, 19(1):178 – 188, 2016. doi: https://doi.org/10.1016/j.jestch.2015.06.002.

M. Schiffer and G. Walther. The electric location routing problem with time windows and partial recharging. *European Journal of Operational Research*, 260(3):995–1013, 2017. ISSN 0377-2217. doi: https://doi.org/10.1016/j.ejor.2017.01.011. URL `http://www.sciencedirect.com/science/article/pii/S0377221717300346`.

M. Schiffer and G. Walther. An adaptive large neighborhood search for the location-routing problem with intra-route facilities. *Transportation Science*, 52(2):331–352, 2018a.

M. Schiffer and G. Walther. Strategic planning of electric logistics fleet networks: A robust location-routing approach. *Omega*, 80:31–42, 2018b.

M. Schiffer, M. Schneider, and G. Laporte. Designing sustainable mid-haul logistics networks with intra-route multi-resource facilities. *European Journal of Operational Research*, 265(2):517–532, 2018.

M. Schneider, A. Stenger, and D. Goeke. The electric vehicle-routing problem with time windows and recharging stations. *Transportation Science*, 48(4):500–520, 2014.

A. Schrijver. On the history of the transportation and maximum flow problems. *Mathematical Programming*, 91(3):437–445, 2002.

T. Sedran. The Volkswagen Group: Our roadmap to become a leading provider of sustainable mobility – Status update, 1 2018. Retrieved on 18/11/2019 from https://www.volkswagenag.com/presence/investorrelation/publications/presentations/2018/01_january/2018_01_22_Goldman%20Sachs_Mobility_Conference_Volkswagen_Group.pdf.

A. Sonoc, J. Jeswiet, and V. K. Soo. Opportunities to improve recycling of automotive lithium ion batteries. *Procedia CIRP*, 29:752–757, 2015. ISSN 2212-8271. The 22nd CIRP Conference on Life Cycle Engineering.

K. Soonpracha, A. Mungwattana, G. K. Janssens, and T. Manisri. Heterogeneous VRP review and conceptual framework. In *Proceedings of the International MultiConference of Engineers and Computer Scientists 2014 Vol II*. Newswood Limited, 2014.

Southern California Edison. Electric vehicle rates for businesses, 10 2019. Retrieved on 14/12/2019 from https://www.sce.com/business/rates/electric-car-business-rates/business/rates/electric-car-business-rates.

M. G. Speranza. Trends in transportation and logistics. *European Journal of Operational Research*, 264(3):830–836, 2018.

G. Suizo. Large & recharged: Top electric fleets, 07 2013. Retrieved on 05/02/2019 from https://www.greenfleetmagazine.com/155563/large-recharged-top-electric-fleets.

T. M. Sweda, I. S. Dolinskaya, and D. Klabjan. Adaptive routing and recharging policies for electric vehicles. *Transportation Science*, 51(4):1326–1348, 2017.

T. T. Taefi, J. Kreutzfeldt, T. Held, R. Konings, R. Kotter, S. Lilley, H. Baster, N. Green, M. S. Laugesen, S. Jacobsson, M. Borgqvist, and C. Nyquist. Comparative analysis of European examples of freight electric vehicles schemes—A systematic case study approach with examples from Denmark, Germany, the Netherlands, Sweden and the UK. In *Dynamics in Logistics*, pages 495–504. Springer, 2016.

P. Toth and D. Vigo. *Vehicle routing: problems, methods, and applications*. SIAM, 2014.

K. Uddin, A. Picarelli, C. Lyness, N. Taylor, and J. Marco. An acausal li-ion battery pack model for automotive applications. *Energies*, 7(9):5675–5700, 2014.

USEPA. Fast facts on transportation greenhouse gas emissions, 06 2019. Retrieved on 18/11/2019 from https://https://www.epa.gov/greenvehicles/fast-facts-transportation-greenhouse-gas-emissions.

J. Vetter, P. Novák, M. Wagner, C. Veit, K.-C. Möller, J. Besenhard, M. Winter, M. Wohlfahrt-Mehrens, C. Vogler, and A. Hammouche. Ageing mechanisms in lithium-ion batteries. *Journal of Power Sources*, 147(1):269–281, 2005.

T. Vidal, T. G. Crainic, M. Gendreau, N. Lahrichi, and W. Rei. A hybrid genetic algorithm for multidepot and periodic vehicle routing problems. *Operations Research*, 60(3):611–624, 2012.

J. Villegas, C. Guéret, J. E. Mendoza, and A. Montoya. The technician routing and scheduling problem with conventional and electric vehicle. Working paper or preprint, 0 2018. URL https://hal.archives-ouvertes.fr/hal-01813887.

J. G. Villegas, C. Prins, C. Prodhon, A. L. Medaglia, and N. Velasco. A matheuristic for the truck and trailer routing problem. *European Journal of Operational Research*, 230 (2):231–244, 2013.

J. Wang, P. Liu, J. Hicks-Garner, E. Sherman, S. Soukiazian, M. Verbrugge, H. Tataria, J. Musser, and P. Finamore. Cycle-life model for graphite-$LiFePO_4$ cells. *Journal of Power Sources*, 196(8):3942–3948, 2011.

Y.-W. Wang, C.-C. Lin, and T.-J. Lee. Electric vehicle tour planning. *Transportation Research Part D: Transport and Environment*, 63:121 – 136, 2018.

T. C. Wanger. The lithium future–resources, recycling, and the environment. *Conservation Letters*, 4(3):202–206, 2011.

M. Wen, J.-F. Cordeau, G. Laporte, and J. Larsen. The dynamic multi-period vehicle routing problem. *Computers & Operations Research*, 37(9):1615–1623, 2010.

M. Wen, E. Linde, S. Ropke, P. Mirchandani, and A. Larsen. An adaptive large neighborhood search heuristic for the electric vehicle scheduling problem. *Computers & Operations Research*, 76:73–83, 2016.

M. Wohlfahrt-Mehrens, C. Vogler, and J. Garche. Aging mechanisms of lithium cathode materials. *Journal of Power Sources*, 127(1–2):58–64, 2004.

B. Xu. Degradation-limiting optimization of battery energy storage systems operation. Master's thesis, ETH Zurich, Switzerland, 2013.

M. Yaghini, M. Momeni, and M. Sarmadi. An improved local branching approach for train formation planning. *Applied Mathematical Modelling*, 37(4):2300–2307, 2013.

J. Yang and H. Sun. Battery swap station location-routing problem with capacitated electric vehicles. *Computers & Operations Research*, 55:217–232, 2015.

J. Y. Yong, V. K. Ramachandaramurthy, K. M. Tan, and N. Mithulananthan. A review on the state-of-the-art technologies of electric vehicle, its impacts and prospects. *Renewable and Sustainable Energy Reviews*, 49:365–385, 2015.

X. Zeng, J. Li, and N. Singh. Recycling of spent lithium-ion battery: A critical review. *Critical Reviews in Environmental Science and Technology*, 44(10):1129–1165, 2014. doi: 10.1080/10643389.2013.763578. URL https://doi.org/10.1080/10643389.2013.763578.

D. Zhang, X. Wang, S. Li, N. Ni, and Z. Zhang. Joint optimization of green vehicle scheduling and routing problem with time-varying speeds. *PloS ONE*, 13(2), 2018a.

S. Zhang, Y. Gajpal, S. Appadoo, and M. Abdulkader. Electric vehicle routing problem with recharging stations for minimizing energy consumption. *International Journal of Production Economics*, 2018b.

L. Zhen, Z. Xu, K. Wang, and Y. Ding. Multi-period yard template planning in container terminals. *Transportation Research Part B: Methodological*, 93:700–719, 2016.

H. Zheng and S. Peeta. Routing and charging locations for electric vehicles for intercity trips. *Transportation Planning and Technology*, 40(4):393–419, 2017.

# Appendices

# Appendix A

# Variable and parameter definitions

## A.1 Problem definitions

| | |
|---|---|
| $0$ | Node representing the depot |
| $\mathcal{P}$ | Set of periods ($\mathcal{P} = \{0, \ldots, P_{max} - 1\}$); $p \in \mathcal{P}$ |
| $E_p$ | Earliest departure time from depot to perform routes during period $p$ |
| $L_p$ | Latest arrival time to depot after performing routes of period $p$ |
| $\mathcal{I}$ | Set of visit nodes (customers or routes as it may apply); $i \in \mathcal{I}$ |
| $\delta_i$ | Service time of customer $i$ |
| $t_{ij}$ | Driving time from $i$ to $j, i, j \in \mathcal{I} \cup \{0\}$ |
| $e_{ij}$ | Energy consumption from $i$ to $j, i, j \in \mathcal{I} \cup \{0\}$ |
| $t_i$ | Duration of route $i$ |
| $e_i$ | Energy consumption of route $i$ |
| $p_i$ | Period in which an EV must visit node $i$ |
| $\mathcal{K}$ | Set of homogeneous EVs with battery capacity $Q$; $k \in \mathcal{K}$ |
| $Q_0^k$ | Energy of EV $k$ at the beginning of the planning horizon |
| $\mathcal{M}$ | Set of charging modes available at the depot; $m \in \mathcal{M}$ |
| $A_m$ | Number of available chargers with mode $m$ |
| $u_m$ | Fixed cost per charge with mode $m$ |
| $v_m$ | Charging power of mode $m$ |
| $B_v$ | Set of breakpoints of the piecewise linear approximation of charging function for power $v$; $b \in B_v$ |
| $c_{v,b}$ | Charging time of breakpoint $b$ |
| $a_{v,b}$ | SOC of breakpoint $b$ |
| $PW_{max}$ | Grid power capacity |
| $\Pi$ | Set of breakpoints of the piecewise linear approximation of the cumulative wear cost; $\beta \in \Pi$ |
| $l_\beta$ | SOC of breakpoint $\beta$ |
| $n_\beta$ | Cumulative wear cost of breakpoint $\beta$ |
| $\zeta_\beta$ | Slope of the segment between $l_{\beta-1}$ and $l_\beta$ of breakpoint $\beta$ |
| $T$ | End of the planning horizon |

## A.2 MILP formulations

| | |
|---|---|
| $\mathcal{H}$ | (Totally ordered) set of charges an EV battery can go through during the time horizon; $h \in \mathcal{H}$ |
| $d_p^{start}$ | Starting depot node for period $p$ |
| $\mathcal{D}^{start}$ | Set of the starting depot nodes |
| $d_p^{end}$ | Ending depot node for period $p \in \mathcal{P} \cup \{-1\}$ |
| $\mathcal{D}^{end}$ | Set of the ending depot nodes |
| $\mathcal{D}$ | Set of depot nodes |
| $\mathcal{C}_h$ | Set of charging nodes associated with charge $h$ |
| $\mathcal{C}$ | Set of all charging nodes; $i \in \mathcal{C}$ |
| $\mathcal{I}_p$ | Set of nodes (customers or routes as it may apply) that must be visited in period $p$ |
| $m(i)$ | Charging mode associated with charging node $i$ |
| $h(i)$ | Charge associated with charging node $i$ |
| $i(m,h)$ | Charging node related with charging mode $m$ and charge $h$ |
| $G = (\mathcal{V}, \mathcal{A})$ | Multigraph for the M-E-VRP, the MP-E-VRACSP, and the MP-E-VRACSPm |
| $\mathcal{O}_m$ | Set of charging operations associated with charging mode $m$ |
| $\mathcal{O}$ | Set of all charging operations; $o \in \mathcal{O}$ |
| $o_{mh}^k \in \mathcal{O}$ | Charging operation associated with EV $k$, charging mode $m$, and charge $h$ |
| $m(o)$ | Charging mode associated with charging operation $o$ |
| $h(o)$ | Charge associated with charging operation $o$ |
| $k(o)$ | EV associated with charging operation $o$ |
| $\varphi^-$, $\varphi^+$ | Dummy charging operations for power grid / charging modes capacity constraints |
| $\mathcal{O}^-(o), \mathcal{O}^+(o)$ | Set of charging operations that can be done before and after charging operation $o$ |
| $\mathcal{O}_m^-(o), \mathcal{O}_m^+(o)$ | Set of charging operations with mode $m$ that can be done before and after charging operation $o$ |

## A.3 Variables

| | |
|---|---|
| $x_{ij}^k$ | Equal to 1 if vehicle $k$ travels on arc $(i,j) \in \mathcal{A}$, and 0 otherwise |
| $\tau_{ij}^k$ | Time when EV $k$ departs from node $i \in \mathcal{V}$ to travel on arc $(i,j) \in \mathcal{A}$ |
| $y_{ij}^k$ | Energy when the EV $k$ departs from node $i \in \mathcal{V}$ to travel on arc $(i,j) \in \mathcal{A}$ |
| $\underline{q}_o$, $\overline{q}_o$ | Energy of EV upon starting and after charging operation $o$ |
| $\underline{s}_o$, $\overline{s}_o$ | Starting and ending time of charging operation $o$ |
| $\Delta_o$ | Duration of the charging operation $o$ |
| $\underline{\theta}_{ob}, \overline{\theta}_{ob}$ | Equal to 1 if energy of an EV upon starting and after completing charging operation $o$ is between $a_{m(o),b-1}$ and $a_{m(o),b}$ |
| $\underline{\rho}_{ob}$, $\overline{\rho}_{ob}$ | Coefficient associated with the breakpoint $(c_{m(o),b}, a_{m(o),b})$ in the piecewise linear approximation of the charging function, when an EV starts and ends charging operation $o$ |
| $w_{oo'}$ | Equal to 1 if charging operation $o' \in \mathcal{O}^+(o)$ starts after the completion of charging operation $o \in \mathcal{O} \cup \{\varphi^+\}$ |
| $z_{oo'}$ | Quantity of power transferred from charging operation $o \in \mathcal{O} \cup \{\varphi^+\}$ to charging operation $o' \in \mathcal{O}^+(o)$ |
| $f_{oo'}$ | Number of chargers of charging mode $m$ transferred from charging operation $o \in \mathcal{O}_m \cup \{\varphi^+\}$ to charging operation $o' \in \mathcal{O}_m^+(o)$ |
| $\alpha_{o\beta}$ | Percentage of energy charged on the segment that lies between points $(l_{\beta-1}, n_{\beta-1})$ and $(l_{\beta-1}, n_{\beta-1})$ of the cumulative wear cost function associated with charging operation $o$ |
| $\sigma_{o\beta}$ | Equal to 1 if and only if the charging operation involves the segment between points $(l_{\beta-1}, n_{\beta-1})$ and $(l_{\beta-1}, n_{\beta-1})$ of the cumulative wear cost function associated with charging operation $o$ |
| $\gamma_o$ | Cumulative wear cost due to charging operation $o$ |
| $\eta_{p\beta}^k$ | Percentage of energy discharged on the segment that lies between points $(l_{\beta-1}, n_{\beta-1})$ and $(l_{\beta-1}, n_{\beta-1})$ of the cumulative wear cost function associated with the route performed by EV $k$ in period $p$ |
| $\phi_{p\beta}^k$ | Equal to 1 if and only if the discharge involves the segment between points $(l_{\beta-1}, n_{\beta-1})$ and $(l_{\beta-1}, n_{\beta-1})$ of the cumulative wear cost function associated with the route performed by EV $k$ in period $p$ |
| $\varepsilon_p^k$ | Cumulative wear cost due to the route performed by EV $k$ in period $p$ |

# Appendix B

# Compute Canada cluster characteristics

We carried out the experiments in the general-purpose cluster Cedar. Table B.1 provides the node characteristics.

Table B.1: Compute Canada's Cedar node characteristics. Source: `https://docs.computecanada.ca/wiki/Cedar`

| Nodes | Cores | Available memory | CPU |
|---|---|---|---|
| 576 | 32 | 125G | 2 x Intel E5-2683 v4 Broadwell @ 2.1Ghz |
| 96 | 32 | 250G | 2 x Intel E5-2683 v4 Broadwell @ 2.1Ghz |
| 24 | 32 | 502G | 2 x Intel E5-2683 v4 Broadwell @ 2.1Ghz |
| 24 | 32 | 1510G | 2 x Intel E5-2683 v4 Broadwell @ 2.1Ghz |
| 4 | 32 | 3022G | 4 x Intel E7-4809 v4 Broadwell @ 2.1Ghz |
| 114 | 24 | 125G | 2 x Intel E5-2650 v4 Broadwell @ 2.2GHz |
| 32 | 24 | 250G | 2 x Intel E5-2650 v4 Broadwell @ 2.2GHz |
| 192 | 32 | 187G | 2 x Intel Silver 4216 Cascade Lake @ 2.1GHz |
| 640 | 48 | 187G | 2 x Intel Platinum 8160F Skylake @ 2.1Ghz |
| 768 | 48 | 187G | 2 x Intel Platinum 8260 Cascade Lake @ 2.4Ghz |

## Résumé :

Cette thèse étudie l'optimisation du routage et de la programmation de la charge des véhicules électriques (VEs) sur un horizon de planification de plusieurs périodes dans le but de limiter la dégradation des batteries associée à ces opérations. Nous introduisons le problème qui en résulte sous le nom de « Multi-period Electric Vehicle Routing Problem » (MP-E-VRP). Nous définissons formellement le MP-E-VRP et développons des méthodes pour le résoudre.

Pour tenir compte de l'impact des pratiques de charge et des tournées sur le vieillissement des batteries des VE, nous associons les coûts de dégradation aux opérations de charge et aux routes. Nous transformons la relation non linéaire entre les paramètres de fonctionnement et l'état de santé de la batterie en coûts linéaires par morceaux qui peuvent être inclus dans le MP-E-VRP.

Nous fournissons ensuite une formulation de programmation linéaire mixte en nombres entiers (PLNE) pour le MP-E-VRP, ci-après dénommée $[F^1]$. Notre formulation modélise le temps de manière continue et utilise des variables de suivi basées sur les arcs. En outre, elle utilise des modèles de flux pour tenir compte des contraintes de capacité du réseau électrique et de l'infrastructure de charge, et des modèles de combinaison convexe pour représenter le coût de dégradation des batteries et les fonctions de charge. Étant donné que le MP-E-VRP est un nouveau problème dans la littérature sur les E-VRP, nous présentons la procédure que nous avons suivie pour générer des instances basées sur des informations fournies par des entreprises utilisant des VE. Les résultats des calculs indiquent que, généralement, le modèle ne peut pas être utilisé directement pour résoudre des cas réalistes. Par conséquent, $[F^1]$ nous permet d'avoir une idée de la difficulté du problème et de la pertinence de concevoir des stratégies plus complexes.

Nous proposons ensuite une stratégie de décomposition dans laquelle nous générons d'abord un pool de routes de bonne qualité, puis nous sélectionnons les routes du pool, nous leur attribuons des VEs et nous ordonnons les opérations de chargement. Nous proposons trois méthodes qui suivent cette stratégie de décomposition. Elles utilisent toutes une heuristique existante pour échantillonner l'espace des routes possibles. Pour résoudre le second sous-problème (la sélection de routes et l'affectation des VE), nous proposons une heuristique constructive, une formulation PLNE et une approche basée sur « *local branching* ». L'heuristique constructive, bien que simple, permet de trouver une solution réalisable en peu de temps. Pour chaque période, l'heuristique attribue la route ayant la plus grande consommation d'énergie au VE ayant la plus grande énergie disponible et poursuit l'attribution jusqu'à ce que toutes les routes de la période soient attribuées. En outre, l'heuristique vérifie la satisfaction des contraintes de l'infrastructure de recharge. La solution obtenue peut alors être fournie pour accélérer le processus de recherche dans les autres stratégies de décomposition.

La méthode de décomposition basée sur une formulation PLNE s'appuie sur $[F^1]$, ci-après dénommée $[F^{2m}]$. Peu de modifications sont nécessaires dans $[F^1]$ pour formuler le nouveau problème concernant l'affectation des VE aux routes et l'ordonnancement des opérations de chargement. Enfin, la matheuristique « *local branching* » basée sur $[F^{2m}]$ consiste à ajouter des contraintes linéaires à cette formulation, pour explorer l'espace de

solution en effectuant des recherches locales sur des voisinages définis en vue de trouver des solutions de bonne qualité. La définition du voisinage et la stratégie de diversification sont modifiées pour tenir compte des caractéristiques du MP-E-VRP. Les résultats expérimentaux nous permettent d'identifier cette méthode comme la meilleure pour trouver des solutions pour des instances de grande taille.

## Mots clés :

Problè me de tournées des véhicule électriques, dégradation de la batterie, programmation linéaire mixte en nombres entiers, matheuristique, local branching

## Abstract :

Recent innovations in battery technology have significantly improved electric vehicles' (EVs) driving range. As a result, companies exploiting EVs for urban operations do not longer need to plan for mid-route battery charging and can restrict all charging operations to take place overnight (or between shifts) at the depot. However, the trivial policy of fully charging all vehicles every night can lead to poor fleet management decisions. First, this policy may be infeasible because of charging infrastructure constraints (e.g., grid constraints, the maximum number of available chargers). Second, this practice accelerates battery degradation. To solve these issues, routing and charge scheduling decisions must be taken simultaneously over a planning horizon of (at least) a few days/shifts. In this thesis, we introduce the resulting problem as the Multi-period Electric Vehicle Routing Problem (MP-E-VRP). We formally define the MP-E-VRP and develop methods for solving it.

To account for the impact of charging and routing practices on EVs battery aging, we associate degradation costs with charging operations and routes. We transform the nonlinear relationship between operating parameters and battery health into piecewise linear costs that can be easily included in the MP-E-VRP. These costs can be easily computed with readily available data, provided by battery manufacturers or relative to the operations themselves.

We then provide a Mixed integer linear programming (MILP) formulation for the MP-E-VRP, hereinafter referred to as $[F^1]$. Our formulation models time on a continuous basis and uses arc-based tracking variables. Moreover, it uses flow models to account for the power grid and charging infrastructure capacity constraints, and convex combination models to represent the battery degradation cost and charging functions. Since the MP-E-VRP is a new problem in the E-VRP literature, we present the procedure we followed to generate instances based on some insights provided by companies using EVs. Computational results indicate that, generally, the model cannot be directly used to solve realistic instances. Therefore, $[F^1]$ allows us to have an idea about the difficulty of the problem and the relevance of designing more complex strategies.

We then propose a decomposition strategy in which we first generate a pool of high-quality routes and then we select the routes from the pool, assign EVs to them, and schedule the charging operations. We propose three methods following this decomposition strategy. All of them use an existing heuristic to sample the space of feasible routes. To solve the second subproblem (routes selection, assignment of EVs, and scheduling of charging operations), we propose a constructive heuristic, a MILP formulation, and a local branching-based approach. The constructive heuristic, yet simple, allows finding a feasible solution in a short time. For each period, the heuristic assigns the route with the highest energy consumption to the EV with the most available energy and continues the assignment until all routes of the period are assigned. In addition, the heuristic checks for the satisfaction of the charging infrastructure constraints. The solution obtained can then be provided to speed up the search process in the other decomposition strategies.

The decomposition method based on a MILP formulation is built upon $[F^1]$, referred to as $[F^{2m}]$. Few modifications are needed in $[F^1]$ to formulate the new problem concerning the assignment of EVs to routes and the scheduling of the charging operations. Finally,

the local branching matheuristic is based on $[F^{2m}]$ and lies in adding linear inequalities to this formulation, to explore the solution space by performing local searches on defined neighborhoods looking for good quality solutions. The neighborhood definition and the diversification strategy are modified to consider MP-E-VRP features. Computational experiments allow us to identify this method as the best for finding solutions in large-size instances.

## Keywords :

Electric vehicle routing problem, battery degradation, mixed integer linear programming, matheuristic, local branching